SECONDARY INSTABILITY IN EKMAN BOUNDARY FLOW

David B. Zaff
B.S., Columbia University
(1978)

Submitted to the
Department of Mathematics
in partial fulfillment of the requirements for the degree of

Doctor of Philosophy

at the

Massachusetts Institute of Technology
January 1987

Signature of author____________________

Certified by____________________
Professor Willem V.R. Malkus
Thesis Supervisor

Accepted by____________________
Professor Willem V. R. Malkus, Chairman
Committee on Applied Mathematics

Accepted by____________________
Professor Sigurdur Helgason, Chairman
Departmental Graduate Committee
Department of Mathematics

Acknowledgements

I would like to express my appreciation to Professor Willem V.R. Malkus for the intellectually stimulating insights he has generously shared with me over the past years. Perhaps more important, for the successful completion of this thesis, was his patient understanding and constant encouragement in spite of often slow outward progress. My desk in his downstairs lab was at times my "home away from home".

I wish to thank Prof. Dave Benney, Prof. K.K. Tung, and Dr. Fred Pearson for taking the time and effort to act as thesis committee members. Prof. Tung went out of his way to help, especially in obtaining part time employment for me at A.E.R.. This provided my financial support while I was writting my masters thesis. I would like to thank Prof. E.T. Onat, for introducing me to the fascinating study of dynamical systems, and the difficulties of doing research, during the summer I was at Yale.

The many years spent at M.I.T. would certainly have been duller without the friendship of Dale Worley, Steve Lowe, Bob Thurstans, and George Fann. Sharing the graduate student experience usually made things a lot easier to take. It always made them more interesting.

Finally, I thank my family for the immeasurable support and confidence that I have benefited from. This was fundamental to my productive development, and given of, I believe, far more than I (or anyone else) could possibly deserve.

TO GERTRUDE T. ZAFF

SECONDARY INSTABILITY IN EKMAN BOUNDARY FLOW

David B. Zaff

Submitted to the Department of Mathematics
in partial fulfillment of the requirements for the degree of
Doctor of Philosophy
Massachusetts Institute of Technology
February 1987

Abstract

This thesis examines the linear secondary instability to finite amplitude vorticity waves in narrow gap Ekman flow. A deductive path is taken in which a linear primary instability is first investigated and its equilibration determined from a parametric expansion, giving the Reynolds number as a function of the equilibrium amplitude. As the gap size decreases the primary vorticity waves become longitudinally directed. Comparison is drawn between Ekman and Poiseuille flow. The presence of a small amplitude transverse wave links the fourier components of the secondary instability, permitting a more complex '3-D' disturbance, with a streamwise fourier component, to grab energy directly from the mean shear. A large streamwise velocity, u_0^{3D}, is induced. Strong '3-D' amplification results because the streamwise mode is very effective in generating power via the correlation $u_0^{3D}(w_0^{3d})^*(dU_M/dz)$. Longitudinally directed primary vorticity waves force a large streamwise velocity, which alternately steepen and flatten the velocity field. In this case, the energy supplied to a secondary instability comes mostly from the primary wave, and relies on a primary wave amplitude sufficiently large to produce inflections in the local velocity field. In narrow gap Ekman flow ($G \cong 2.5$) secondary instability develops sporadically along vortex filaments as a small scale finely hashed perturbation (appearing like a string of beads), and is considerably milder than the bursting phenomenon associated with subcritical transition for Poiseuille flow.

Thesis Supervisor: Willem V.R. Malkus
Professor of Applied Mathematics

Contents

Introduction.

Considerable effort has been devoted to uncovering the various transition mechanisms which lead to turbulence. It has become clear that several processes quite distinct in character are possible scenarios for the breakdown of shear flow. Of these, secondary instability appears promising. Its basic nature is in general agreement with many observations, it is applicable to a wide variety of flows, and is predictable on a purely deductive basis directly from the Navier-Stokes equations without further hypothesis. Secondary instability provides a link between wave interactions (global instability) and turbulent spots (local instability) which suggests (Malkus' conjecture) that turbulent spots exist as an isolated 'island' instability beyond the scope of weakly non-linear theory.

The transition process in boundary layers, pipes, and channels is of practical interest, especially with regards to boundary layer control, aerodynamic stability, and drag reduction. Because of its relatively simple velocity profile, Poiseuille (pressure driven) channel flow has served in the capacity as role model. In contrast to pipe flow, Poiseuille channel flow can experience linear instability at Reynolds numbers in excess of 5772. Realistically this distinction may be of little importance since both flows are subject to burstlike disturbances at Reynolds numbers as low as 1000. Reconciling the observed low Reynolds number transition with previous theoretical studies proved to be quite a mystery. S. Orzag and A. Patera proposed that spots are the development of a highly structured (but global) three dimensional instability on a finite amplitude wave. Both the three dimensionality of the instability and the finite amplitude of the primary wave are necessary conditions. For Poiseuille flow, the existence of a quasi-steady finite amplitude wave is posited. This is consistent as, the secondary instability grows on a fast convective time scale, while any pre-existing wave will decay slowly. In the analysis, the primary wave characteristics are chosen to resemble those on the upper branch of the finite amplitude stability curve. The exact wave number and amplitude that leads to instability are left unspecified, and secondary instability becomes operational when rapid three dimensional growth can overcompensate the two dimensional decay.

Turbulent boundary layers are subject to spots, bursts, and a collection of coherent structures such as horseshoe vortices. Remarkably, as discovered by Emmons, the spots are characterized by a definite spreading angle, growth rate, and phase speed. The onset of transition in boundary layers is, however, distinctly different than that of Poiseuille channel flow or pipe flow. The experiments of Klebanoff, Tidstrom & Sargent first demonstrated that a well ordered sequence of triggering steps connects transition with weakly non-linear wave interactions. In boundary layers the Reynolds number increases downstream, so spatial development substitutes for temporal evolution. In the Blasius boundary layer, linear Tolmien-Shlichting waves amplify and become unstable to a three dimensional disturbance. The warping of the velocity field increases producing the appearance of 'peak-valley' splitting. This is accompanied by high frequency spikes having periods which are an integral multiple of the fundamental linear wave. A longitudinal pattern of streaks intensifies, and within typically one or two wavelengths the flow field breaks down, becoming highly disordered.

The early work by D.J. Benney gives a surprisingly good account of the observed two and three dimensional non-linear wave interactions. One of the most interesting features of his analysis is that a three-dimensional primary oscillation induces a mean second order vorticity into the flow, having a component ξ_0^2 in the downstream direction. It is this mechanism which produces a spanwise momentum exchange and causes a warping of the original velocity profile. His theory correctly predicts that breakdown originates near the ‘peak’ (a spanwise distributed region where the velocity field is enhanced by the local wave field). As the local velocity profile is inflectional around each peak, much speculation was generated regarding a subsequent inviscid, Rayliegh, instability at these periodically spaced locations.

In contrast to Benneys work, T. Herbert considers the secondary instability as the transition mechanism in the Blasius boundary layer. An important distinction is that the three dimensional disturbance arises as an instability to a finite amplitude wave field, and this makes its properties calculable from maximum linear growth rate considerations. The spanwise wavenumber is determined by this condition. For this reason the phase velocity of the secondary instability matches that of the primary wave. The three dimensional instability that results from secondary instability is highly structured. The non-separability of the ensuing boundary value calculation introduces oblique and longitudinal vorticity modes at the same order. The cross-stream eigenstructure that is predicted from this theory is not merely of an Orr-Sommerfeld type, but has a more complex nature involving a coupling of modal components through interaction with the primary wave. Herbert has gone to considerable length to demonstrate agreement between the predicted and observed cross-stream velocity structure. His work also supports the premise used by Patera, that the exact form of the primary wave is not crucial for secondary instability.

R. Pierrehumbert and S. Widnall analyze secondary instability of Stuart vorticies. Pierrehumbert has concluded on the basis of additional work that vorticies of a general nature will become unstable to secondary disturbances. On the basis of their eigenvalue calculation they show that in this case the secondary instability has no high wavenumber cutoff, a characteristic of inviscid instability, and a mechanism for generating a cascade to smaller length scales.

F. Busse and M. Nagata examine secondary instability in flow down an inclined plane, with heating. The primary instability is generated by a cubic inflectional velocity profile. Waves equilibrate, and subsequently undergo vortex pairings.

The previously mentioned works relate almost exclusively to primary disturbances aligned so that the vorticity is originally transverse to the flow. C.F. Pearson has studied the evolution of a streamwise diffusing vortex core, in an unbounded linear shear. He finds that even for modest vortex Reynolds numbers $(\Gamma/(2\pi\nu))$, the vorticity forces a large longitudinal velocity response.

Thus several characteristic features of secondary instability appear to be worthy of further study and possible clarification. What is the general relationship that exists between the mean shear, the primary wave, and possible secondary instabilities? Patera found that transverse vorticity waves serve to mediate the transfer of energy from the mean shear to the 3-D perturbation. How is this accomplished? Can the 2-D wave ever supply the secondary disturbance with energy directly? What is the cross-stream structure of the secondary instability? Is it concentrated near the boundary or highly structured throughout the interior and of a more inviscid nature? Is it located near inflections (maximum vorticity regions) in the local velocity profile? Does it have a high wavenumber cutoff?

This thesis explores stability and secondary instability in 'narrow gap' Ekman flow, a class of rotational flows parametrized by gap size (Ekman number) and created to permit the variation of wave criticality. Here stable finite amplitude waves are realized making predictions more readily testable, and providing a direct link to weakly non-linear wave theories. In particular for small gap separations the finite amplitude waves are nearly stationary in the rotating frame of reference. Another important distinction is a mean shear along the wave axis and a large induced 'helical' (streamwise) velocity component associated with the vortex wave. These differences contribute to enlarging the notion of secondary instability.

The first part of the thesis establishes the linear stability of narrow gap Ekman flow. The mean profiles are dependent on the local Rossby number and are conveniently developed in a regular perturbation expansion. The stability analysis that follows considers that the basic flow is a parallel shear flow at small Rossby number. The experimental analogue is then pressure driven flow between two rotating discs where the aspect ratio of the disc radius to the gap thickness is large. Several nonlinear wave problems are then treated. The method of modified perturbation theory is used to parametrize the finite amplitude stability curves. The method of amplitude expansions is also developed. In particular the two wave interaction using the technique of multiple scales and the case of three wave resonance are examined. The former expansion results in a coupled set of non-linear Schrödinger equations. Ekman flow is a very good case in point for distinguishing between wave chaos and turbulence. The third part of the thesis concerns mapping out the secondary stability properties of supercritical Ekman vorticies. This is contrasted with secondary instability in Poiseuille flow with a quasi-steady primary wave. An energy equation points to the significance of the correlation product, $u_0^{3d}(w_0^{3d})^*(dU_M/dz)$, in generating power for the rapid secondary instability growth.

In this chapter the basic mean velocity profiles for narrow gap Ekman flow are derived via a perturbation expansion in the Rossby number. The first term of the solution is physically representative of the flow in an infinitely long gap, and will approximate the velocity field far from the origin. We start with the Navier-Stokes equations in polar- cylindrical coordinates, in a uniformly rotating reference frame.

$$u_t + (\mathbf{u}\cdot\nabla)u - \frac{v^2}{r} - 2\Omega v = -\frac{p_r}{\rho} + \nu(\nabla^2 u - \frac{2v_\theta}{r^2} - \frac{u}{r^2}) \tag{1}$$

$$v_t + (\mathbf{u}\cdot\nabla)v + \frac{vu}{r} + 2\Omega u = -\frac{p_\theta}{\rho r} + \nu(\nabla^2 v + \frac{2u_\theta}{r^2} - \frac{v}{r^2}) \tag{2}$$

$$w_t + (\mathbf{u}\cdot\nabla)w = -\frac{p_z}{\rho} + \nu(\nabla^2 w) \tag{3}$$

Where $(\mathbf{u}\cdot\nabla) \equiv (u\partial_r + \frac{v}{r}\partial_\theta + w\partial_z)$ and $\nabla^2 \equiv (\partial_r^2 + \frac{1}{r}\partial_r + \frac{1}{r^2}\partial_\theta^2 + \partial_z^2)$.
In addition mass conservation for an incompressible fluid requires,

$$\frac{1}{r}\partial_r(ru) + \frac{1}{r}\partial_\theta v + \partial_z w = 0 \tag{4}$$

i.e. $\nabla\cdot\mathbf{u} = \mathbf{0}$. We follow A.J. Faller (J.F.M. 1963) in nondimensionalizing the Navier-Stokes equations. The characteristic length, time, and velocities determine the appropriate scaling and relevant parameters. Then

$$z' = zD \quad , \quad r' = rR \quad , \quad t' = t/(2\Omega)$$

$$u' = \frac{cu}{r} \quad , \quad v' = \frac{cv}{r} \quad , \quad w' = Dcw/R$$

$$p_r' = \frac{R\Omega c}{r}p_r \quad , \quad p_\theta' = \frac{R\Omega c}{r}p_\theta \quad , \quad p_z' = \frac{R\Omega c}{r}p_z$$

where $D = \sqrt{\frac{\nu}{\Omega}}$ is the characteristic boundary layer depth, $c = S/(\pi RD)$ is the characteristic speed, and S is the forced volume flux per unit time. R is a dimensional outer radius and H is the dimensional gap size. The dimensionless parameters are the Rossby number, $Ro = c/(\Omega r^2 R)$, the Ekman number,

$Ek = (\nu/(\Omega H^2))^{\frac{1}{2}} = D/H$, and the Taylor number, $T = \Omega^2 R^2/\nu^2 = R^4/D^4$. The Rossby number number is a function of radial position and its rate of variation is a measure of non-parallelness in the basic velocity profile. The inverse of the Ekman number expresses the gap thickness in terms of boundary layer units. The inverse of the Taylor number turns out to be exceeding small in the present study.

Assuming the underlying steady-state velocity field, (U,V,W), to be axisymmetric and making the above scaling transformations Equations [1.1-4] can be reduced to,

$$Ro(rU\frac{\partial U}{\partial r} - U^2 - V^2 + r^2 W\frac{\partial U}{\partial z}) - 2V = -p_r + \frac{\partial^2 U}{\partial z^2} + T^{-\frac{1}{2}}(r\frac{\partial}{\partial r}(\frac{1}{r}\frac{\partial U}{\partial r})) \tag{5}$$

$$Ro(rU\frac{\partial V}{\partial r} + r^2 W\frac{\partial V}{\partial z}) + 2U = \frac{\partial^2 V}{\partial z^2} + T^{-\frac{1}{2}}(r\frac{\partial}{\partial r}(\frac{1}{r}\frac{\partial V}{\partial r})) \tag{6}$$

$$Ro(rU\frac{\partial W}{\partial r} + r^2 W\frac{\partial W}{\partial z}) = -T^{\frac{1}{2}}\frac{p_z}{r} + \frac{\partial^2 W}{\partial z^2} + T^{-\frac{1}{2}}(\frac{\partial^2 W}{\partial r^2} + \frac{1}{r}\frac{\partial W}{\partial r}) \tag{7}$$

$$\frac{\partial U}{\partial r} + r\frac{\partial W}{\partial z} = 0 \tag{8}$$

The solution is developed in a power series in the Rossby number, which is conveniently written $Ro = \epsilon/r^2$, in terms of the small quantity ϵ. The Taylor number is determined by the relation $T^{-\frac{1}{2}} = \epsilon\mu$ where μ is also small. The expansions are

$$U(z,r) = U_0(z) + RoU_1(z) + Ro^2U_2(z) + Ro^3U_3(z) + Ro^4U_4(z) + \ldots$$

$$V(z,r) = V_0(z) + RoV_1(z) + Ro^2V_2(z) + Ro^3V_3(z) + Ro^4V_4(z) + \ldots$$

$$W(z,r) = \frac{Ro}{r^2}W_1(z) + \frac{Ro^2}{r^2}W_2(z) + \frac{Ro^3}{r^2}W_3(z) + \frac{Ro^3}{r^2}W_4(z) + \ldots$$

$$T^{-\frac{1}{2}}W(z,r) = \mu Ro^2 W_1(z) + \mu Ro^3 W_2(z) + \mu Ro^4 W_3(z) + \ldots$$

$$p_r = P_0 + Ro(P_I + \frac{T^{-\frac{1}{2}}}{r^2}P_1(z)) + Ro^2(P_{II} + \frac{T^{-\frac{1}{2}}}{r^2}P_2(z)) + Ro^3(P_{III} + \frac{T^{-\frac{1}{2}}}{r^2}P_3(z)) + \ldots$$

$$\frac{p_z}{r} = -\frac{T^{-\frac{1}{2}}}{3r^2}Ro\dot{P}_1(z) - \frac{T^{-\frac{1}{2}}}{5r^2}Ro^2\dot{P}_2(z) - \frac{T^{-\frac{1}{2}}}{7r^2}Ro^3\dot{P}_3(z) - \frac{T^{-\frac{1}{2}}}{9r^2}Ro^4\dot{P}_4(z) - \ldots$$

A set of equations at each order of the Rossby number results. The first three are

$O(1)$:

$$-2V_0 = -P_0 + \frac{\partial^2 U_0}{\partial z^2}$$
$$2U_0 = \frac{\partial^2 V_0}{\partial z^2}$$

$O(Ro)$:

$$-(U_0^2 + V_0^2) - 2V_1 = -P_I + \frac{\partial^2 U_1}{\partial z^2}$$
$$2U_1 = \frac{\partial^2 V_1}{\partial z^2}$$
$$\frac{\dot{P}_1(z)}{3} + \frac{\partial^2 W_1}{\partial z^2} = 0$$
$$-2U_1 + \dot{W}_1 = 0$$

$O(Ro^2)$:

$$(-4U_0U_1 - 2V_0V_1 + W_1\frac{\partial U_0}{\partial z}) - 2V_2 = -(P_{II} + \mu P_1(z)) + \frac{\partial^2 U_2}{\partial z^2} + 8\mu U_1$$
$$(-2U_0V_1 + W_1\frac{\partial V_0}{\partial z}) + 2U_2 = \frac{\partial^2 V_2}{\partial z^2} + 8\mu V_1$$
$$-4(U_0W_1) = \frac{\dot{P}_2(z)}{5} + \frac{\partial^2 W_2}{\partial z^2} + 16\mu W_1$$
$$-4U_2 + \dot{W}_2 = 0$$

A few words concerning the solution of these equations are in order, especially with regards to the decomposition of the pressure and the role of the constants $P_0, P_I, P_{II}, \ldots$ A solution to these equations which transports a given radial flux is sought. At $O(1)$ the constant P_0 is chosen to meet the radial flux requirement. The first two equations at $O(Ro)$ are used to solve for U_1 and V_1 and the value of P_I is picked to maintain the net radial flux. Continuity determines W_1 , and then $P_1(z)$ is easily obtained by integrating the third equation. Similarly at $O(Ro^2)$ the first two equations determine U_2 and V_2 and the constant P_{II} is chosen to meet the flux requirement. It should be clear that by adding a multiple of the homogeneous solution to the forced equations the flux condition can be met.

For the case of narrow-gap Ekman flow $U(0) = U(H) = V(0) = V(H) = 0$ and the $O(1)$ solution is

$$U_0(z) = -\frac{P_0}{2}A^{-1}(\exp^{(z-H)}\sin z + \exp^{-z}\sin{(H-z)} - \exp^{(H-z)}\sin z - \exp^{z}\sin{(H-z)}) \quad (9)$$

$$V_0(z) = \frac{P_0}{2} - \frac{P_0}{2}A^{-1}(\exp^{(z-H)}\cos z + \exp^{-z}\cos{(H-z)} + \exp^{(H-z)}\cos z + \exp^{z}\cos{(H-z)}) \quad (10)$$

with $A = (\exp^{-H}(1+\exp^{H}\cos H) + \exp^{H}(1+\exp^{-H}\cos H))$. The flux requirement that $\int_0^H U(z)dz = -1$ determines $P_0 = 2A/(\exp^{-H} - \exp^{H} + 2\sin(H))$.

If the upper boundary is taken to be infinity and a stess free boundary condition, $U(\infty) = \dot{V}(\infty) = 0$, is applied then the $O(1)$ flow is the Ekman boundary layer, $U_0(z) = \frac{P_0}{2}(\exp^{-z}\sin z)$ and $V_0(z) = \frac{P_0}{2}(1 - \exp^{-z}\cos z)$. In this case the O(Ro) correction term is

$$U_1(z) = \frac{P_I}{P_0}U_0 + \frac{P_0^2}{4}(\exp^{-z}(\frac{1}{2}z\sin z - \frac{1}{2}z\cos z - \frac{2}{5}\sin z + \frac{1}{5}\cos z) - \frac{1}{5}\exp^{-2z})$$

$$V_1(z) = \frac{P_I}{P_0}V_0 + \frac{P_0^2}{4}(\exp^{-z}(\frac{1}{2}z\sin z + \frac{1}{2}z\cos z - \frac{1}{5}\sin z + \frac{3}{5}\cos z) - \frac{1}{10}\exp^{-2z} - \frac{1}{2})$$

The flux requirement that $\int_0^\infty U(z)dz = -\frac{1}{2}$ then fixes $P_0 = -2$ and $P_I = -\frac{1}{5}$.

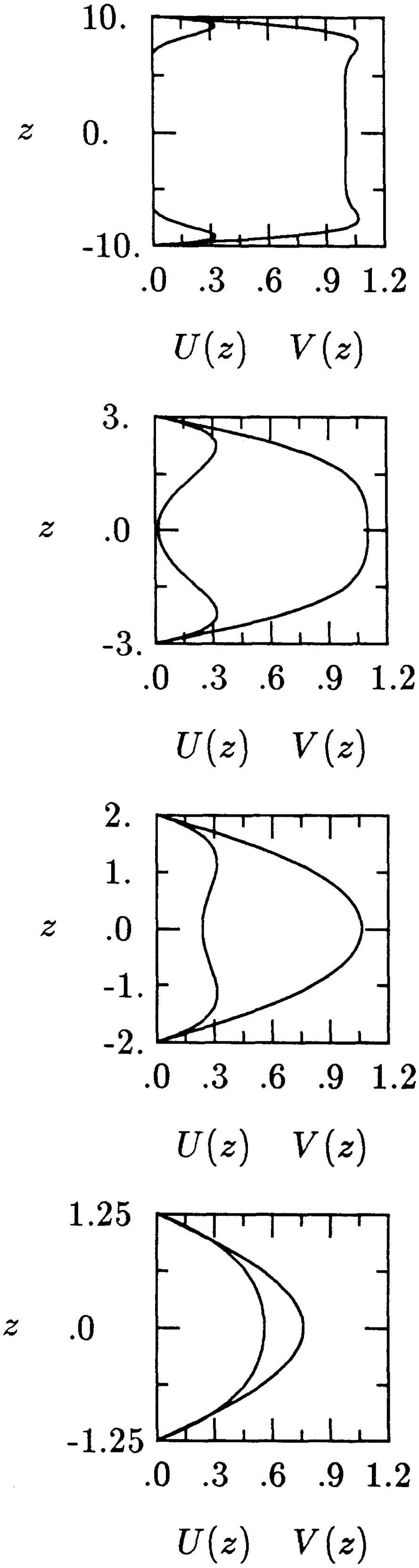

Figure 1: Radial and Azimuthal Velocities

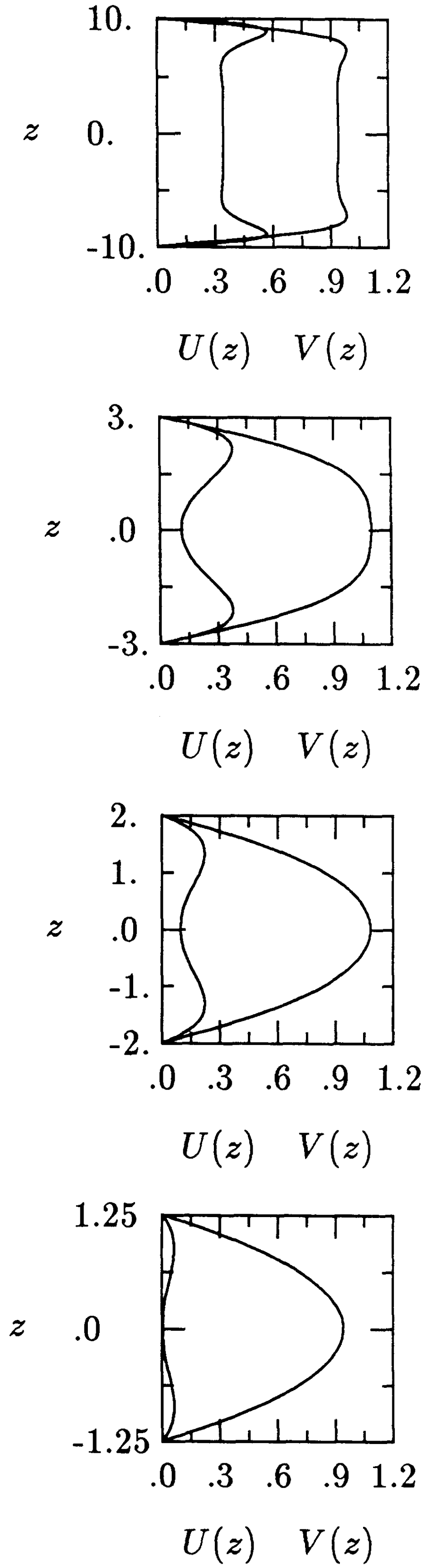

Figure 2: Rotated Velocity Profiles

Chapter 2. Linear Theory of Narrow Gap Ekman Flow

In this chapter the linear stability characteristics of narrow gap Ekman flow are examined in the small Rossby number limit. A brief outline is first given. At large enough gap sizes the flow is best thought of as two uncoupled Ekman boundary layers separated by an interior geostrophic flow. The stability characteristics of this then reduce immediately to what was given in D.K. Lilly, J.A.S. 1966 (see H.P.Greenspan for a concise review). As the gap width is decreased waves that can be justly thought to propagate along either top or bottom surface (i.e. mathematically the sum and/or difference of a symmetric/antisymmetric pair of modes) begin to interact. The gap distance at which coupling becomes significant is properly a function of the wavelength, (the linear eigenfuction decays exponentially as the wavenumber in the vertical direction) and for the wavelength of fastest growth is approximately of 15 boundary layer thicknesses. It will be shown in a later chapter, that a reasonable model for this is given by two coupled Shrödinger equations. Further reducing the gap size increases the intensity of the interaction. Not surprisingly the critical Reynolds number for the symmetric mode is decreased while the critical Reynolds number for the antisymmetric mode is increased. A minimum critical Reynolds number is reached for gap size nearly six boundary layer distances wide. With gaps smaller than about eight boundary layer widths separation it is no longer appropriate to consider the disturbance as two interacting waves and a look at the perturbation streamlines indicates that the two vorticity centers have merged. Physically however the instability still has its energy source in the two inflectional points of the velocity profile perpendicular to the roll axis. Further decreasing the gap size greatly reduces the mean shear associated with the inflectional velocity profile. This results in the critical Reynolds number shooting up fast. In fact for gaps of less than one boundary layer thickness a new linear instability, namely that associated with the nearly Poiseuille velocity component, occurs. Not only is this instability subcritical but there are finite amplitude effects such as bursts which will dominate the stability of the flow at lower Reynolds numbers and thus larger gaps. This must be taken to account with gaps less than about two boundary layers across.

The stability analysis herein treats narrow-gap Ekman flow in terms of a parallel shear flow model. The local velocity profiles are used in the Orr-Sommerfeld/Vertical Vorticity equations which are coupled through rotational terms. The validity of this approach requires that certain assumptions be met and while these conditions are not very restrictive it is best to be clear as to the approximations that are made. In the previous chapter the narrow-gap velocity profiles were determined as a power series in the Rossby number. The leading term is the solution at infinity, i.e. it is approached far enough from the center of the rotating disks. It would be a solution for the problem of a pressure induced flow between uniformly rotating infinite parallel plates. In this idealization the parallel flow stability computation is exact. Recall however that the narrow-gap Ekman profiles are dependent on the radial distance from the disks center. The magnitude of the basic velocity profiles vary inversely as the radial distance and are additionally altered in shape, a modification whose magnitude depends on the inverse of the radial distance squared. Then in terms of dimensionless parameters, the Reynolds number increases inversely as the radial distance while the Rossby number increases inversely as the radial distance squared.

A stability calculation that treats the local velocity profiles as though they were uniformly extended throughout space is approximate on the grounds that it neglects the change of the mean with position and thus requires that the flow change slowly. By 'slow' it is meant that the change in the velocity field is small over distances of the order of several disturbance wavelengths. Since the major interest concerns the small Rossby number region, all the restrictions are satisfied at large distances from the origin. These conditions are experimentally achieved by working with a large enough disk and focusing attention near the outer boundary. (For small gaps the Rossby number correction may alter the small inflectional velocity component and Rossby effects should be included.)

For viscous flow in a rotating boundary layer in which the fluid is incompressible with constant density, the equations of motion are given by

$$\frac{d\vec{V}}{dt} = -\nabla\frac{p}{\rho} - 2\,\vec{\Omega}\times\vec{V} + \nu\nabla^2\,\vec{V} \tag{1}$$

$$\nabla\cdot\vec{V} = 0 \tag{2}$$

Equation [2.1] is the 'Navier-Stokes' equation for the momentum of the fluid when viewed in the non-inertial frame of reference in which the observer moves with the constant angular velocity $\hat{k}\Omega$ of the physical system. Thus the left hand term represents the acceleration of the fluid which is balanced by (respectively) a pressure gradient, the Coriolis force, and the viscous dissipation. The density, ρ, is also assumed to be a constant however it should be clear that an additional set of equations relating temperature with density stratification could be included to make the analysis that follows more generally applicable to atmospheric circulation (c.f. Brown). These equations are the starting point of this paper. The following convention should be mentioned. The centrifugal force $\vec{\Omega}\times(\vec{\Omega}\times\vec{r}) = -\nabla\left(\frac{\Omega r^2}{2}\right)$ is in balance with the radial pressure gradient and the gravitational force (which is also conservative) is balanced by the hydrostatic pressure so they have been combined with p in (1) so that p is actually the reduced pressure. As a matter of convention and in keeping with Lilly's notation we consider a rotation of the coordinate axes through an angle ϵ, counterclockwise, bringing the y-axis into alignment with the direction of wave propagation. Surfaces of constant phase then lie parallel with the x-axis so that derivatives of the perturbed quantities vanish along this direction, i.e. $\frac{\partial u_i'}{\partial x'} = 0$. Under this transformation;

$$\begin{pmatrix} x' \\ y' \end{pmatrix} = \begin{pmatrix} \cos\epsilon & \sin\epsilon \\ -\sin\epsilon & \cos\epsilon \end{pmatrix} \begin{pmatrix} x \\ y \end{pmatrix}$$

The Ekman boundary layer profiles then become $U_E = (\cos\epsilon - e^{-z}\cos(z+\epsilon))$ and $V_E = (-\sin\epsilon + e^{-z}\sin(z+\epsilon))$. Both $\vec{V}$ and $\vec{V}_E$ satisfy (1)-(2). Subtracting

$$\vec{V}_E \cdot\nabla \vec{V}_E + \nabla\frac{p_E}{\rho} + 2\Omega\hat{k}\times \vec{V}_E = \nu\nabla^2 \vec{V}_E \tag{3}$$

$$\nabla\cdot \vec{V}_E = 0 \tag{4}$$

from (1)-(2) with $\vec{V} = \vec{V}_E + \vec{v}^*$ yields,

$$\frac{\partial \vec{v}^*}{\partial t} + \vec{V}_E \cdot\nabla \vec{v}^* + \vec{v}^* \cdot\nabla \vec{V}_E + \vec{v}^* \cdot\nabla \vec{v}^* +$$

$$\nabla\frac{p^*}{\rho} + 2\Omega\hat{k}\times \vec{v}^* = \nu\nabla^2 \vec{v}^* \tag{5}$$

$$\nabla\cdot \vec{v}^* = 0 \tag{6}$$

The linear theory is obtained by ignoring products of perturbed quantities. In component form, with the Reynolds number $R = \frac{VD}{\nu}$, this reduces to

$$\frac{\partial u^*}{\partial t} + V_E\frac{\partial u^*}{\partial y} + w^*\frac{\partial U_E}{\partial z} = \qquad + \frac{2}{R}v^* + \frac{1}{R}\left(\frac{\partial^2 u^*}{\partial y^2} + \frac{\partial^2 u^*}{\partial z^2}\right) \tag{7}$$

$$\frac{\partial v^*}{\partial t} + V_E\frac{\partial v^*}{\partial y} + w^*\frac{\partial V_E}{\partial z} = -\frac{\partial p^*}{\partial y} - \frac{2}{R}u^* + \frac{1}{R}\left(\frac{\partial^2 v^*}{\partial y^2} + \frac{\partial^2 v^*}{\partial z^2}\right) \tag{8}$$

$$\frac{\partial w^*}{\partial t} + V_E\frac{\partial w^*}{\partial y} \qquad = -\frac{\partial p^*}{\partial z} \qquad + \frac{1}{R}\left(\frac{\partial^2 w^*}{\partial y^2} + \frac{\partial^2 w^*}{\partial z^2}\right) \tag{9}$$

$$\frac{\partial v^*}{\partial y} + \frac{\partial w^*}{\partial z} = 0 \tag{10}$$

with the perturbation boundary conditions, $u^* = v^* = w^* = 0$ at $z = \pm H$ for the finite gap problem. For the semi-infinite problem the perturbation velocities vanish $u^* = v^* = w^* = 0$ at $z = 0$ and a zero stress condition is applied at infinity so $\frac{\partial u^*}{\partial z} = \frac{\partial v^*}{\partial z} = w^* = 0$ at $z = \infty$.

The two dimensional incompressibility condition allows for the introduction of a streamfunction potential for which

$$v^* = -\frac{\partial \psi^*}{\partial z} \qquad w^* = \frac{\partial \psi^*}{\partial y} \tag{11}$$

A vorticity equation is formed by cross differentiating (5-6), and with $\xi^* = (\frac{\partial w}{\partial y}^* - \frac{\partial v}{\partial z}^*)$ the perturbation equations take the form:

$$\frac{\partial \xi^*}{\partial t} + V_E \frac{\partial \xi^*}{\partial y} - w^* \frac{d^2 V_E}{dz^2} = \frac{2}{R}\frac{\partial u^*}{\partial z} + \frac{1}{R}(\frac{\partial^2 \xi^*}{\partial y^2} + \frac{\partial^2 \xi^*}{\partial z^2}) \tag{12}$$

$$\frac{\partial u^*}{\partial t} + V_E \frac{\partial u^*}{\partial y} - w^* \frac{dU_E}{dz} = \frac{2}{R}v^* + \frac{1}{R}(\frac{\partial^2 u^*}{\partial y^2} + \frac{\partial^2 u^*}{\partial z^2}) \tag{13}$$

A linear eigenproblem is obtained by the substitution of the normal modes $\psi^* = \varphi(z)e^{i\alpha(y-ct)}$, $u^* = \mu(z)e^{i\alpha(y-ct)}$ which represent vorticity waves traveling along the y-axis in the form of longitudinal rolls. Note that the presence of a mean velocity along the roll axis gives the perturbation a 'helical' (streamwise) component. Here α is the wave number and $c = c_r + ic_i$ is the complex phase speed. This results in the following boundary value problem:

$$\overbrace{\varphi^{iv} - 2\alpha^2\ddot{\varphi} + \alpha^4 - i\alpha R[(V_E - c)(\ddot{\varphi} - \alpha^2\varphi) - \ddot{V}_E\varphi]}^{\mathcal{OS}} + 2\dot{\mu} = 0 \tag{14}$$

$$\underbrace{\ddot{\mu} - \alpha^2\mu - i\alpha R[(V_E - c)\mu + \dot{U}_E\varphi]}_{\mathcal{LV}} - 2\dot{\varphi} = 0 \tag{15}$$

The boundary conditions become $\varphi = \dot{\varphi} = \mu = 0$ at $z = \pm H$ for the narrow-gap case. For the semi-infinite Ekman layer the boundary conditions are $\varphi = \dot{\varphi} = \mu = 0$ at $z = 0$ and $\dot{\varphi} = \ddot{\varphi} = \dot{\mu} = 0$ at $z = \infty$, where '$\cdot$' signifies $\frac{d}{dz}$.

This is an appropriate place to mention some of the more basic properties of the stability equations. For a unidirectional parallel shear flow without rotation the linear stability analysis leads to the Orr-Sommerfeld ($\mathcal{OS}$) equation for the streamfunction, (that portion of Equation (14) which is overbraced). The theorem of Squire states that a minimum critical Reynolds number is obtained for two dimensional waves propagating in the direction of the flow. Moreover it provides a transformation from the linear three-dimensional stability problem at a higher Reynolds number to an equivalent two-dimensional stability problem at a lower Reynolds number with an identical spectrum. For three dimensional waves, that is waves whose phase varies along both coordinate axes, still without rotation, a complimentary equation for the longitudinal velocity (the underbraced portion of equation (15)) needs to be included. However it can be shown that the homogeneous operator of the longitudinal velocity ($\mathcal{L}\mathcal{V}$) equation has no unstable modes, and thus the Orr-Sommerfeld equation can first be solved and then used to determine the forced response of the longitudinal velocity. Note that the forced response of the longitudinal velocity increases proportionally with the Reynolds number. There are modes of the longitudinal velocity equation which are only weakly damped which allows for the possibility of 'direct resonance' with modes of the Orr-Sommerfeld equation should two or more eigenvalues of these operators be equal or nearly so (see D.J. Benney & L.H. Gustavson or T. Akylas and Benney). For a one wave system an equivalent set of independent variables are the vertical velocity and vertical vorticity, which are just scalar multiples of the streamfunction and longitudinal velocity. But the formulation in terms of vertical vorticity also carries over to more general systems of waves for which there is no preferred coordinate system which permits a streamfunction. In the presence of uniform rotation the Orr-Sommerfeld equation and longitudinal velocity equation are weakly, $O(\frac{1}{R})$, coupled. (the important term is $2\dot{\mu}$ in Equation (14), while the term $-2\dot{\varphi}$ in Equation (15) is only of minor significance). In Ekman flow the rotational coupling allows energy to be efficiently supplied from the shear of the velocity component, $U_E(z)$, that is parallel with the disturbance vorticity. This initiates a low Reynolds number, Type II, instability that otherwise cound not be obtained. While the source of the instability remains the mean inflectional velocity profile, $V_E(z)$, the induced helical velocity component redirects the roll alignment and selects the wavenumber so as to better utilize the power provided through the correlation $u^{2d}(w^{2d})^*(dU_E/dz)$.

For each value of R, α, ϵ, (14-15) is an eigenproblem for the phase speed c. The locus of points in (R, α, ϵ) space for which an eigenvalue c has a positive imaginary part constitutes a region of linear instability, while the locus of points in (R, α, ϵ) space in which no eigenvalues have non-negative imaginary part constitutes the region of linear stability which (providing the eigenfuctions form a complete set) indicates that the flow is stable to all infinitesimal periodic waves. These regions are separated by the 'neutral surface' on which c has zero imaginary part. This is illustrated in figure 2.6 (a-d) taken from D.K. Lilly.

The number of potentially realizable linear instabilities present in the system will be equal to the number of local positive maxima in the growth rate function(s) $(\alpha c_i)(\epsilon, \alpha)$. At such points $\frac{\partial}{\partial \epsilon}(\alpha c_i) = \frac{\partial}{\partial \alpha}(\alpha c_i) = 0$. Each maximum traces a branch of the curve of greatest growth rate when parametrized by the Reynold number. Intersection of each branch with the neutral surface occurs at critical points $(R, \alpha, \epsilon)_{cr}$ corresponding to the onset of an observable instability.

For Ekman flow (semi-infinite gap) the Type II or 'parallel' instability occurs first at a Reynolds number of 55, a wavenumber of .3, and with the phase velocity .6, oriented -22 degrees counterclockwise from the geostrophic direction. The Type I or inviscid instability has a critical Reynolds number of 115, and a corresponding wavenumber of .5, and nearly stationary phase speed of .06, directed 8 degrees counterclockwise from the geostrophic flow. By varying the wavenumber and wave orientation the eigenvalue and eigenmode of a Type I and Type II instability can be continuously transformed into each other.

In viewing the eignenfunctions of narrow gap Ekman flow, an important characteristic to keep in mind is the ratio of the maximum magnitudes of the streamfuction to streamwise velocity.

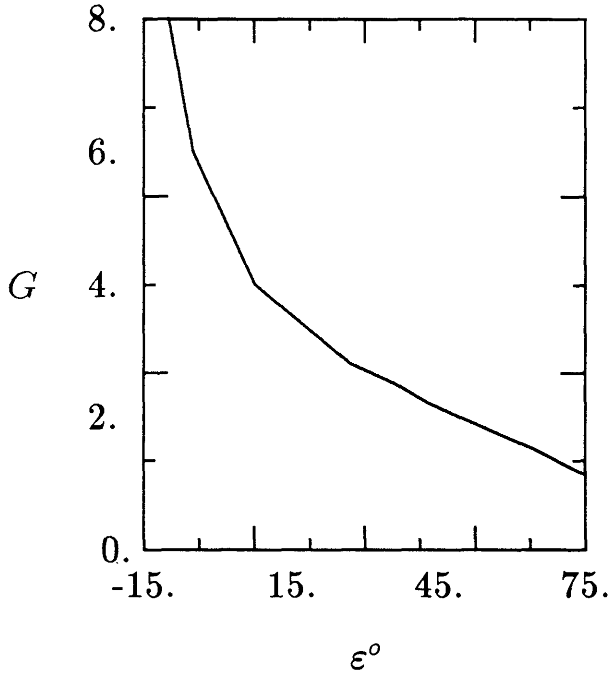

Figure 1: Gap size vs. Critical Wave Angle

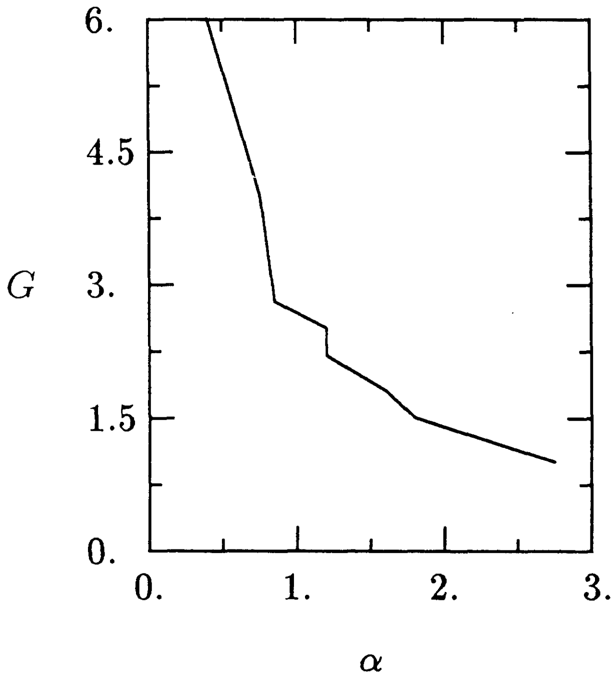

Figure 2: Gap size vs. Critical Wave No.

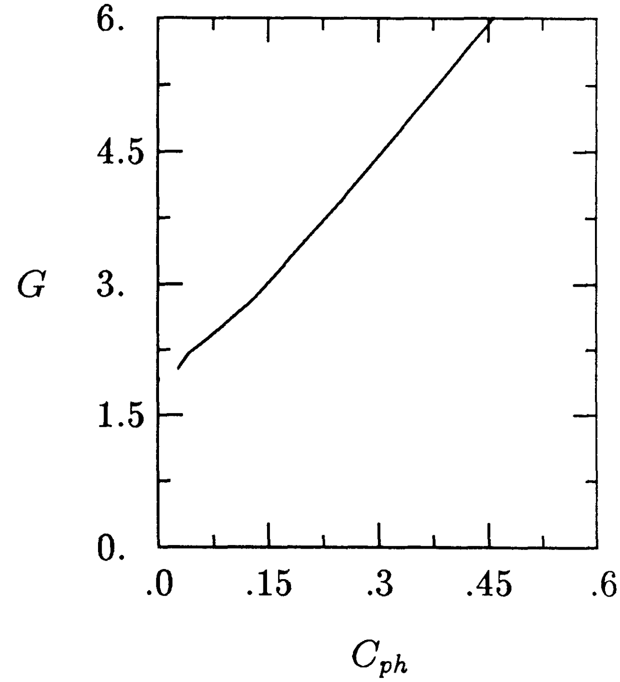

Figure 3: Gap size vs. Critical Wave Speed

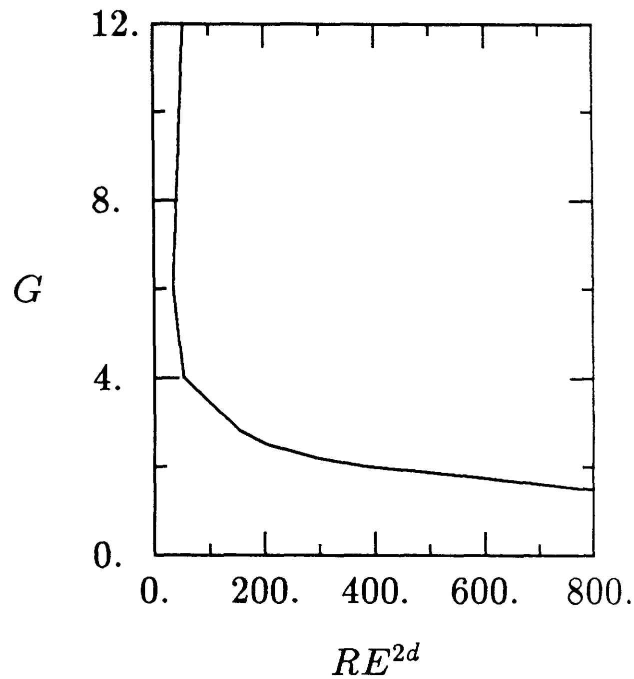

Figure 4: Gap size vs. Critical Reynolds No.

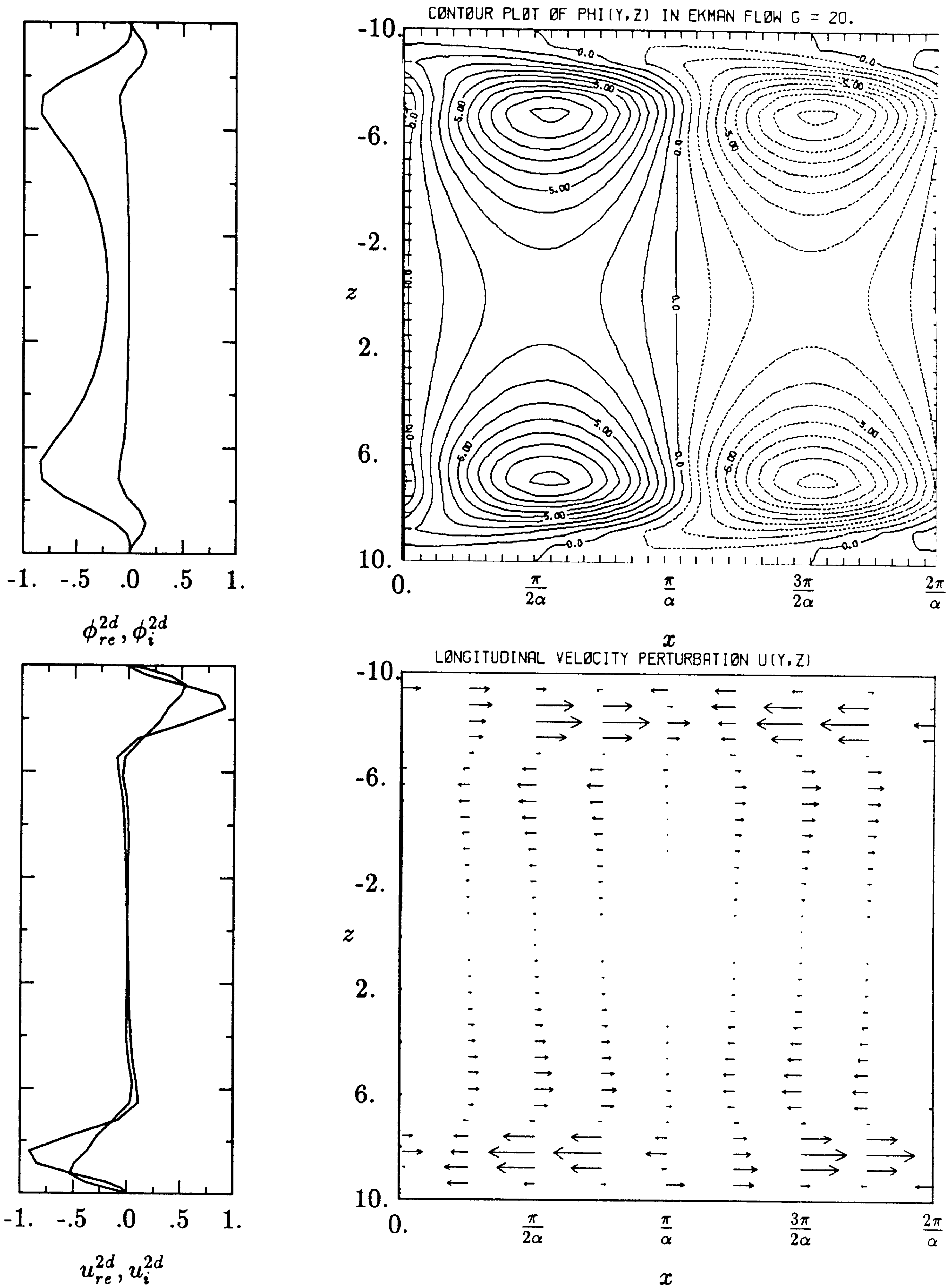

CØNTØUR PLØT ØF PHI(Y,Z) IN EKMAN FLØW G = 20.
LØNGITUDINAL VELØCITY PERTURBATIØN U(Y,Z)
-10.
-6.
-2.
z
2.
6.
10.
0.
π/2α
π/α
3π/2α
2π/α
x
-1.
-.5
.0
.5
1.
$\phi_{re}^{2d}, \phi_i^{2d}$
u_{re}^{2d}, u_i^{2d}
0.0
5.00

This is the most complete text of the thesis available. The following page(s) were not included in the copy of the thesis deposited in the Institute Archives by the author:

Pg 24

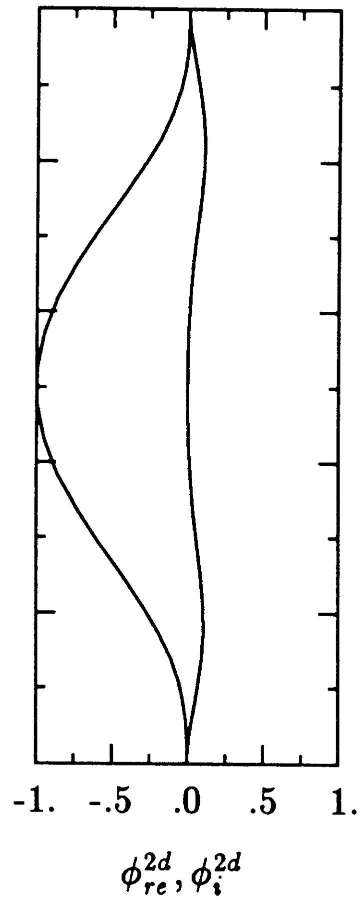
-1.
-.5
.0
.5
1.
$\phi_{re}^{2d}, \phi_{i}^{2d}$

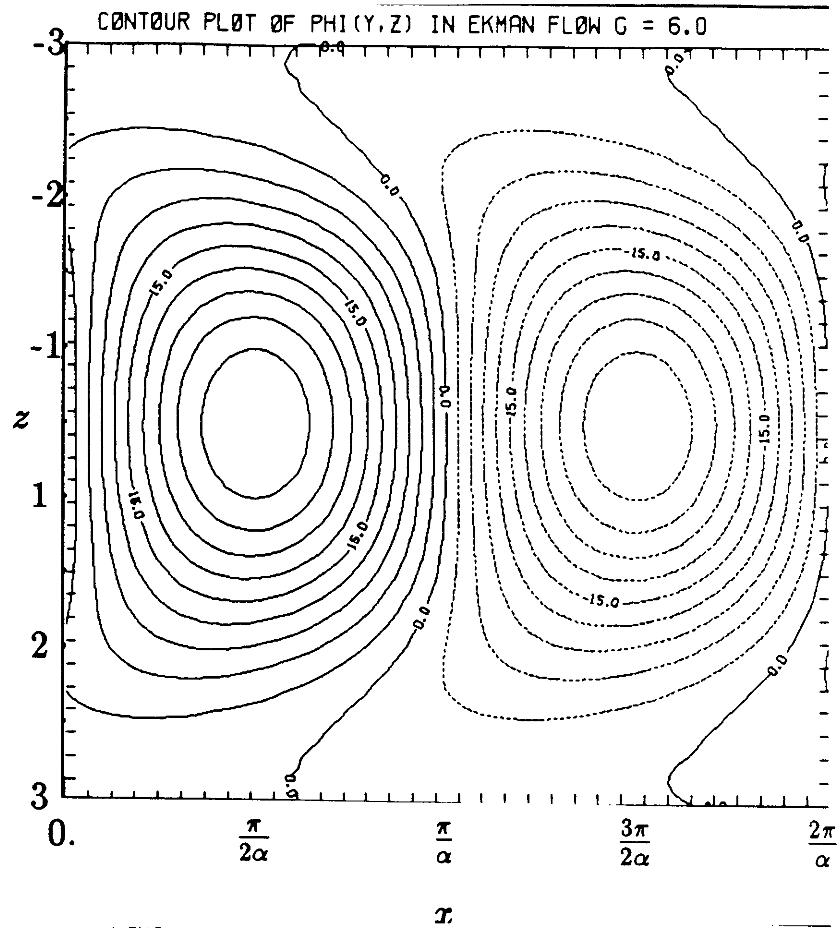
CØNTØUR PLØT ØF PHI(Y,Z) IN EKMAN FLØW G = 6.0
-3
-2
-1
z
1
2
3
0.
$\frac{\pi}{2\alpha}$
$\frac{\pi}{\alpha}$
$\frac{3\pi}{2\alpha}$
$\frac{2\pi}{\alpha}$
x
0.0
15.0
-15.0

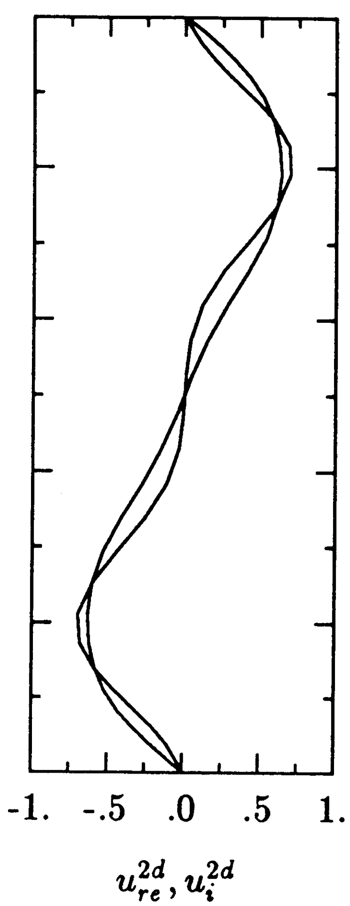
-1.
-.5
.0
.5
1.
u_{re}^{2d}, u_{i}^{2d}

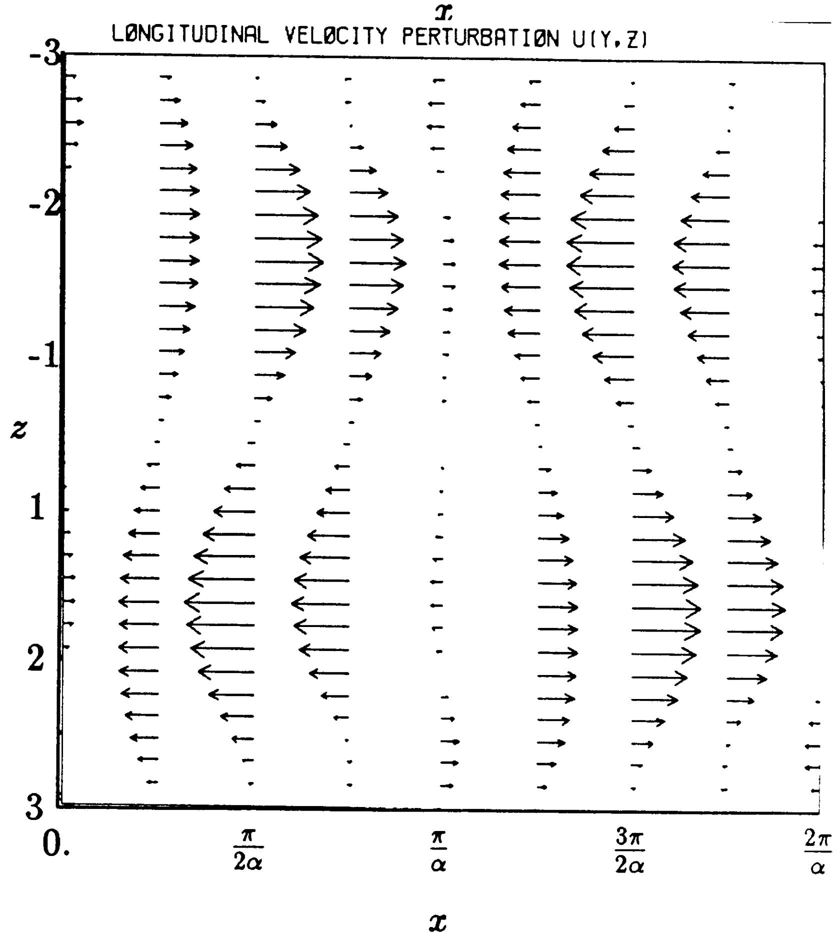
LØNGITUDINAL VELØCITY PERTURBATIØN U(Y,Z)
-3
-2
-1
z
1
2
3
0.
$\frac{\pi}{2\alpha}$
$\frac{\pi}{\alpha}$
$\frac{3\pi}{2\alpha}$
$\frac{2\pi}{\alpha}$
x

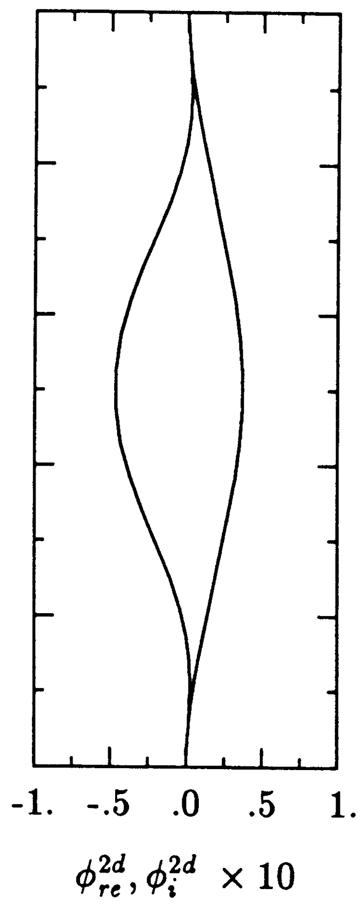
-1. -.5 .0 .5 1.
$\phi_{re}^{2d}, \phi_i^{2d} \times 10$

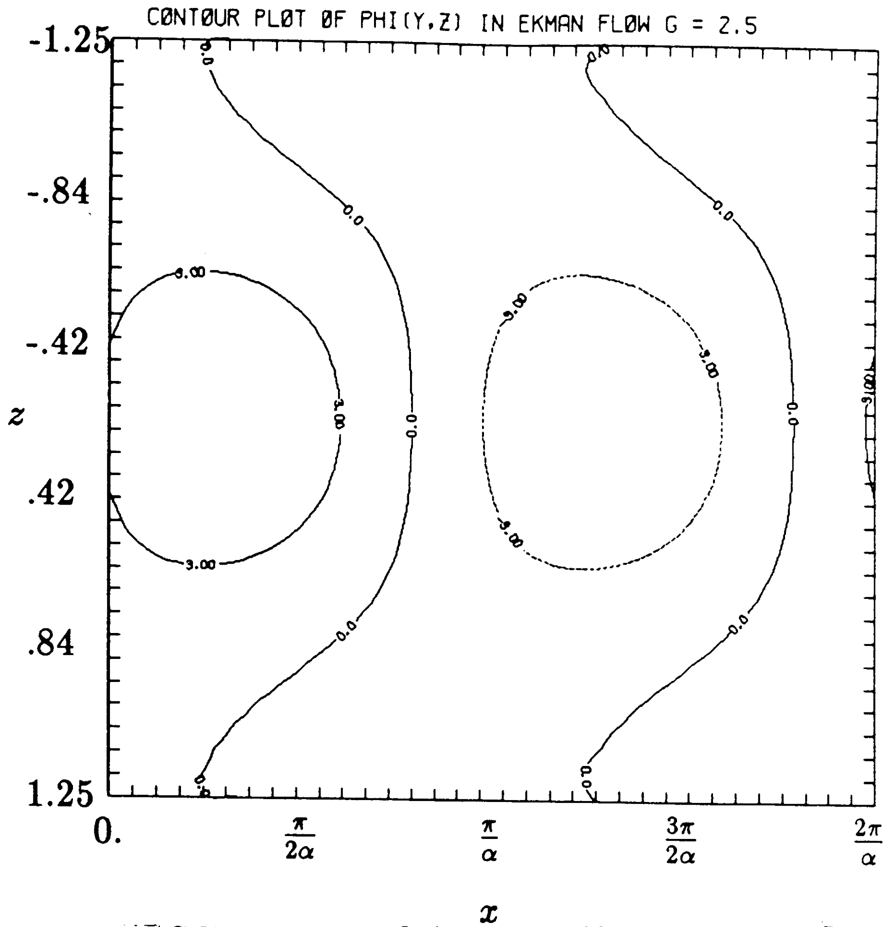
CØNTØUR PLØT ØF PHI(Y,Z) IN EKMAN FLØW G = 2.5
-1.25
-.84
-.42
z
.42
.84
1.25
0.
$\frac{\pi}{2\alpha}$
$\frac{\pi}{\alpha}$
$\frac{3\pi}{2\alpha}$
$\frac{2\pi}{\alpha}$
x

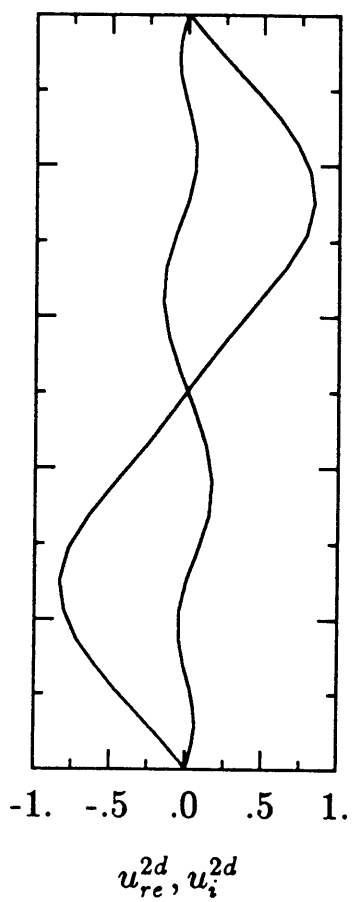
-1. -.5 .0 .5 1.
u_{re}^{2d}, u_i^{2d}

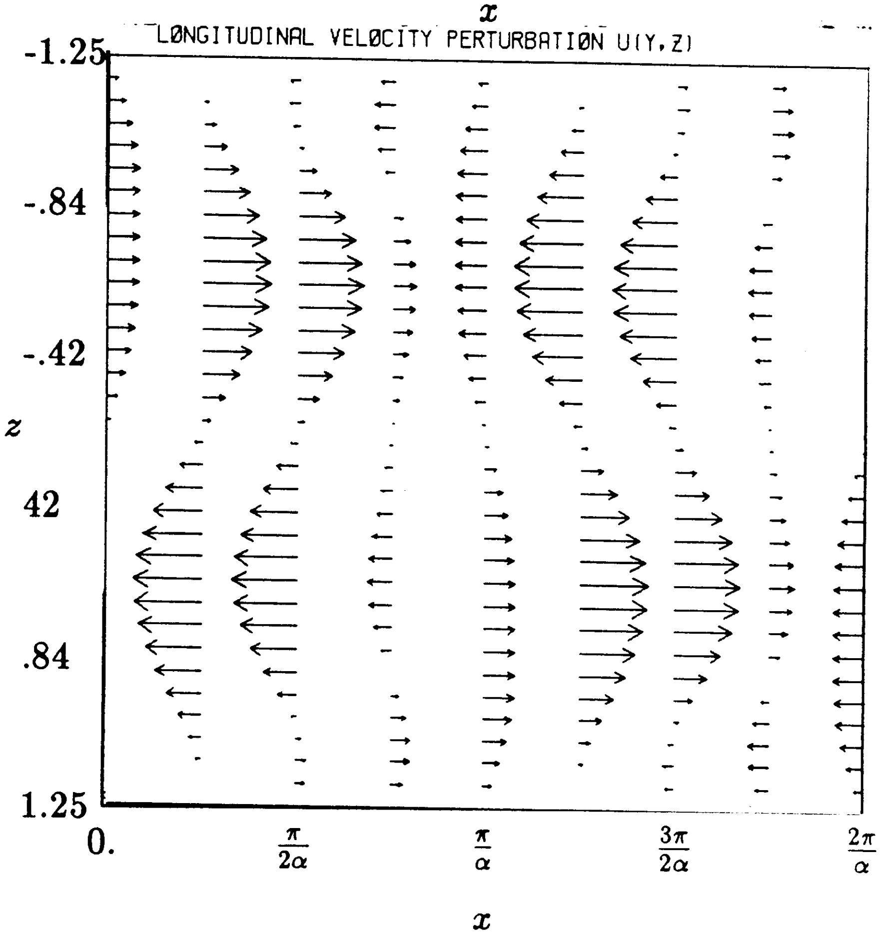
LØNGITUDINAL VELØCITY PERTURBATIØN U(Y,Z)
-1.25
-.84
-.42
z
42
.84
1.25
0.
$\frac{\pi}{2\alpha}$
$\frac{\pi}{\alpha}$
$\frac{3\pi}{2\alpha}$
$\frac{2\pi}{\alpha}$
x

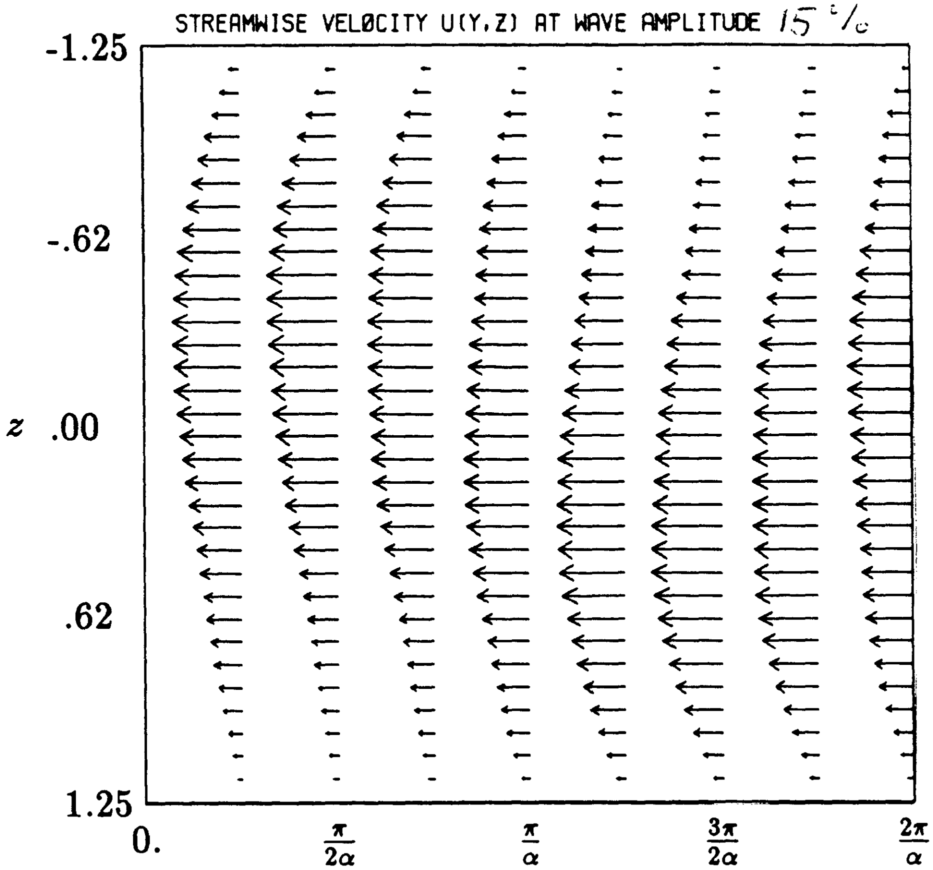
STREAMWISE VELØCITY U(Y,Z) AT WAVE AMPLITUDE 15 %
-1.25
-.62
z .00
.62
1.25
0.
π/2α
π/α
3π/2α
2π/α

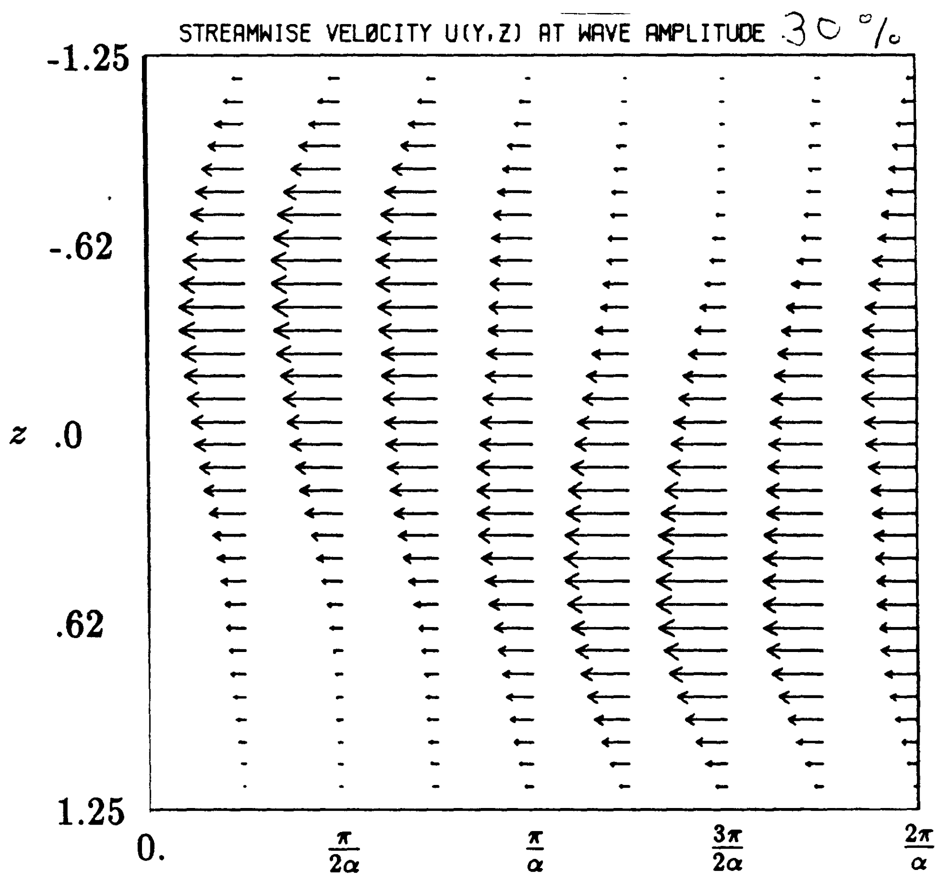
STREAMWISE VELØCITY U(Y,Z) AT WAVE AMPLITUDE 30 %
-1.25
-.62
z .0
.62
1.25
0.
π/2α
π/α
3π/2α
2π/α

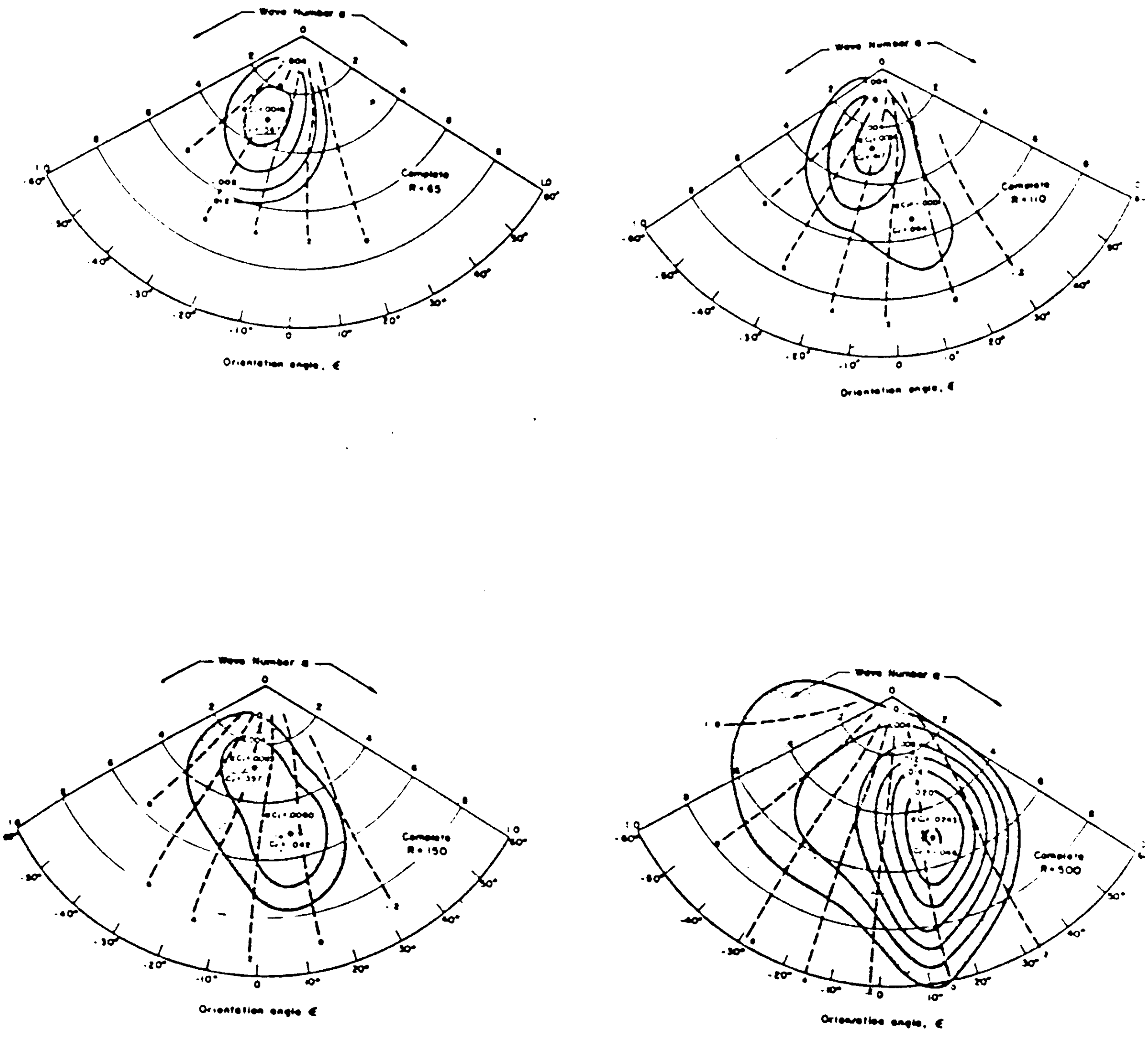

Figure 2-1 (FROM LILLY)

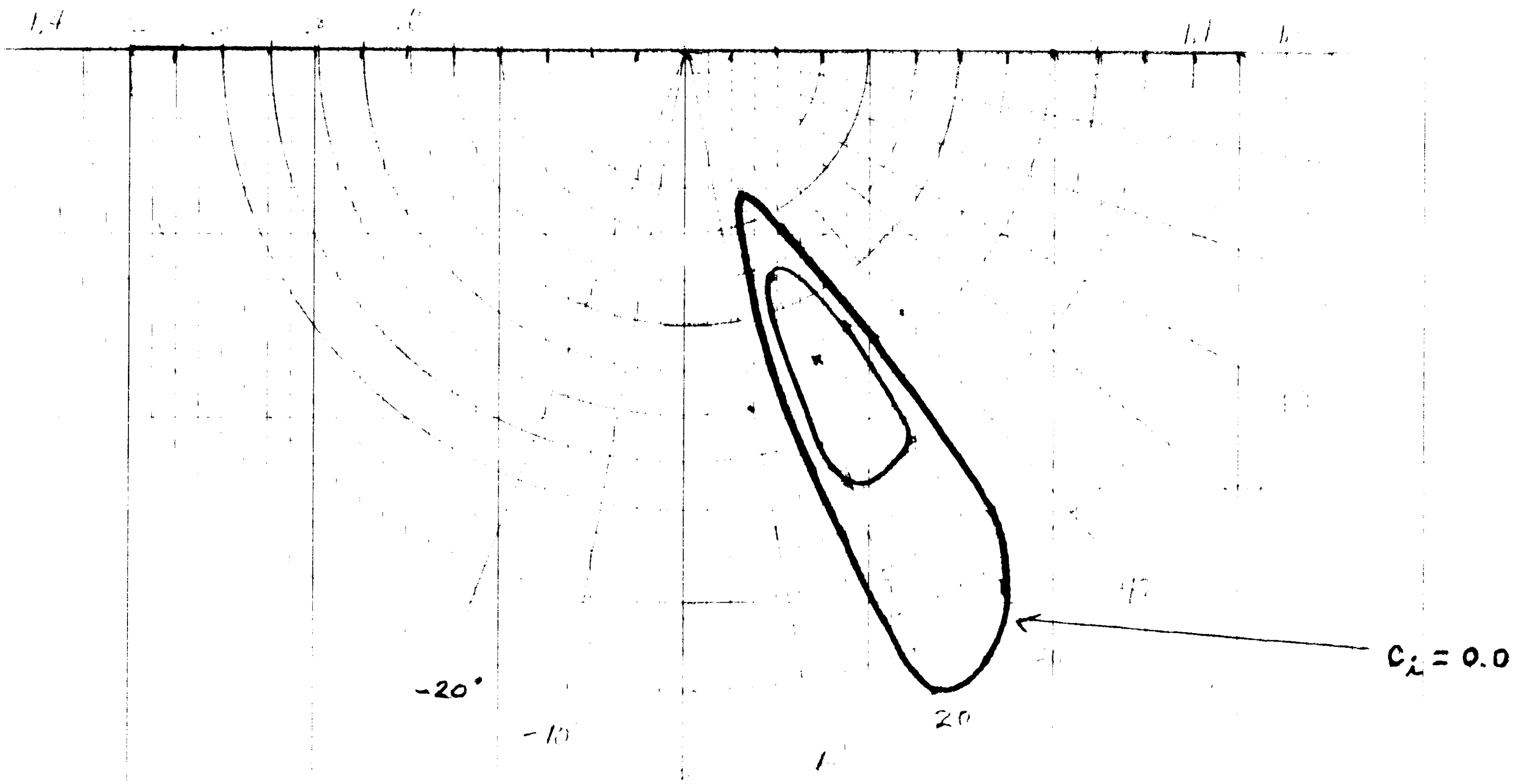

Stability diagram for N.G. Ekman Flow

Gap size = 3.0

Rosby # = 0.0

Reynolds # = 200.

x most unstable mode: $\epsilon \doteq 22^\circ$

$C_{max} = (.150 + .007i)$, $\alpha \doteq .75$

Chapter 3. Parametric Expansions of Equilibrated Flow

The finite amplitude parametric scheme of Malkus and Veronis is applied to determine the criticality of incompressible parallel shear flows with arbitrary velocity profiles (U(z),V(z),0). The foremost examples for this study are Poiseuille flow and narrow gap Ekman flow, however the analysis applies directly to a wide class of other laminar flows. Some of the more prominent of which are the Blasius boundary layer, flow over sweptback wings, Oceanic boundary layers, and flow over rotating disks. The laminar velocity profiles over rotating disks (Kaufman et al., J.F.M. 1983) are in fact very similar to those of the Ekman boundary layer.

Of the various perturbation schemes, the Malkus and Veronis expansion (J.F.M. 1958) is the most efficient in determining the finite amplitude equilibrium near criticality. Here the Reynolds number and phase speed are parametrized by the equilibrium amplitude ϵ. (ϵ is strictly defined as the magnitude of the projection of the wave on the linear eigenfunction). Then

$$R = R_0 + R_1\epsilon^2 + R_2\epsilon^4 + \dots \tag{1}$$

$$c = c_0 + c_1\epsilon^2 + c_2\epsilon^4 + \dots \tag{2}$$

where the constants R_i and c_i are determined by solvability conditions. The analytical structure of the equilibrium curve at the critical Reynolds number is obtained with one set of calculations. Note that because the plan form is simply a plane wave (as opposed to cells of hexagons or squares which occur in the study of convection) the self-interaction does not result in a solvability condition and the parametric series depends only on the square of the amplitude. With $l_n = n(\alpha^2+\beta^2)^{\frac{1}{2}}$, the underlying finite amplitude wave has the fourier representation

$$\sum_{n=1}^{\infty}[\phi_n \exp^{(in\alpha x+in\beta y-il_n ct)} + (*)]$$

This representation is then substituted into the Navier-Stokes equations where the eigenfunctions $\phi_i = (w_i, \eta_i)$ are further expanded as:

$$\phi_1(z,R) = \epsilon\phi_{10}(z) + \epsilon^3\phi_{11}(z) + \epsilon^5\phi_{12}(z) + \dots \tag{3}$$

$$\phi_2(z,R) = \epsilon^2\phi_{20}(z) + \epsilon^4\phi_{11}(z) + \epsilon^6\phi_{22}(z) + \dots \tag{4}$$

$$\dots$$

$$\phi_k(z,R) = \epsilon^k\phi_{k,0}(z) + \epsilon^{k+2}\phi_{k,1}(z) + \epsilon^{k+4}\phi_{k,2}(z) + \dots \tag{5}$$

The linear operator is a function of R, c, and the mean flow and so it to is developed in powers of ϵ^2.

$$\mathcal{L}_R = \mathcal{L}_0 + \epsilon^2\mathcal{L}_1 + \epsilon^4\mathcal{L}_2 + \dots \tag{6}$$

We have adopted the following notation. Let $\vec{V}$ be the velocity profile $(U, V, 0)$ and $\vec{\alpha}$ be the wave number vector (α, β). Then define

$$\mathcal{L}_R[\vec{V}, \vec{\alpha}] =$$

$$\begin{pmatrix} (D^2-(\alpha^2+\beta^2))^2 - R(i\alpha U + i\beta V - ilc)(D^2-(\alpha^2+\beta^2)) + R(i\alpha D^2U + i\beta D^2V) & -2D \\ R(i\beta DU - i\alpha DV) + 2D & (D^2-(\alpha^2+\beta^2)) - R(i\alpha U + i\beta V - ilc) \end{pmatrix}$$

$$\mathcal{L}_0[\vec{V}, \vec{\alpha}] =$$

$$\begin{pmatrix} (D^2-(\alpha^2+\beta^2))^2 - R_0(i\alpha U_0 + i\beta V_0 - ilc_0)(D^2-(\alpha^2+\beta^2)) + R_0(i\alpha D^2U_0 + i\beta D^2V_0) & -2D \\ R_0(i\beta DU_0 - i\alpha DV_0) + 2D & (D^2-(\alpha^2+\beta^2)) - R_0(i\alpha U_0 + i\beta V_0 - ilc_0) \end{pmatrix}$$

and for $n = 1, 2, 3, \ldots$

$$\mathcal{L}_n[\vec{V}, \vec{\alpha}] =$$

$$\begin{pmatrix} \sum_{k=0}^{n}[-R_k(i\alpha U_{n-k}+i\beta V_{n-k}-ilc_{n-k})(D^2-(\alpha^2+\beta^2))+R_k(i\alpha D^2U_{n-k}+i\beta D^2V_{n-k})] & 0 \\ \sum_{k=0}^{n} R_k(i\beta DU_{n-k}-i\alpha DV_{n-k}) & \sum_{k=0}^{n} -R_k(i\alpha U_{n-k}+i\beta V_{n-k}-ilc_{n-k}) \end{pmatrix}$$

The eigenproblems that arise from the preceding development are ordered first with respect to the harmonic component to which they contribute (the first subscript) and then according to the degree of the correction (the second subscript).

$O(\epsilon)$:

$$\mathcal{L}_0[\vec{V}, \vec{\alpha}]\phi_{10} = 0$$

$O(\epsilon^3)$:

$$\mathcal{L}_0[\vec{V}, \vec{\alpha}]\phi_{11} = -\mathcal{L}_1[\vec{V}, \vec{\alpha}]\phi_{10} + \langle Nonlinear\ terms\rangle$$

...

$O(\epsilon^{2n+1})$:

$$\mathcal{L}_0[\vec{V}, \vec{\alpha}]\phi_{1n} = -\sum_{k=1}^{n} \mathcal{L}_k[\vec{V}, \vec{\alpha}]\phi_{1,n-k} + \langle Nonlinear\ terms\rangle$$

$O(\epsilon^2)$:

$$\mathcal{L}_0[\vec{V}, \vec{2\alpha}]\phi_{20} = \langle Nonlinear\ terms\rangle$$

...

$O(\epsilon^{2n+2})$:

$$\mathcal{L}_0[\vec{V}, \vec{2\alpha}]\phi_{2,n} = -\sum_{k=1}^{n} \mathcal{L}_k[\vec{V}, \vec{2\alpha}]\phi_{2,n-k} + \langle Nonlinear\ terms\rangle$$

$\ldots$

$O(\epsilon^m)$:

$$\mathcal{L}_0[\vec{V}, \vec{m\alpha}]\phi_{m,0} = \langle Nonlinear\ terms \rangle$$

$\ldots$

$O(\epsilon^{2n+m})$:

$$\mathcal{L}_0[\vec{V}, \vec{m\alpha}]\phi_{m,n} = -\sum_{k=1}^{n} \mathcal{L}_k[\vec{V}, \vec{m\alpha}]\phi_{m,n-k} + \langle Nonlinear\ terms \rangle$$

The bracketed 'Nonlinear terms' is meant to indicate all nonlinear terms that occur in the particular problem. In practice they are determined by a coded algorithm without having to write them out explicitly. (Appendix 1)

The expansion for the mean flow is given by:

$$U_M = U_B + \epsilon^2 U_C = U_{00} + \epsilon^2 U_{01} + \epsilon^4 U_{02} + \ldots \tag{7}$$

$$V_M = V_B + \epsilon^2 V_C = V_{00} + \epsilon^2 V_{01} + \epsilon^4 V_{02} + \ldots \tag{8}$$

To arrive upon the equations governing the mean flow it is convenient to introduce a set of functions $\{P_i\}$ which operate on pairs of subscripted sequences. Take

$$P_0(A_1, B_1) \triangleq A_{10}B_{10}$$

$$P_1(A_1, B_1) \triangleq (A_{10}B_{11} + A_{11}B_{10})$$

$$\ldots$$

$$P_n(A_l, B_k) \triangleq \sum_{i=0}^{n} A_{l,i}B_{k,n-i}$$

For the steady mean flow,

$$R\frac{d}{dz}(\sum_{i=1}^{\infty}(u_i w_i^* + u_i^* w_i)) = 2\overline{v} + \frac{d^2\overline{u}}{dz^2}$$

$$R\frac{d}{dz}(\sum_{i=1}^{\infty}(v_i w_i^* + v_i^* w_i)) = -2\overline{u} + \frac{d^2\overline{v}}{dz^2}$$

and in the notation above:

$O(\epsilon^2)$:

$$\ddot{U}_{01} + 2V_{01} = R_0 \frac{d}{dz}(P_0(u_1, w_1^*) + (*))$$
$$\ddot{V}_{01} - 2U_{01} = R_0 \frac{d}{dz}(P_0(v_1, w_1^*) + (*))$$

...

$O(\epsilon^{2n})$:

$$\ddot{U}_{0n} + 2V_{0n} = \sum_{j=1}^{n}\sum_{i=0}^{n-j} R_i \frac{d}{dz}(P_{n-j-i}(u_j, w_j^*) + (*))$$
$$\ddot{V}_{0n} - 2U_{0n} = \sum_{j=1}^{n}\sum_{i=0}^{n-j} R_i \frac{d}{dz}(P_{n-j-i}(v_j, w_j^*) + (*))$$

We will call the (R_i, c_i) Linsted coefficients. (R_i, c_i) are found by taking the inner product of the equation for $\phi_{1,n}$ with the adjoint eigenfunction $\phi_{10}^\dagger = (w_{10}^\dagger, \eta_{10}^\dagger)$ and integrating between boundaries (the solvability conditions.) Thus

$$\int (\mathcal{L}_0[\vec{V}, \vec{\alpha}]\phi_{1,n}) \cdot \phi_{10}^{\dagger *} dz = -\sum_{i=0}^{n-1} \int (\mathcal{L}_i[\vec{V}, \vec{\alpha}]\phi_{1,n-i}) \cdot \phi_{10}^{\dagger *} dz + \int \langle Nonlinear\ terms \rangle \cdot \phi_{10}^{\dagger *} dz$$
$$= \int \phi_{1,n} \cdot (\mathcal{L}_0^\dagger[\vec{V}, \vec{\alpha}]\phi_{10}^\dagger)^* dz = 0. \tag{9}$$

Here the adjoint operator is given as:

$$\mathcal{L}^\dagger[\vec{V}, \vec{\alpha}] =$$

$$\begin{pmatrix} (D^2-(\alpha^2+\beta^2))^2 - R_0(i\alpha U_0 + i\beta V_0 - ilc_0^*)(D^2-(\alpha^2+\beta^2)) + R_0(i\alpha DU_0 + i\beta DV_0)D & (i\alpha DV_0 - i\beta DU_0) - 2D \\ +2D & (D^2-(\alpha^2+\beta^2)) + R_0(i\alpha U_0 + i\beta V_0 - ilc_0^*) \end{pmatrix}$$

Some algebraic manipulation is performed and yields the formula for (R_n, c_n), the n-th Linsted coefficient.

$$R_n\Big[\int[-(i\alpha U_0+i\beta V_0-ilc_0)(D^2-(\alpha^2+\beta^2))w_{10}\cdot w_{10}^{\dagger}+(i\beta\dot{U}_0-i\alpha\dot{V}_0)w_{10}\cdot\eta_{10}^{\dagger}-(i\alpha U_0+i\beta V_0-ilc_0)\eta_{10}\cdot\eta_{10}^{\dagger}]dz\Big]$$

$$+c_n\Big[\int[ilR_0(D^2-(\alpha^2+\beta^2))w_{10}\cdot w_{10}^{\dagger}+ilR_0\eta_{10}\cdot\eta_{10}^{\dagger}]dz\Big] =$$

$$\int[R_0(i\alpha U_n+i\beta V_n)(D^2-(\alpha^2+\beta^2))w_{10}\cdot w_{10}^{\dagger}+\sum_{k=1}^{n-1}[R_k(i\alpha U_{n-k}+i\beta V_{n-k}-ilc_{n-k})(D^2-(\alpha^2+\beta^2))]w_{10}\cdot w_{10}^{\dagger}$$

$$-\sum_{k=0}^{n-1}(R_k(i\alpha\ddot{U}_{n-k}+i\beta\ddot{V}_{n-k})w_{10}\cdot w_{10}^{\dagger}-\sum_{k=0}^{n-1}(R_k(i\beta\dot{U}_{n-k}-i\alpha\dot{V}_{n-k})w_{10}\cdot\eta_{10}^{\dagger}$$

$$R_0(i\alpha U_n+i\beta V_n)\eta_{10}\cdot\eta_{10}^{\dagger}+\sum_{k=1}^{n-1}(R_k(i\alpha U_{n-k}+i\beta V_{n-k}-ilc_{n-k}))\eta_{10}\cdot\eta_{10}^{\dagger}]dz$$

$$-\sum_{i=0}^{n-1}\int(\mathcal{L}_i[\vec{V},\vec{\alpha}]\phi_{1,n-i})\cdot\phi_{10}^{\dagger}dz+\int\langle Nonlinear\ terms\rangle\cdot\phi_{10}^{\dagger}dz$$

The ordering of the problems to be solved in this formulation is most easily discerned as a tabular array diagramed as follows:

		ϕ_0	ϕ_1	ϕ_2	ϕ_3	ϕ_4	ϕ_5
$O(1)$		ϕ_{00}					
$O(\epsilon)$	(R_0, c_0)		ϕ_{10}				
$O(\epsilon^2)$		ϕ_{01}		ϕ_{20}			
$O(\epsilon^3)$	(R_1, c_1)		ϕ_{11}		ϕ_{30}		
$O(\epsilon^4)$		ϕ_{02}		ϕ_{21}		ϕ_{40}	
$O(\epsilon^5)$	(R_2, c_2)		ϕ_{12}		ϕ_{31}		ϕ_{50}
...				...			

One proceeds in solving the problems for the related eigenfunctions from left to right across each row and continues on to the next row down. At $O(\epsilon^{2n+1})$ the n-th Linsted coefficient is obtained. The diagram for the parametric expansion is identical to the one given in Herbert for Stuart-Watson theory (where we have only replaced the Landau constants by the Linsted coefficients).

The actual numerical calculation of the Linsted coefficients is easier to do in matrix form, with the linear operator divided up into four parts.

$$\mathcal{L}[\vec{V},\vec{\alpha}] =$$

$$\begin{pmatrix} \left[\sum_{k=1}^{n-1} -R_k(i\alpha U_{n-k}+i\beta V_{n-k}-ilc_{n-k})(D^2-(\alpha^2+\beta^2))+\sum_{k=0}^{n-1} R_k(i\alpha \ddot{U}_{n-k}+i\beta \ddot{V}_{n-k})\right] & 0 \\ \sum_{k=0}^{n-1} R_k(i\beta \dot{U}_{n-k}-i\alpha \dot{V}_{n-k}) & \sum_{k=1}^{n-1} -R_k(i\alpha U_{n-k}+i\beta V_{n-k}-ilc_{n-k}) \end{pmatrix}$$

$$+R_n \begin{pmatrix} \left[-(i\alpha U_0+i\beta V_0-ilc_0)(D^2-(\alpha^2+\beta^2))+(i\alpha \ddot{U}_0+i\beta \ddot{V}_0)\right] & 0 \\ (i\beta \dot{U}_0-i\alpha \dot{V}_0) & -(i\alpha U_0+i\beta V_0-ilc_0) \end{pmatrix}$$

$$+c_n \begin{pmatrix} +R_0 il(D^2-(\alpha^2+\beta^2)) & 0 \\ 0 & +R_0 il \end{pmatrix}$$

$$+ \begin{pmatrix} -R_0(i\alpha U_n+i\beta V_n)(D^2-(\alpha^2+\beta^2)) & 0 \\ 0 & -R_0(i\alpha U_n+i\beta V_n) \end{pmatrix}$$

One final technical point; the adjoint equation need never be solved for. (R_n, c_n) can be more accurately determined through gaussian reduction and elimination.

Table 1. LINSTED COEFFICIENTS

POISEUILLE FLOW† $\alpha = 1.02$		
i	R_i	c_i
0	.5772E+04	.2639E+00
1	-.1676E+08	.2683E+03
2	.8278E+12	-.8600E+07
3	-.4434E+17	.4358E+12
4	.2673E+22	-.2597E+17

†with the normalization w(0) = 1

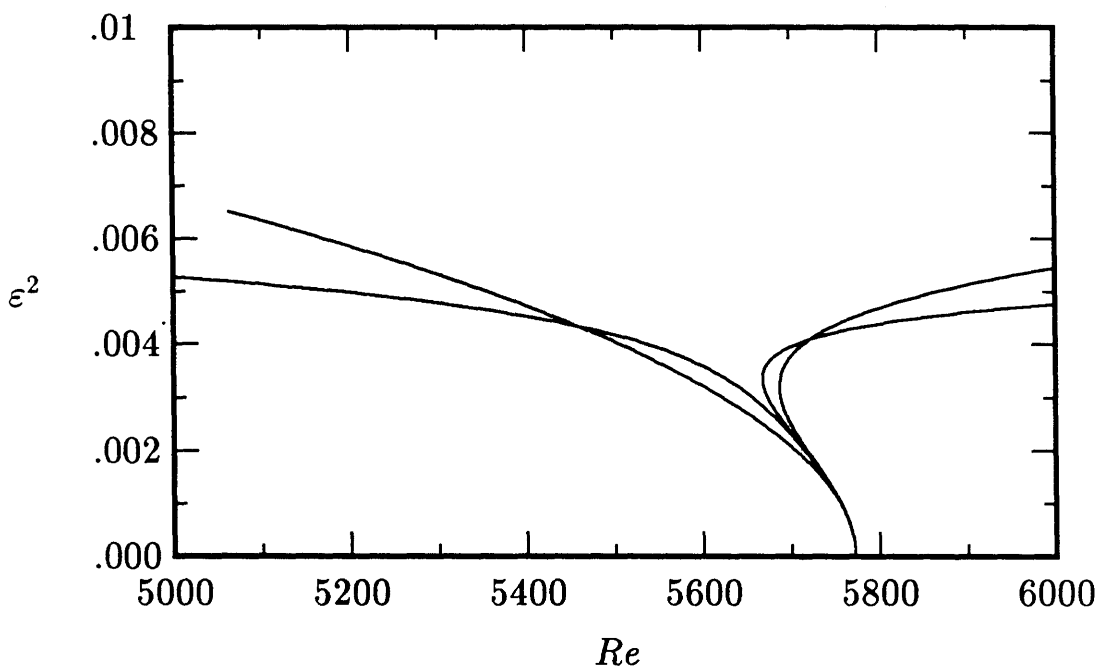

Figure 1: THE FIRST FOUR APPROXIMATIONS : POISEUILLE FLOW

Table 2.1 LINSTED COEFFICIENTS

NARROW GAP EKMAN FLOW								
	GAP=20.		GAP=6.0		GAP=4.0		GAP=2.5	
i	R_i	c_i	R_i	c_i	R_i	c_i	R_i	c_i
0	.5437e2	.5833e0	.3476e2	.4580e0	.5333e2	.2571e0	.2044e3	.0729e0
1	.3689e5	-.9229e2	.4940e4	-.1971e2	.2359e4	.2059e0	.4686e4	.1916e1
2	.5671e8	-.1887e6	.1265e7	-.5314e4	.1603e6	.2272e2	.1958e6	.7329e2
3	.1087e12	-.4173e9	.3913e9	-.1699e7	.1380e8	.1642e4	.8255e7	.3791e4
4	.2372e15	-.9789e12	.1333e12	-.5961e9	.1330e10	.1334e6	.1740e9	.2442e6

Table 2.2 MARGINAL WAVE CHARACTERISTICS

NARROW GAP EKMAN FLOW				
	GAP = 20.	GAP = 6.0	GAP = 4.0	GAP = 2.5
R_{cr}	54.37	34.76	53.33	204.4
c_{cr}	.5833	.4580	.2571	.0780
wave no. (β)	.30	.40	.75	1.2
wave angle ϵ°	$-20.^{\circ}$	-5.0°	7.5°	$36.^{\circ}$
normalization	$w(-.8) = 1.$	$w(0.) = 1.$	$w(0.) = 1.$	$\eta(.5) = 1.$

Figure 2: THE FIRST FOUR APPROXIMATIONS : GAP = 20.

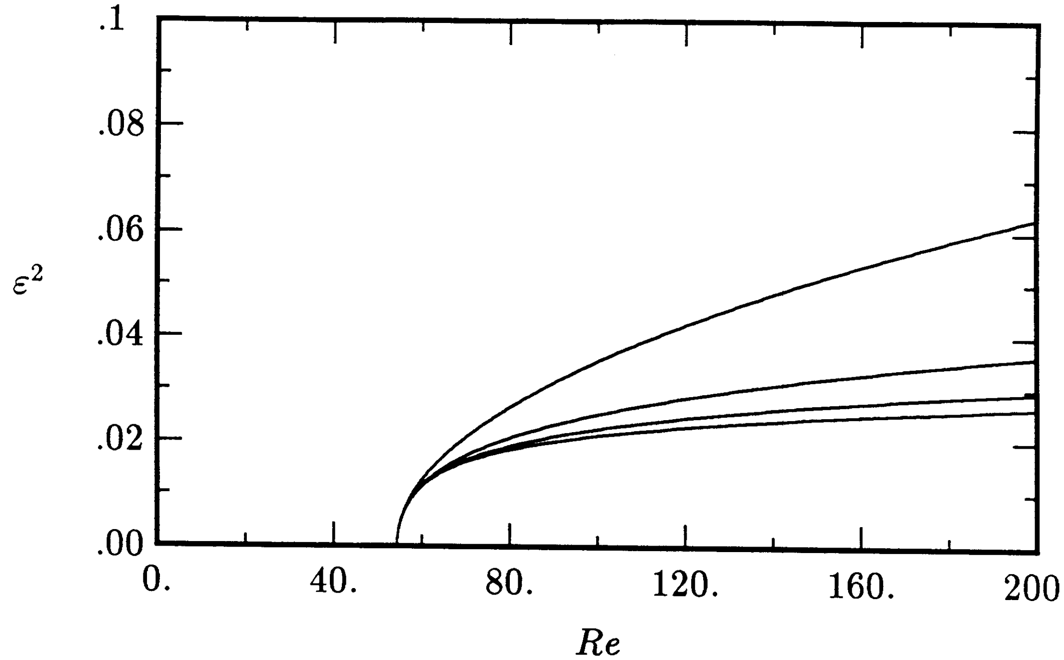

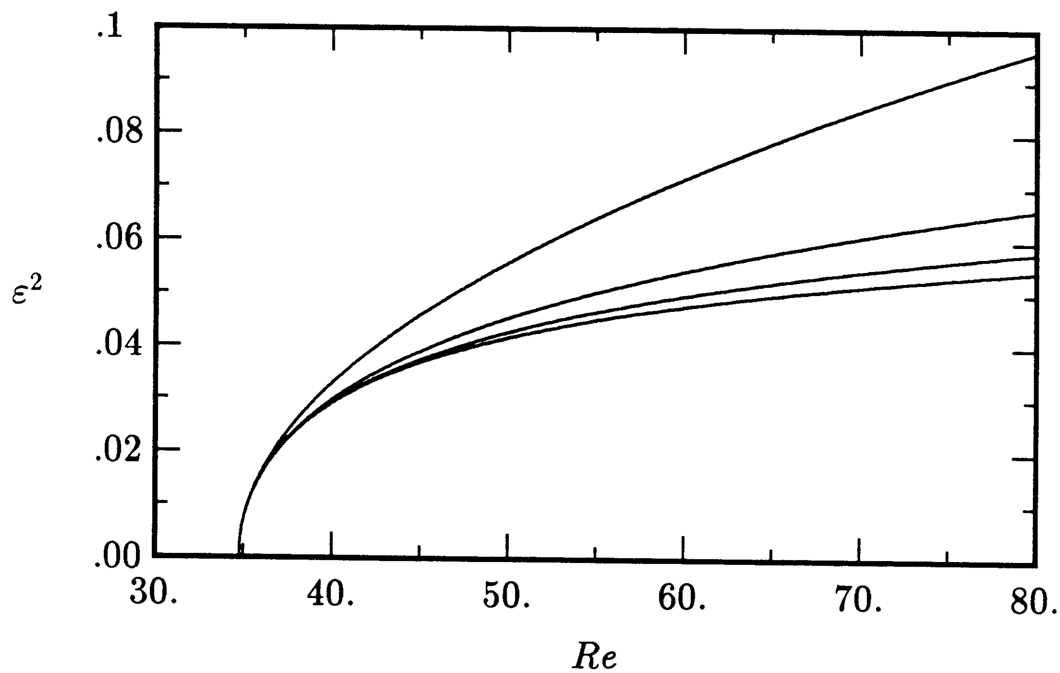

Figure 3: THE FIRST FOUR APPROXIMATIONS : GAP = 6.

Figure 4: THE FIRST FOUR APPROXIMATIONS : GAP = 4.

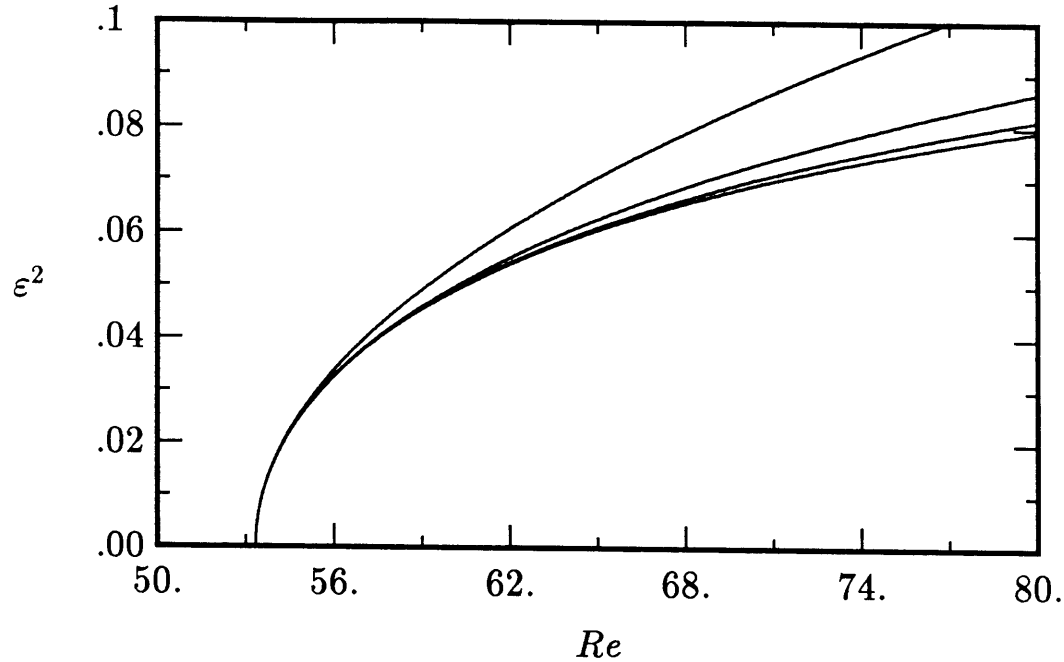

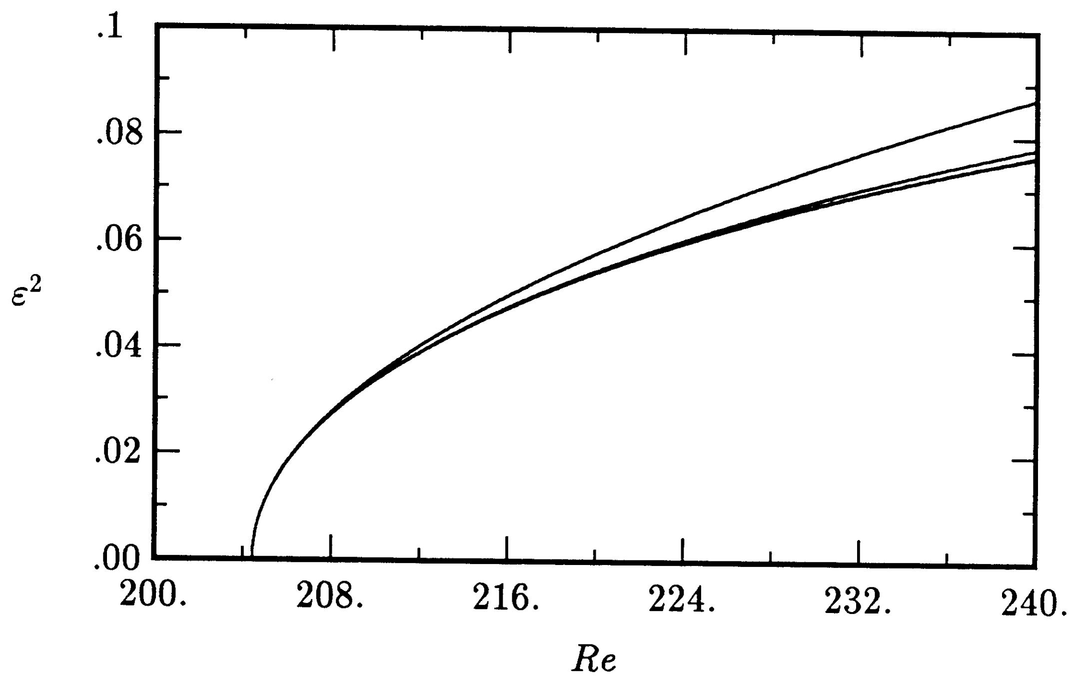

Figure 5: THE FIRST FOUR APPROXIMATIONS : GAP = 2.5

Chapter 4. Weakly Non-Linear Theory: Stuart-Watson Expansions

Linear theory can account for the initial development of a wave disturbance under the approximation that it represents an infinitesimally small perturbation of the basic flow. If exponential growth is predicted the latter assumption soon fails to hold and nonlinearity must be accounted for. The nonlinear expansions applied to this problem have been developed by J.T. Stuart and J. Watson in related papers (J.F.M. 1960). In this approach the Reynolds number is fixed and the evolution of the wave is followed in time until an equilibrium state (if one exists) is reached. Stuart's expansion takes the form of a series in the wave amplitude with the linear growth rate αc_i treated as order A^2 . The original conjecture, due to Landau, gave the first terms of the initial departure of the wave disturbance from equilibrium as $dA/dt = \alpha c_i A + kA^2A^*$. The implications of the Stuart-Landau equation are easily grasped. If $\Re e\{k\} < 0$ and $c_i > 0$ an initially infinitesimal disturbance will undergo exponential amplification in accord with the linear theory. This will be altered as the wave amplitude becomes small with the resulting finite amplitude equilibrium given by $|A|_{EQ}^2 = -\frac{\alpha c_i}{\Re e\{k\}}$. If c_i and $\Re e\{k\} > 0$ the equilibrium state is unstable and small perturbations will lead to instability if they are larger than the threshold equilibrium amplitude. This latter situation is referred to as subcritical. The constant k is commonly known as the Landau constant. For high Reynolds number parallel shear flow, Herbert has shown that many terms in the expansion need to be computed to achieve reasonable quantitative agreement with the analytical solution. In both the single and two wave expansions the same procedure is adopted. A nonlinear perturbation equation is obtained from (2.1) and (2.2). The perturbed quantities are decomposed into a spatial mean and periodic part. The periodic part is represented as a fourier series and the resulting equation for each harmonic are subject to an expansion in the wave amplitude, which is considered to be a slowly varying function of time.

The Single Mode Expansion.

The nonlinear perturbation equations are:

$$\frac{\partial u^*}{\partial t} + V_E \frac{\partial u^*}{\partial y} + w^* \frac{\partial U_E}{\partial z} + v^* \frac{\partial u^*}{\partial y} + w^* \frac{\partial u^*}{\partial z} = +\frac{2}{R} v^* + \frac{1}{R}\left(\frac{\partial^2 u^*}{\partial y^2} + \frac{\partial^2 u^*}{\partial z^2}\right) \quad (1)$$

$$\frac{\partial v^*}{\partial t} + V_E \frac{\partial v^*}{\partial y} + w^* \frac{\partial V_E}{\partial z} + v^* \frac{\partial v^*}{\partial y} + w^* \frac{\partial v^*}{\partial z} = -\frac{\partial p^*}{\partial y} - \frac{2}{R} u^* + \frac{1}{R}\left(\frac{\partial^2 v^*}{\partial y^2} + \frac{\partial^2 v^*}{\partial z^2}\right) \quad (2)$$

$$\frac{\partial w^*}{\partial t} + V_E \frac{\partial w^*}{\partial y} + w^* \frac{\partial w^*}{\partial z} = -\frac{\partial p^*}{\partial z} + \frac{1}{R}\left(\frac{\partial^2 w^*}{\partial y^2} + \frac{\partial^2 w^*}{\partial z^2}\right) \quad (3)$$

These give rise to the nonlinear vorticity equations:

$$\frac{\partial \xi^*}{\partial t} + V_E \frac{\partial \xi^*}{\partial y} - w^* \frac{d^2 V_E}{dz^2} + v^* \frac{\partial \xi^*}{\partial y} + w^* \frac{\partial \xi^*}{\partial z} = \frac{2}{R}\frac{\partial u^*}{\partial z} + \frac{1}{R}\left(\frac{\partial^2 \xi^*}{\partial y^2} + \frac{\partial^2 \xi^*}{\partial z^2}\right) \quad (4)$$

$$\frac{\partial u^*}{\partial t} + V_E \frac{\partial u^*}{\partial y} - w^* \frac{dU_E}{dz} + v^* \frac{\partial u^*}{\partial y} + w^* \frac{\partial u^*}{\partial z} = \frac{2}{R} v^* + \frac{1}{R}\left(\frac{\partial^2 u^*}{\partial y^2} + \frac{\partial^2 u^*}{\partial z^2}\right) \quad (5)$$

The streamwise velocity and vorticity perturbations are further decomposed into a mean and a fluctuating part, so that $u^* = \bar{u} + u'$ and $\xi^* = \bar{\xi} + \xi'$ where the overbar indicates the averaged component and the prime the fluctuating part. Substitution of these into (4.1-3) and taking the average of the equations over a wavelength in the y direction results in the equations for the mean flow distortion:

$$\frac{\partial \bar{\xi}}{\partial t} + \overline{v' \frac{\partial \xi'}{\partial y}} + \overline{w' \frac{\partial \xi'}{\partial z}} = \frac{2}{R}\frac{\partial \bar{u}}{\partial z} + \frac{1}{R}\frac{\partial^2 \bar{\xi}}{\partial z^2} \quad (6)$$

$$\frac{\partial \bar{u}}{\partial t} + \overline{v' \frac{\partial u'}{\partial y}} + \overline{w' \frac{\partial u'}{\partial z}} = \frac{2}{R}\bar{v} + \frac{1}{R}\frac{\partial^2 \bar{u}}{\partial z^2} \quad (7)$$

Subtraction of the mean flow equations above from the perturbation equations yields the equations for the periodic part of the disturbance:

$$\frac{\partial \xi'}{\partial t} + (V_E + \bar{v} + v')\frac{\partial \xi'}{\partial y} + w'\frac{\partial}{\partial z}(\xi_E + \bar{\xi} + \xi') - \overline{v'\frac{\partial \xi'}{\partial y}} - \overline{w'\frac{\partial \xi'}{\partial z}}$$
$$= \frac{2}{R}\frac{\partial u'}{\partial z} + \frac{1}{R}(\frac{\partial^2 \xi'}{\partial y^2} + \frac{\partial^2 \xi'}{\partial z^2}) \tag{8}$$

$$\frac{\partial u'}{\partial t} + (V_E + \bar{v} + v')\frac{\partial u'}{\partial y} + w'\frac{\partial}{\partial z}(U_E + \bar{u} + u') - \overline{v'\frac{\partial u'}{\partial y}} - \overline{w'\frac{\partial u'}{\partial z}}$$
$$= \frac{2}{R}v' + \frac{1}{R}(\frac{\partial^2 u'}{\partial y^2} + \frac{\partial^2 u'}{\partial z^2}) \tag{9}$$

It is easier to work with the mean flow velocity components obtained by averaging (4.1-3) and these are:

$$\frac{\partial \bar{u}}{\partial t} + \frac{\partial \overline{u'w'}}{\partial z} = \frac{2}{R}\bar{v} + \frac{1}{R}\frac{\partial^2 \bar{u}}{\partial z^2} \tag{10}$$

$$\frac{\partial \bar{v}}{\partial t} + \frac{\partial \overline{v'w'}}{\partial z} = -\frac{2}{R}\bar{u} + \frac{1}{R}\frac{\partial^2 \bar{v}}{\partial z^2} \tag{11}$$

Now the fluctuating quantities are $\frac{2\pi}{\alpha}$ periodic and so

$$u' = \sum_{n=1}^{\infty}\left(u_n(z,t)e^{in\alpha(y-c_r t)} + (*)\right)$$

$$\xi' = \sum_{n=1}^{\infty}\left(\xi_n(z,t)e^{in\alpha(y-c_r t)} + (*)\right)$$

Thus each term in the fourier series will satisfy a component equation:

$$-i\alpha c_r u_1 + \frac{\partial u_1}{\partial t} + i\alpha(V_E + \bar{v})u_1 + 2i\alpha v_1^* u_2 - i\alpha u_1^* v_2 + w_1 \frac{\partial}{\partial z}(U_E + \bar{u})$$

$$+ w_1^* \frac{\partial u_2}{\partial z} + w_2 \frac{\partial u_1^*}{\partial z} = \frac{1}{R}(2v_1 - \alpha^2 u_1 + \frac{\partial^2 u_1}{\partial z^2}) \tag{12}$$

$$-2i\alpha c_r u_2 + \frac{\partial u_2}{\partial t} + 2i\alpha(V_E + \bar{v})u_2 + i\alpha v_1 u_1 + w_2 \frac{\partial}{\partial z}(U_E + \bar{u}) + w_1 \frac{\partial u_1}{\partial z}$$

$$= \frac{1}{R}(2v_2 - 4\alpha^2 u_2 + \frac{\partial^2 u_2}{\partial z^2}) \tag{13}$$

$$-i\alpha c_r \xi_1 + \frac{\partial \xi_1}{\partial t} + i\alpha(V_E + \bar{v})\xi_1 + 2i\alpha v_1^* \xi_2 - i\alpha \xi_1^* v_2 + w_1 \frac{\partial}{\partial z}(\xi_E + \bar{\xi})$$

$$+ w_1^* \frac{\partial \xi_2}{\partial z} + w_2 \frac{\partial \xi_1^*}{\partial z} = \frac{1}{R}(2\frac{\partial u_1}{\partial z} - \alpha^2 \xi_1 + \frac{\partial^2 \xi_1}{\partial z^2}) \tag{14}$$

$$-2i\alpha c_r \xi_2 + \frac{\partial \xi_2}{\partial t} + 2i\alpha(V_E + \bar{v})\xi_2 + i\alpha v_1 \xi_1 + w_2 \frac{\partial}{\partial z}(\xi_E + \bar{\xi}) + w_1 \frac{\partial \xi_1}{\partial z}$$

$$= \frac{1}{R}(2\frac{\partial u_2}{\partial z} - 4\alpha^2 \xi_2 + \frac{\partial^2 \xi^2}{\partial z^2}) \tag{15}$$

With the equations for the mean flow distortion becoming:

$$\frac{\partial \bar{u}}{\partial t} + \frac{\partial}{\partial z}(u_1 w_1^* + u_1^* w_1 + w_2 u_2^* + w_2^* u_2) = \frac{2}{R}\bar{v} + \frac{1}{R}\frac{\partial^2 \bar{u}}{\partial z^2} \tag{16}$$

$$\frac{\partial \bar{v}}{\partial t} + \frac{\partial}{\partial z}(v_1 w_1^* + v_1^* w_1 + w_2 v_2^* + w_2^* v_2) = -\frac{2}{R}\bar{u} + \frac{1}{R}\frac{\partial^2 \bar{v}}{\partial z^2} \tag{17}$$

A stream function can be introduced for each harmonic such that

$$\xi_1 = (-\alpha^2 + \frac{\partial^2}{\partial z^2})\psi_1 \qquad \xi_2 = (-\alpha^2 + \frac{\partial^2}{\partial z^2})\psi_2$$

(4.14-15) can now be revised to,

$$\begin{aligned}
&(-i\alpha c_r + \frac{\partial}{\partial t})(-\alpha^2 + \frac{\partial^2}{\partial z^2})\psi_1 + i\alpha(V_E + \bar{v})(-\alpha^2 + \frac{\partial^2}{\partial z^2})\psi_1 \\
&-2i\alpha\frac{\partial \psi_1^*}{\partial z}(-4\alpha^2 + \frac{\partial^2}{\partial z^2}\psi_2) + i\alpha\frac{\partial \psi_2}{\partial z}(-\alpha^2 + \frac{\partial^2}{\partial z^2})\psi_1^* + i\alpha\psi_1\frac{\partial^2}{\partial z^2}(V_E + \bar{v}) \\
&- i\alpha\psi_1^*\frac{\partial}{\partial z}(-4\alpha^2 + \frac{\partial^2}{\partial z^2})\psi_2 + 2i\alpha\psi_2\frac{\partial}{\partial z}(-\alpha^2 + \frac{\partial^2}{\partial z^2})\psi_1^* = \frac{1}{R}(2\frac{\partial u_1}{\partial z} + (-\alpha^2 + \frac{\partial^2}{\partial z^2})^2\psi_1)
\end{aligned} \tag{18}$$

$$\begin{aligned}
&(-2i\alpha c_r + \frac{\partial}{\partial t})(-4\alpha^2 + \frac{\partial^2}{\partial z^2})\psi_2 + 2i\alpha(V_E + \bar{v})(-4\alpha^2 + \frac{\partial^2}{\partial z^2})\psi_2 \\
&-i\alpha\frac{\partial \psi_1}{\partial z}(-\alpha^2 + \frac{\partial^2}{\partial z^2})\psi_1 - 2i\alpha\psi_2(\frac{\partial^2}{\partial z^2}(V_E + \bar{v}) + i\alpha\psi_1\frac{\partial}{\partial z}(-\alpha^2 + \frac{\partial^2}{\partial z^2})\psi_1 \\
&\qquad = \frac{1}{R}(2\frac{\partial u_2}{\partial z} + (-4\alpha^2 + \frac{\partial^2}{\partial z^2})^2\psi_2)
\end{aligned} \tag{19}$$

with similar changes to (4.12-13). The Stuart-Watson ordering, in the form of a separable solution, is given to order A^3 by:

$$\psi_1(z,t) = A(t)\phi_1(z) + A^2(t)A^*(t)\phi_{11}(z) + o(A^5) \tag{20}$$

$$\psi_2(z,t) = A^2(t)\phi_2(z) + o(A^4) \tag{21}$$

$$u_1(z,t) = A(t)\mu_1(z) + A^2(t)A^*(t)\mu_{11}(z) + o(A^5) \tag{22}$$

$$u_2(z,t) = A^2(t)\mu_2(z) + o(A^4) \tag{23}$$

The first mean flow correction occurs at order AA^* so that,

$$\bar{u}(z,t) = AA^*\bar{\mu}(z) + o(A^4) \tag{24}$$

$$\bar{v}(z,t) = AA^*\bar{\nu}(z) + o(A^4) \tag{25}$$

With the slow time dependence of the wave amplitude given by

$$\frac{dA}{dt} = \alpha c_i A + kA^2A^* + o(A^5) \tag{26}$$

the leading order problem is complete and seen to be consistent. The formal substitution of (4.18-26) into the equations for the harmonic components results in a corresponding problem at each order of A .

The Linear Problem:

$$(-\alpha^2 + \frac{\partial^2}{\partial z^2})^2\phi_1 - i\alpha R(V_E - c)(-\alpha^2 + \frac{\partial^2}{\partial z^2})\phi_1 + i\alpha R\phi_1\frac{\partial^2 V_E}{\partial z^2} + 2\frac{\partial \mu_1}{\partial z} = 0$$

$$(-\alpha^2 + \frac{\partial^2}{\partial z^2})\mu_1 - i\alpha R(V_E - c)\mu_1 - i\alpha R\phi_1\frac{\partial U_E}{\partial z} - 2\frac{\partial \phi_1}{\partial z} = 0$$

The Problem at $O(A^2)$:

$$(-4\alpha^2 + \frac{\partial^2}{\partial z^2})^2\phi_2 - 2i\alpha R(V_E - c)(-4\alpha^2 + \frac{\partial^2}{\partial z^2})\phi_2 + 2i\alpha R\phi_2\frac{\partial^2 V_E}{\partial z^2} + 2\frac{\partial \mu_2}{\partial z}$$
$$= i\alpha R\phi_1\frac{\partial}{\partial z}(-\alpha^2 + \frac{\partial^2}{\partial z^2})^2\phi_1 - i\alpha R\frac{\partial \phi_1}{\partial z}(-\alpha^2 + \frac{\partial^2}{\partial z^2})^2\phi_1$$

$$(-4\alpha^2 + \frac{\partial^2}{\partial z^2})\mu_2 - 2i\alpha R(V_E - c)\mu_2 - 2i\alpha R\phi_2\frac{\partial U_E}{\partial z} - 2\frac{\partial \phi_2}{\partial z}$$
$$-i\alpha R\frac{\partial \phi_1}{\partial z}\mu_1 + i\alpha R\phi_1\frac{\partial \mu_1}{\partial z}$$

The order AA^* Mean flow distortion:

$$2R\alpha c_i\bar{\nu} + i\alpha R\frac{d}{dz}(\dot{\phi}_1\phi_1^* - \dot{\phi}_1^*\phi_1) = -2\bar{\mu} + \frac{\partial^2\bar{\nu}}{\partial z^2}$$

$$2R\alpha c_i\bar{\mu} + i\alpha R\frac{d}{dz}(\mu_1^*\phi_1 - \mu_1\phi_1^*) = 2\bar{\nu} + \frac{\partial^2\bar{\mu}}{\partial z^2}$$

The Problem for Landau's Constant:

$$(-\alpha^2 + \frac{\partial^2}{\partial z^2})^2\phi_{11} - i\alpha R(V_E - c)(-\alpha^2 + \frac{\partial^2}{\partial z^2})\phi_{11} + i\alpha R\phi_{11}\frac{\partial^2 V_E}{\partial z^2} + 2\frac{\partial\mu_{11}}{\partial z} =$$

$$R(i\alpha\bar{\nu} + k)(-\alpha^2 + \frac{\partial^2}{\partial z^2}\phi_1 - i\alpha R\phi_1\frac{\partial^2\nu}{\partial z^2} - 2i\alpha R\frac{\partial\phi_1^*}{\partial z}(-4\alpha^2 + \frac{\partial^2}{\partial z^2})\phi_2$$

$$+i\alpha R\frac{\partial\phi_2}{\partial z}(-\alpha^2 + \frac{\partial^2}{\partial z^2})\phi_1^* - i\alpha R\phi_1^*\frac{\partial}{\partial z}(-4\alpha^2 + \frac{\partial^2}{\partial z^2})\phi_2 + 2i\alpha R\phi_2(-\alpha^2 + \frac{\partial^2}{\partial z^2})\frac{\partial\phi_1^*}{\partial z}$$

$$(-\alpha^2 + \frac{\partial^2}{\partial z^2})\mu_{11} - i\alpha R(V_E - c)\mu_{11} - i\alpha R\phi_{11}\frac{\partial U_E}{\partial z} - 2\frac{\partial\phi_{11}}{\partial z} =$$

$$R(i\alpha\bar{\nu} + k)\mu_1 + i\alpha R\phi_1\frac{\partial\bar{\mu}}{\partial z} - 2i\alpha R\frac{\partial\phi_1^*}{\partial z}\mu_2 + i\alpha R\mu_1^*\frac{\partial\phi_2}{\partial z}$$

$$-i\alpha R\phi_1^*\frac{\partial\mu_2}{\partial z} + 2i\alpha R\phi_2\frac{\partial u_1^*}{\partial z}$$

These systems of differential equations can now be solved in the following manner. The linear eigenvalue problem is first solved and the resulting eigenfunction substituted into the inhomogeneous terms on the right hand side of the order A^2 , and the mean flow distortion equations. Now the linear operator for the order A^2 problem is not singular if $(2\alpha, c)$ is not an eigenvalue of the homogeneous problem. The homogeneous operator associated with the order AA^* mean flow distortion contains only an exceptional set of eigenvalues (Davey 1978). The solutions of these equations are therefore obtained by inverting their corresponding operators. Having obtained these solutions the inhomogeneity of the order A^2A^* problem is determined up to the unknown Landau constant, k. The differential operator is identical with that of the linear problem (that is the linear eigenfuction is a homogeneous solution). The Landau constant is therefore determined by the Fredholm alternative, which requires that the inhomogeneity be orthogonal to the adjoint eigenfunction of the homogeneous problem. The adjoint system (c.f. Ince) to (2.13-14), with respect to the inner product $(f,g) = \int_0^\infty f \cdot g^* dz$ is given by:

$$(-\alpha^2 + \frac{\partial^2}{\partial z^2})^2 \chi + i\alpha R(V_E - c^*)(-\alpha^2 + \frac{\partial^2}{\partial z^2})\chi + i\alpha R \frac{\partial U_E}{\partial z} N$$
$$+ 2i\alpha R \frac{\partial V_E}{\partial z}\frac{\partial \chi}{\partial z} + 2\frac{\partial N}{\partial z} = 0 \tag{27}$$

$$(-\alpha^2 + \frac{\partial^2}{\partial z^2})N + i\alpha R(V_E - c^*)N - 2\frac{\partial \chi}{\partial z} = 0 \tag{28}$$

together with the boundary conditions $\chi = \dot{\chi} = N = 0$ at $z = 0$, and $\chi = \ddot{\chi} = \dot{N} = 0$ at $z = \infty$. The Landau constant can be given explicitly as

$$k = \frac{\int_0^\infty \{(I) \cdot \chi^* + (II) \cdot N^*\} \, dz}{\int_0^\infty (\xi_1 \chi^* + u_1 N^*) dz} \tag{29}$$

where the linear eigenfunction has been normalized by

$$max(sup\ \phi(z), sup\ u(z)) = 1 \tag{30}$$

and with

$$(I) = (-i\alpha\bar{v}\xi_1 + i\alpha\phi_1\frac{d^2\bar{v}}{dz^2} + 2i\alpha\dot{\phi}_1^*\xi_2 - i\alpha\dot{\phi}_2\xi_1^* + i\alpha\phi_1^*\dot{\xi}_2 - 2i\alpha\phi_2\dot{\phi}_1^*)$$

$$(II) = (-i\alpha\bar{v}\mu_1 - i\alpha\phi_1\bar{\dot{\mu}} + 2i\alpha\dot{\phi}_1^*\mu_2 - i\alpha\mu_1^*\dot{\phi}_2 + i\alpha\phi_1^*\dot{\mu}_2 - 2i\alpha\phi_2\dot{\mu}_1)$$

Table 3.1 LANDAU CONSTANTS

NARROW GAP EKMAN FLOW			
GAP	Without Second Harmonic	Without Mean flow Correction	Total Landau Constant
1.5	(-1.0697,2.0220)	(.0983,-.1520)	(-.9714,1.870)
1.8	(-.6342,.46687)	(.1005,-.1112)	(-.5337,.3557)
2.0	(-.5922,-.6490)	(.1354,-.1123)	(-.4568,-.7613)
2.2	(-.6315,-2.164)	(.1932,-.1241)	(-.4383,-2.2881)
2.5	(-.5789,-.4.5277)	(.1354,-.0942)	(-.4435,-4.6219)
4.0	(-1.2458,-.7405)	(.3391,-.01388)	(-.9067,.7544)
10.	(-2.3420,5.2265)	(.2293,4.1977)	(-2.1127,4.0348)

Chapter 5. WNLTs and Secondary Instability

We want to compare the weakly non-linear theories (WNLTs) and secondary instability. The weakly non-linear theories start with a basic mean flow. The theories account for first non-linear effects of one or several waves each of which is nearly marginally stable. The physical effects that these theories incorporate are (1) a mean flow distortion, (2) the generation of harmonics, (3) a correction to the linear wave speed, and (4) a modification of the linear eigenstructure. The computations show that the mean flow distortion predominates over the generation of harmonics. Poiseuille flow is subcritical because the Reynolds stress exerted by a small but finite amplitude wave destabilizes the mean toward the growth of the wave. Thus an equilibrated mean -wave field exists below the linear critical Reynolds number. Similarly Ekman flow is supercritical largely because the Reynolds stress exerted by a finite amplitude wave stabilizes the mean toward the growth of the wave. For viscous shear flow, the linear eigenproblem (the Orr-Sommerfeld equation) is singular with a critical layer of thickness $(\alpha R)^{-1/3}$. In using the method of amplitude expansions the initial growth rate, αc_i, should be small compared to the dimensions of the critical layer. If the basic mean flow has more than one linearly unstable mode, Figure 5.1, the WNLTs can account for the wave interactions, that one would naturally anticipate, along the lines of (1)-(4) above. (Chapters 6-8).

The 3-D instability of the kind considered here (Chapter 9), Figure 5.2, results from a secondary instability to a finite amplitude wave field. The secondary instability does not occur without the presence of the primary wave, which serves to link the fourier modes of the secondary instability. This permits the 3-D eigenstructure to assume a form capable of rapid linear growth. In the language of the WNLTs the important consideration is the modification to the secondary eigenstructure that a primary wave of given amplitude effects. This is perhaps best illustrated in Poiseuille flow where calculations show that the eigenvalue of the secondary instability is accurately determined by a three mode representation, consisting of a downstream roll and two complimentary oblique waves. Squires theorem precludes the possibility of a linearly unstable downstream roll (which would be essentially sinusoidal, i.e. the solution of a forth order constant coefficient O.D.E.). The existence of the primary transverse 2-d wave locks the oblique wave mode to the downstream component. The downstream mode is altered near the boundary (inside the viscous sublayer) by coupling with the oblique mode (see Figure 9.2, on page 92). A small but finite 2-d wave amplitude is sufficient to link the downstream and oblique components into a rapidly growing 3-D perturbation. Strong growth results because the downstream mode is very effective in generating power via the correlation $u_0^{3d}(w_0^{3d})^*(dU_M/dz)$. A preferred spanwise wave number and the phase speed for the 3-D instability are determined from maximal linear growth rate arguments.

We also wish to distinguish between finite amplitude procedures and asymptotics. In the asymptotic analysis one chooses a physical scale as a small parameter and usually expands in 'slow' and 'fast' variables. The difference in scales reflects the characteristics of the various processes that occur. The physical situation we have in mind is the interaction of waves ensuing secondary instability. The interaction is between a finite amplitude wave and a small secondary perturbation. Here an appropriate scale for the fast variables might be the derivative of the linear growth rate of the secondary instability with respect to the Reynolds number, $\frac{\partial \alpha c_{i2}}{\partial R}|_{R=R_{c2}}$. The wave properties such as phase velocity and wavelength are associated with the fast time and small spatial scales while the wave envelopes have a large length scale and slow time scale over which modulations can develop. The asymptotics captures the physics in some small neighborhood of parameter space. In contrast what is implied by a finite amplitude expansion is a well defined and extendible procedure by which the equilibrium solution can be explicitly computed to arbitrary accuracy. The Malkus & Veronis finite amplitude expansion does just this, providing an algorithmic framework in which the Reynolds number and the phase speed are parametrized as functions of the equilibrium amplitude. The asymptotics reveals the stability of this equilibrium and the nature of small departures from it. Consistency is very important and the governing asymptotic equations are no longer valid once any of the neglected terms becomes significant or whenever the scaling assumptions no longer apply. Thus if the wave amplitude becomes large enough the higher order nonlinear terms not only become important but will dominate the physics and asymptotic equations which neglect these terms cannot be applicable.

Largely because of the singular character of high Reynolds number flow the finite amplitude expansions have a very limited range of convergence. Pade summation (T. Herbert, JFM 1983) will accelerate the convergence of the series. Shanks transformation (Sen et al., JFM 1983) even gives the 'correct' (analytically continued) sum of the series beyond its first singularity. But both of these procedures require a large number of terms to be computed with high accuracy (to ensure numerical stability). For Poiseuille (subcritical) flow the upper stable branch of the equilibrium curve remains inaccessible.

H. Zhou (1982) has considered a method that combines a fourier mode integration with a modified Stuart-Watson amplitude expansion. Alternatively it seems possible to expand about a previously obtained finite amplitude equilibrium in a stepwise fashion. (What might appropriately be called "Integrating with Malkus & Veronis".) The crucial factor is that the eigenfuction in which one expands is changed. At each step the new equilibrium flow is calculated and the expansion is developed using the eigenfunction generated by the new mean field. This procedure was suggested by Meksyn & Stuart where in the limit of large Reynolds number the value of $(U''(z)/U'(z))|_{z=z_c}$ evaluated at the critical level (where $U(z) - c = 0$) is what needs to be updated along the neutral curve. Moreover that the equilibrated finite amplitude eigenfunction differs in shape only slightly from the linear eigenfunction (as has been pointed out in some ongoing research of W.V.R. Malkus) is indicative that a more efficient perturbation scheme might be developed in which one stretches the cross stream coordinate.

Obviously any valid asymptotic theory will match first finite amplitude results. Here it will be instructive to display the relationship between the lowest order results obtained via the the Malkus-Veronis finite amplitude scheme and those from the Stuart-Watson asymptotic technique. For the critical Reynolds number, R_0, at which marginal stability occurs the real part of the Landau constant, k_1, is related to the first Malkus-Veronis coefficient R_1 by the formula:

$$R_1 \left(\frac{\partial[\alpha c_i]}{\partial R} \right) |_{R=R_0} = \Re e\{k_1|_{R=R_0}\} \tag{1}$$

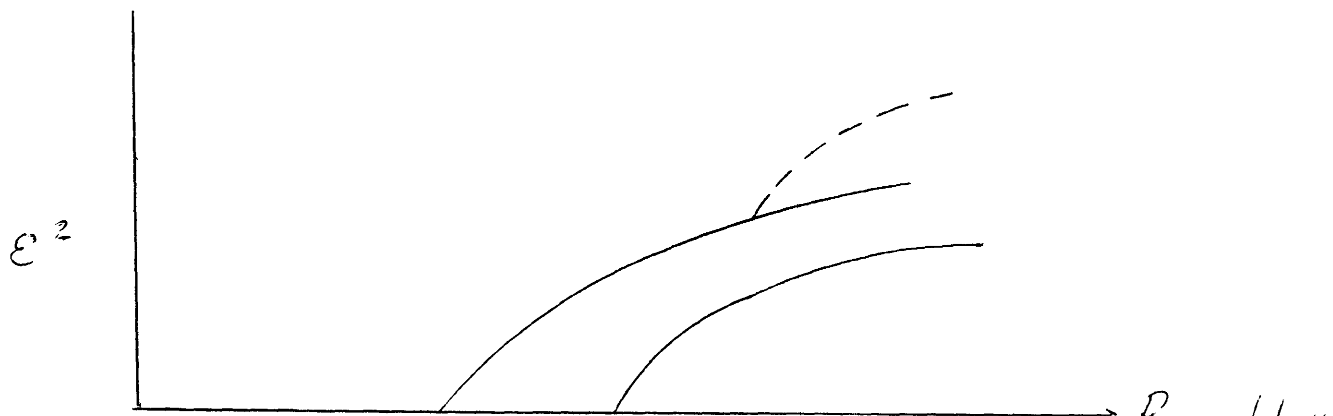

Figure 5.1 In Ekman flow there are two linear unstable waves.

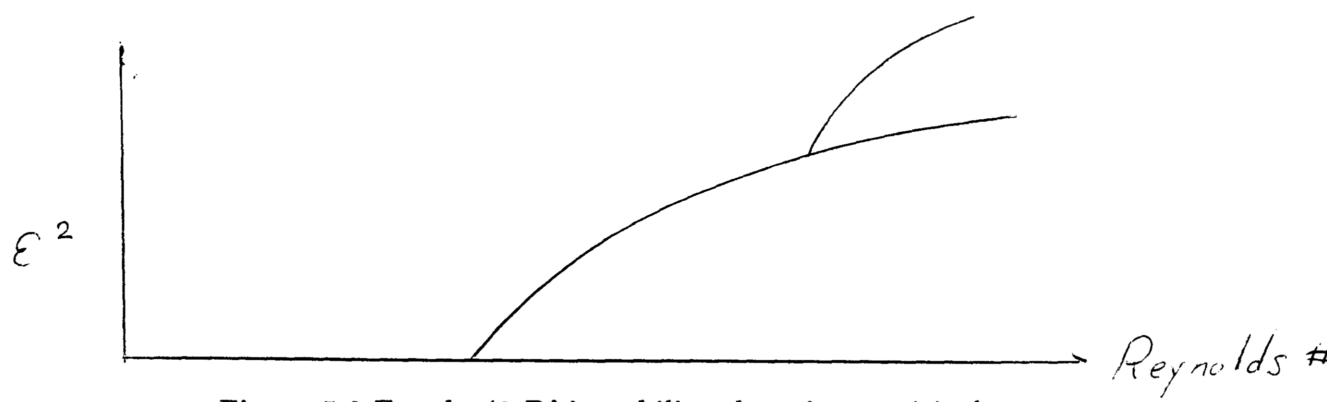

Figure 5.2 For the '3-D' instability there is no critical Reynolds number without the primary finite amplitude wave

Chapter 6. The Two Wave Interaction

The evolution of many physical systems involve successive instabilities upon an equilibrated secondary state. In the case of the Ekman boundary flow two wave modes are linearly unstable over a given range of the Reynolds number. The presence of more than one unstable wave disturbance enriches the possible dynamic behavior that can be expected. One purpose of the asymptotic analysis is to qualitatively characterize the observable dynamics in a neighborhood of criticality. In itself this provides insight into the nature of the system under study. Furthermore if one is fortuitous, the prediction has a range of validity that extends well beyond any rigorously justifiable domain.

The physical situation considered is the simultaneous growth of the two Ekman wave modes upon an undisturbed Ekman flow. It should be pointed out that this may be different than the evolution of a wave system consisting of one pre-existing finite amplitude wave subject to the onset of a second wave if the magnitude of the finite amplitude wave is sufficiently large.

The new effects introduced into the problem consist of wave-wave interactions. In addition to the previously considered wave-mean flow effects the two waves couple to produce overtones which interact with both waves and mean flow. A stream function can no longer be introduced to simplify the computations. These complications can be overcome in a fairly straight forward generalization of the single mode case albeit, the computational work becomes somewhat more involved. The nonlinear perturbation equations must now contain variations along all three coordinate axes and so assume the form:

$$\frac{\partial u^*}{\partial t} + U_E\frac{\partial u^*}{\partial x} + V_E\frac{\partial u^*}{\partial y} + w^*\frac{\partial U_E}{\partial z} + S_1 = -\frac{\partial p^*}{\partial x} + \frac{2}{R}v^* + \frac{1}{R}\nabla^2 u^* \tag{1}$$

$$\frac{\partial v^*}{\partial t} + U_E\frac{\partial v^*}{\partial x} + V_E\frac{\partial v^*}{\partial y} + w^*\frac{\partial V_E}{\partial z} + S_2 = -\frac{\partial p^*}{\partial y} - \frac{2}{R}u^* + \frac{1}{R}\nabla^2 v^* \tag{2}$$

$$\frac{\partial w^*}{\partial t} + U_E\frac{\partial w^*}{\partial x} + V_E\frac{\partial w^*}{\partial y} + S_3 = -\frac{\partial p^*}{\partial z} + \frac{1}{R}\nabla^2 w^* \tag{3}$$

where we have used the notation (from Benney and Gustavson)

$$S_1 = \frac{\partial}{\partial x}(u^*)^2 + \frac{\partial}{\partial y}(u^*v^*) + \frac{\partial}{\partial z}(u^*w^*)$$

$$S_2 = \frac{\partial}{\partial x}(u^*v^*) + \frac{\partial}{\partial y}(v^*)^2 + \frac{\partial}{\partial z}(v^*w^*)$$

$$S_1 = \frac{\partial}{\partial x}(u^*w^*) + \frac{\partial}{\partial y}(v^*w^*) + \frac{\partial}{\partial z}(w^*)^2$$

In addition the incompressibility equation will be

$$\frac{\partial u^*}{\partial x} + \frac{\partial v^*}{\partial y} + \frac{\partial w^*}{\partial z} = 0 \tag{4}$$

The perturbation equations (6.1-3) can be reduced by taking the laplacian, $\triangle$, of (6.3) and eliminating the pressure. When normal mode solutions are sought the resulting linearized boundary value problem is the Orr-Sommerfeld equation of the preceding section. The complimentary equation for the vertical vorticity is obtained by cross differentiating (6.1) and (6.2).

$$\left(\frac{\partial}{\partial t} + U_E\frac{\partial}{\partial x} + V_E\frac{\partial}{\partial y}\right)\triangle w^* - \frac{\partial w^*}{\partial y}\frac{\partial^2}{\partial z^2}V_E - \frac{\partial w^*}{\partial x}\frac{\partial^2}{\partial z^2}U_E$$
$$+ \left(\frac{\partial^2}{\partial x^2} + \frac{\partial^2}{\partial y^2}\right)S_3 - \frac{\partial^2 S_1}{\partial x \partial z} - \frac{\partial^2 S_2}{\partial y \partial z} = -\frac{2}{R}\frac{\partial \eta^*}{\partial z} + \frac{1}{R}\triangle\triangle w^* \tag{5}$$

$$\left(\frac{\partial}{\partial t} + U_E\frac{\partial}{\partial x} + V_E\frac{\partial}{\partial y}\right)\eta^* + \frac{\partial w^*}{\partial x}\frac{\partial}{\partial z}V_E - \frac{\partial w^*}{\partial y}\frac{\partial}{\partial z}U_E$$
$$+ \frac{\partial S_2}{\partial x} - \frac{\partial S_1}{\partial y} = \left(\frac{2}{R}\frac{\partial w^*}{\partial z} + \frac{1}{R}\triangle\eta^*\right) \tag{6}$$

The velocity components are obtained from the relations,

$$\frac{\partial u^*}{\partial x} + \frac{\partial v^*}{\partial y} = -\frac{\partial w^*}{\partial z} \tag{7}$$

$$\frac{\partial u^*}{\partial y} + \frac{\partial v^*}{\partial x} = \eta^* \tag{8}$$

For the wave modes $u^* = \hat{u}(z)e^{i(\alpha x+\beta y)}$ and $v^* = \hat{v}(z)e^{i(\alpha x+\beta y)}$ (6.7-8) determine the relationships,

$$\hat{u} = \frac{i}{l^2}(\alpha\frac{d\hat{w}}{dz} + \beta\hat{\eta}) \tag{9}$$

$$\hat{v} = \frac{i}{l^2}(\beta\frac{d\hat{w}}{dz} - \alpha\hat{\eta}) \tag{10}$$

with the wave modes $\eta^* = \hat{\eta}(z)e^{i(\alpha x+\beta y)}$ and $w^* = \hat{w}(z)e^{i(\alpha x+\beta y)}$, where each fluctuating quantity (i.e. u', v', w') has a fourier series representation. In the two wave interaction the coefficients assume the form (to leading order);

$$f(x,y,z,t) = (Af_{1000} + A^2A^*f_{2100} + ABB^*f_{1011})e(\alpha,\beta,l_1c_{1r})$$

$$+(Bf_{0010} + B^2B^*f_{0021} + AA^*Bf_{1110})e(\gamma,\delta,l_2c_{2r})$$

$$(A^2f_{2000})e(2\alpha,2\beta,2l_1c_{1r}) + (B^2f_{0020})e(2\gamma,2\delta,2l_2c_{2r})$$

$$+(ABf_{1010})e(\alpha+\gamma,\beta+\delta,l_1c_{1r}+l_2c_{2r}) + (AB^*f_{1001})e(\alpha-\gamma,\beta-\delta,l_1c_{1r}-l_2c_{2r})$$

$$+ (*) \tag{11}$$

Here $e(\alpha,\beta,l_1c_{1r})$ is a concatenation for $e^{i(\alpha x+\beta y-l_1c_{1r}t)}$ while the subscripts on the coefficients associated with the fluctuating quantity denote respectively the power of the amplitudes A, A^*, B, and B^* which multiply it. $(*)$ signifies the complex conjugates of all terms which are explicitly given in the expansion.

A typical expansion representing the product of two fluctuating quantities, f(x,y,z,t) and g(x,y,z,t) is given by:

$$f(x,y,z,t)\cdot g(x,y,z,t) = AA^{*}f_{1000}g_{0100} + BB^{*}f_{0010}g_{0001}$$

$$+(A^{2}A^{*}(f_{0100}g_{2000} + f_{2000}g_{0100}) + ABB^{*}(f_{0010}g_{1001}$$

$$+f_{0001}g_{1010} + f_{1010}g_{0001} + f_{1001}g_{0010}))e(\alpha,\beta,l_1c_{1r})$$

$$(AA^{*}B(f_{1000}g_{0110} + f_{0100}g_{1010} + f_{1010}g_{0100} + f_{0110}g_{1000}$$

$$(B^{2}B^{*}(f_{0001}g_{0020} + f_{0020}g_{0001}))e(\gamma,\delta,l_2c_{2r})$$

$$(A^{2}f_{1000}g_{1000})e(2\alpha,2\beta,2l_1c_{1r}) + (B^{2}f_{0010}g_{0010})e(2\gamma,2\delta,2l_2c_{2r})$$

$$(AB(f_{1000}g_{0010} + f_{0010}g_{1000}))e(\alpha+\gamma,\beta+\delta,l_1c_{1r}+l_2c_{2r})$$

$$(AB^{*}(f_{1000}g_{0001} + f_{0001}g_{1000}))e(\alpha-\gamma,\beta-\delta,l_1c_{1r}-l_2c_{2r})$$

$$(*) \tag{12}$$

Averages are now taken over the x-y plane. The mean flow equations are:

$$\frac{\partial\bar{u}}{\partial t} + \frac{\partial}{\partial z}\overline{u'w'} = \frac{2}{R}\bar{v} + \frac{1}{R}\frac{\partial^2\bar{u}}{\partial z^2} \tag{13}$$

$$\frac{\partial\bar{v}}{\partial t} + \frac{\partial}{\partial z}\overline{v'w'} = -\frac{2}{R}\bar{u} + \frac{1}{R}\frac{\partial^2\bar{u}}{\partial z^2} \tag{14}$$

The equations for the fluctuating quantities are obtained from (6.1-3) by subtraction of the mean flow equations. We find

$$\frac{\partial u'}{\partial t} + U_M\frac{\partial u'}{\partial x} + V_M\frac{\partial u'}{\partial y} + w'\frac{\partial U_M}{\partial z} + S_1' - \overline{S_1'} = -\frac{\partial p'}{\partial x} + \frac{2}{R}v' + \frac{1}{R}\nabla^2 u' \tag{15}$$

$$\frac{\partial v'}{\partial t} + U_M\frac{\partial v'}{\partial x} + V_M\frac{\partial v'}{\partial y} + w'\frac{\partial V_M}{\partial z} + S_2' - \overline{S_2'} = -\frac{\partial p'}{\partial y} - \frac{2}{R}u' + \frac{1}{R}\nabla^2 v' \tag{16}$$

$$\frac{\partial w'}{\partial t} + U_M\frac{\partial w'}{\partial x} + V_M\frac{\partial w'}{\partial y} + S_3' - \overline{S_3'} = -\frac{\partial p'}{\partial z} + \frac{1}{R}\nabla^2 w' \tag{17}$$

with $S_1' = \frac{\partial}{\partial x}(u')^2 + \frac{\partial}{\partial y}(u'v') + \frac{\partial}{\partial z}(u'w')$ and $U_M = U_E + \bar{u}$ etc ... (6.15-17) admit the vertical vorticity formulation,

$$(\frac{\partial}{\partial t} + U_M\frac{\partial}{\partial x} + V_M\frac{\partial}{\partial y})\triangle w' - \frac{\partial w'}{\partial y}\frac{\partial^2}{\partial z^2}V_M - \frac{\partial w'}{\partial x}\frac{\partial^2}{\partial z^2}U_M$$

$$+(\frac{\partial^2}{\partial x^2} + \frac{\partial^2}{\partial y^2})S_3' - \frac{\partial^2 S_1{}'}{\partial x\partial z} - \frac{\partial^2 S_2{}'}{\partial y\partial z} = -\frac{2}{R}\frac{\partial \eta'}{\partial z} + \frac{1}{R}\triangle\triangle w' \tag{18}$$

$$(\frac{\partial}{\partial t} + U_M\frac{\partial}{\partial x} + V_M\frac{\partial}{\partial y})\eta' + \frac{\partial w'}{\partial x}\frac{\partial}{\partial z}V_M - \frac{\partial w'}{\partial y}\frac{\partial}{\partial z}U_M$$

$$+\frac{\partial S_2'}{\partial x} - \frac{\partial S_1'}{\partial y} = (\frac{2}{R}\frac{\partial w'}{\partial z} + \frac{1}{R}\triangle\eta') \tag{19}$$

Observe that (6.5-6) and (6.18-19) are rather identical in form. This is to be expected since η^* and w^* have zero mean. The nonlinear terms involving S_1, S_2, S_3, must now be computed in terms of the fourier and Stuart-Watson expansions of η', and w', a task that requires a formidable amount of labor even after symmetry is exploited. The reader will be spared the details and the results will merely be stated at the correct order where each term appears.

The amplitude equations relevant to the two wave interaction are the natural extension of (4.23).

$$\frac{dA}{dt} = l_1 c_{1i} A + k_1 A^2 A + m_1 B B^* A + o(A^5, B^2A^3, B^4A)$$

$$\frac{dB}{dt} = l_2 c_{2i} B + k_2 B^2 B + m_2 A A^* B + o(B^5, A^2B^3, A^4B) \tag{20}$$

As before the Landau constants k_1 and k_2 arise from the interaction of the mean flow distortion with the fundamental harmonic as well as the self-interaction of the fundamental on its second harmonic. The new features pertinent to the two wave problem are the coupling constants m_1 and m_2 . These nonlinear modifications are brought about through the interaction of each wave with the mean flow distortion induced by the other remaining wave, and also the wave-wave interaction coupling with the fundamentals.

Again the main features of the amplitude equations are salient. For example three new possibilities can arise; (1) Mode-mode suppression whereby the presence of a first instability increases the apparent critical Reynolds number of the second instability. (or mode-mode excitation wherein the first instability decreases the apparent critical Reynolds number). (2) Intermittency with the waves alternately dominating in close proximity of each other. (3) Transition from equilibrium to unbounded growth (in which case the equations will ultimately fail to hold but may still be useful in predicting the onset of a transition).

The fluctuating quantities are assumed to have the form of a fourier series representing a two wave interaction. Thus

$$
\begin{gathered}
w' = w_{\alpha,\beta} e(\alpha, \beta, l_1 c_{1r}) + w_{\gamma,\delta} e(\gamma, \delta, l_2 c_{2r}) + \\
w_{2\alpha,2\beta} e(2\alpha, 2\beta, 2l_1 c_{1r}) + w_{2\gamma,2\delta} e(2\gamma, 2\delta, 2l_2 c_{2r}) \\
w_{\alpha+\gamma,\beta+\delta} e(\alpha+\gamma, \beta+\delta, l_1 c_{1r} + l_2 c_{2r}) + w_{\alpha-\gamma,\beta-\delta} e(\alpha-\gamma, \beta-\delta, l_1 c_{1r} - l_2 c_{2r}) \\
+ (*)
\end{gathered} \tag{21}
$$

$$
\begin{gathered}
\eta' = \eta_{\alpha,\beta} e(\alpha, \beta, l_1 c_{1r}) + \eta_{\gamma,\delta} e(\gamma, \delta, l_2 c_{2r}) + \\
\eta_{2\alpha,2\beta} e(2\alpha, 2\beta, 2l_1 c_{1r}) + \eta_{2\gamma,2\delta} e(2\gamma, 2\delta, 2l_2 c_{2r}) \\
\eta_{\alpha+\gamma,\beta+\delta} e(\alpha+\gamma, \beta+\delta, l_1 c_{1r} + l_2 c_{2r}) + \eta_{\alpha-\gamma,\beta-\delta} e(\alpha-\gamma, \beta-\delta, l_1 c_{1r} - l_2 c_{2r}) \\
+ (*)
\end{gathered} \tag{22}
$$

where typically $w_{\alpha,\beta} = (Aw_{1000} + A^2 A^* w_{2100} + ABB^* w_{1011})$ and the other coefficients are given similarly in accordance with the appropriate generalization of Stuart-Watson theory, equation (6.11).

Each fourier component then gives rise to a system of P.D.E.s. Corresponding to $e^{i(\alpha x + \beta y - l_1 c_{1r} t)}$ there results the set,

$$\left[(\frac{\partial}{\partial t}+il_1c_{1r})+i\alpha U_M+i\beta V_M\right](D^2-(\alpha^2+\beta^2))w_{\alpha,\beta}$$
$$-i\beta(D^2V_M)w_{\alpha,\beta}-i\alpha(D^2U_M)w_{\alpha,\beta}+\frac{2}{R}D\eta_{\alpha,\beta}-\frac{1}{R}(D^2-(\alpha^2+\beta^2))^2w_{\alpha,\beta}$$
$$= \quad < Non-Linear\ \ Terms > \tag{23}$$

$$\left[(\frac{\partial}{\partial t}+il_1c_{1r})+i\alpha U_M+i\beta V_M\right]\eta_{\alpha,\beta}$$
$$-i\beta(DU_M)w_{\alpha,\beta}+i\alpha(DV_M)w_{\alpha,\beta}-\frac{2}{R}Dw_{\alpha,\beta}-\frac{1}{R}(D^2-(\alpha^2+\beta^2))\eta_{\alpha,\beta}$$
$$= \quad < Non-Linear\ \ Terms > \tag{24}$$

with D differentiation with respect to z. Mean flow distortion occurs at leading orders AA^* and BB^* and so,

$$\bar{u}(z,t)=AA^*u_{1100}+BB^*u_{0011}+o(A^4,B^4,A^2B^2) \tag{25}$$

$$\bar{v}(z,t)=AA^*v_{1100}+BB^*v_{0011}+o(A^4,B^4,A^2B^2) \tag{26}$$

Finally the ansatz of all this together with the amplitude equations (6.20) allows for the ordering of the two wave problem in terms of the powers of the wave amplitudes. Collecting terms respective problems whose solution govern the temporal evolution of the nonlinear two wave interaction can be formally stated. Ofcourse the symmetry of the $(\alpha,\beta,\gamma,\delta)$ interaction requires that only the (α,β) problem be given. Again the solution of these equations proceeds in a fashion similar to that for the single mode case. The homogeneous eigenfunctions are obtained and then the mean flow corrections and the second harmonics are determined as a forced response to the fundamental. The problem for the interaction of the fundamentals presents no problem as long as $(\alpha\pm\gamma,\beta\pm\delta,l_1c_{1r}\pm l_2c_{2r})$ is not an eigenvalue of the related homogeneous eigenproblem. The Landau constants and the coupling constants are determined by the application of the Fredholm alternative. As before the adjoint eigenfunction is orthogonal to the respective inhomogeneity and this compatibility condition is used for computational purposes. The adjoint eigenproblem, with respect to the inner product $< \phi, \psi >= \int (\phi \cdot \psi^*) dz$, is given by

$$\frac{1}{R}(D^2 - (\alpha^2 + \beta^2))^2\psi + (i\alpha U_E + i\beta V_E - il_1 c^*)(D^2 - (\alpha^2 + \beta^2))\psi$$

$$+ 2(i\alpha DU_E + i\beta DV_E)D\psi + (i\alpha DV_E - i\beta DU_E)N - \frac{2}{R}DN = 0 \qquad (27)$$

$$\frac{1}{R}(D^2 - (\alpha^2 + \beta^2))N + (i\alpha U_E + i\beta V_E - il_1 c^*)N + \frac{2}{R}D\psi = 0 \qquad (28)$$

together with the boundary conditions $\psi = D\psi = N = 0$ at z $= 0$ and $\psi = D^2\psi = DN = 0$ at $z = \infty$. In the following statement of the two wave problem the definitions $l_1 = (\alpha^2 + \beta^2)^{1/2}$, $l_2 = (\gamma^2 + \delta^2)^{1/2}$ are in use. The coefficients (e, g, i) and (f, h, j) are obtained from (s, t, r) by the transformations $(\alpha, \beta, \gamma, \delta) \longrightarrow (\alpha - \gamma, \beta - \delta, \gamma, \delta)$ and $(\alpha, \beta, \gamma, \delta) \longrightarrow (\alpha + \gamma, \beta + \delta, -\gamma, -\delta)$ respectively.

Stuart-Watson Expansion for the Ekman Boundary Layer

The Linear Problem O(A):

$$\frac{1}{R}(D^2-(\alpha^2+\beta^2))^2 w_{1000}-(i\alpha U_E+i\beta V_E-il_1c_1)(D^2-(\alpha^2+\beta^2))w_{1000}+(i\beta D^2V_E+i\alpha D^2U_E)w_{1000}$$
$$-\frac{2}{R}\eta_{1000}=0$$

$$\frac{1}{R}(D^2-(\alpha^2+\beta^2))\eta_{1000}-(i\alpha U_E+i\beta V_E-il_1c_1)\eta_{1000}-i\alpha(DV_E)w_{1000}+i\beta(DU_E)w_{1000}+\frac{2}{R}Dw_{1000}=0$$

The Second Harmonic O(A^2):

$$\frac{1}{R}(D^2-4(\alpha^2+\beta^2))^2 w_{2000}-(2i\alpha U_E+2i\beta V_E-2il_1c_1)(D^2-4(\alpha^2+\beta^2))w_{2000}+(2i\beta D^2V_E+2i\alpha D^2U_E)w_{2000}$$
$$-\frac{2}{R}\eta_{2000}=2(D^3w_{1000})w_{1000}-2(D^2w_{1000})(Dw_{1000})$$

$$\frac{1}{R}(D^2-4(\alpha^2+\beta^2))\eta_{2000}-(2i\alpha U_E+2i\beta V_E-2il_1c_1)\eta_{2000}-2i\alpha(DV_E)w_{2000}+2i\beta(DU_E)w_{2000}$$
$$+\frac{2}{R}Dw_{2000}=-2(Dw_{1000})\eta_{1000}+2w_{1000}(D\eta_{1000})$$

The Mean Flow Distortion O(AA^*):

$$RD(u_{1000}w_{0100}+u_{0100}w_{1000})=2v_{1100}+D^2u_{1100}$$

$$RD(v_{1000}w_{0100}+v_{0100}w_{1000})=-2u_{1100}+D^2v_{1100}$$

The Interaction at O(AB):

$$\frac{1}{R}(D^2-((\alpha+\gamma)^2+(\beta+\delta)^2))^2 w_{1010}-(i(\alpha+\gamma)+U_E+i(\beta+\delta)V_E-i(l_1c_1+l_2c_2))(D^2-((\alpha+\gamma)^2+(\beta+\delta)^2)w_{1010}$$

$$+(i(\beta+\delta)D^2V_E+i(\alpha+\gamma)D^2U_E)w_{1010}-\frac{2}{R}\eta_{1010}=$$

$$s_1(Dw_{1000})w_{0010}+s_2(Dw_{0100})w_{1000}+s_3\eta_{1000}w_{0010}+s_4\eta_{0010}w_{1000}$$

$$t_1(D^3w_{1000})w_{0010}+t_2(D^2w_{1000})(Dw_{0010})+t_3(D^3w_{0010})w_{1000}+t_4(D^2w_{0010})(Dw_{1000})$$

$$t_5(D^2w_{1000})\eta_{0010}+t_6(Dw_{1000})(D\eta_{0010})+t_7(D^2w_{0010})\eta_{1000}+t_8(Dw_{0010})(D\eta_{1000})$$

$$t_9(D\eta_{1000})\eta_{0010}+t_{10}(D\eta_{0010})(\eta_{1000})+t_{11}w_{0010}(D^2\eta_{1000}+t_{12}w_{1000}(D\eta_{0010})$$

$$\frac{1}{R}(D^2-((\alpha+\gamma)^2+(\beta+\delta)^2))\eta_{1010}-(i(\alpha+\gamma)U_E+i(\beta+\delta)V_E-i(l_1c_1+l_2c_2))\eta_{1010}$$

$$-i(\alpha+\gamma)(DV_E)w_{1010}+i(\beta+\delta)(DU_E)w_{1010}+\frac{2}{R}Dw_{1010}=$$

$$r_1(D^2w_{1000})w_{0010}+r_2(D^2w_{0100})w_{1000}+r_3(Dw_{1000})\eta_{0010}+r_4(Dw_{0010})\eta_{1000}$$

$$+r_5\eta_{1000}\eta_{0010}+r_6w_{0010}(\eta_{1000})+r_7w_{1000}(D\eta_{0010})$$

The Problem for the Landau Constant O(A^2A^*):

$$\frac{1}{R}(D^2-(\alpha^2+\beta^2))^2w_{2100}-(i\alpha U_E+i\beta V_E-il_1c_1)(D^2-(\alpha^2+\beta^2)w_{2100}+(i\beta D^2V_E+i\alpha D^2U_E)w_{2100}-\frac{2}{R}\eta_{2100}=$$

$$k_1(D^2-(\alpha^2+\beta^2))w_{1000}+(i\alpha u_{1100}+i\beta v_{1100})(D^2-(\alpha^2+\beta^2))w_{1000}-i\beta(D^2v_{1100})w_{1000}-i\alpha(D^2u_{1100})w_{1000}$$

$$-(\alpha^2+\beta^2)[3(Dw_{0100})w_{2000}+\frac{3}{2}(Dw_{2000})w_{0100}]$$

$$-[\frac{1}{2}(D^3w_{2000})w_{0100}+(D^2w_{2000})(Dw_{0100})-(D^3w_{0100})w_{2000}-\frac{1}{2}(D^2w_{0100})(Dw_{2000})]$$

$$\frac{1}{R}(D^2-(\alpha^2+\beta^2))\eta_{2100}-(i\alpha U_E+i\beta V_E-il_1c_1)\eta_{2100}-i\alpha(DV_E)w_{2100}+i\beta(DU_E)w_{2100}+\frac{2}{R}Dw_{2100}=$$

$$k_1\eta_{1000}+(i\alpha u_{1100}+i\beta v_{1100})\eta_{1000}+i\alpha(Dv_{1100})w_{1000}-i\beta(Du_{1100})w_{1000}$$

$$+[(Dw_{0100})\eta_{2000}-\frac{1}{2}(Dw_{2000})\eta_{0100}-w_{2000}(D\eta_{0100}+\frac{1}{2}w_{0100}(D\eta_{2000})]$$

The Problem for the Coupling coefficient O(ABB^*):

$$\frac{1}{R}(D^2-(\alpha^2+\beta^2))^2 w_{1011} - (i\alpha U_E + i\beta V_E - il_1c_1)(D^2-(\alpha^2+\beta^2))w_{1011}$$

$$+(i\beta D^2 V_E + i\alpha D^2 U_E)w_{1011} - \frac{2}{R}\eta_{1011} =$$

$$m_1(D^2-(\alpha^2+\beta^2))w_{1000}+(i\alpha u_{0011}+i\beta v_{0011})(D^2-(\alpha^2+\beta^2))w_{1000}-i\beta(D^2 v_{0011})w_{1000}-i\alpha(D^2 u_{0011})w_{1000}$$

$$e_1(Dw_{1001})w_{0010} + e_2(Dw_{0010})w_{1001} + e_3\eta_{1001}w_{0010} + e_4\eta_{0010}w_{1001}$$

$$f_1(Dw_{1010})w_{0001} + f_2(Dw_{0001})w_{1001} + f_3\eta_{1010}w_{0001} + f_4\eta_{0001}w_{1010}$$

$$g_1(D^3 w_{1001})w_{0010} + g_2(D^2 w_{1001})(Dw_{0010}) + g_3(D^3 w_{0010})w_{1001} + g_4(D^2 w_{0010})(Dw_{1001})$$

$$g_5(D^2 w_{1001})\eta_{0010} + g_6(Dw_{1001})(D\eta_{0010}) + g_7(D^2 w_{0010})\eta_{1001} + g_8(Dw_{0010})(D\eta_{1001})$$

$$g_9(D\eta_{1001})\eta_{0010} + g_{10}(D\eta_{0010})(\eta_{1001}) + g_{11}w_{0010}(D^2\eta_{1001} + g_{12}w_{1001}(D\eta_{0010})$$

$$h_1(D^3 w_{1010})w_{0001} + h_2(D^2 w_{1010})(Dw_{0001}) + h_3(D^3 w_{0001})w_{1010} + h_4(D^2 w_{0001})(Dw_{1010})$$

$$h_5(D^2 w_{1010})\eta_{0001} + h_6(Dw_{1010})(D\eta_{0001}) + h_7(D^2 w_{0001})\eta_{1010} + h_8(Dw_{0001})(D\eta_{1010})$$

$$h_9(D\eta_{1010})\eta_{0001} + h_{10}(D\eta_{0001})(\eta_{1010}) + h_{11}w_{0001}(D^2\eta_{1010}) + h_{12}w_{1010}(D\eta_{0001})$$

$$\frac{1}{R}(D^2-(\alpha^2+\beta^2))\eta_{1011} - (i\alpha U_E + i\beta V_E - il_1c_1)\eta_{1011}$$

$$-i\alpha(DV_E)w_{1011} + i\beta(DU_E)w_{1011} + \frac{2}{R}Dw_{1011} =$$

$$m_1\eta_{1000} + (i\alpha u_{0011} + i\beta v_{0011})\eta_{1000} + i\alpha(Dv_{0011})w_{1000} - i\beta(Du_{0011})w_{1000}$$

$$i_1(D^2 w_{1001})w_{0010} + i_2(D^2 w_{0010})w_{1001} + i_3(Dw_{1001})\eta_{0010} + i_4(Dw_{0010})\eta_{1001}$$

$$+i_5\eta_{1001}\eta_{0010} + i_6 w_{0010}(\eta_{1001}) + i_7 w_{1001}(D\eta_{0010})$$

$$j_1(D^2 w_{1010})w_{0001} + j_2(D^2 w_{0001})w_{1010} + j_3(Dw_{1010})\eta_{0001} + j_4(Dw_{0001})\eta_{1010}$$

$$+j_5\eta_{1010}\eta_{0001} + j_6 w_{0001}(\eta_{1010}) + j_7 w_{1010}(D\eta_{0001})$$

The Coefficients of Non-Linear Terms:

$$s_1 = s \cdot (\alpha^2 + \beta^2 - \beta\delta - \alpha\gamma)(\gamma^2 + \delta^2)$$

$$s_2 = s \cdot (\alpha^2 + \beta^2)(\gamma^2 + \delta^2 - \delta\beta - \alpha\gamma)$$

$$s_3 = s \cdot (\alpha\delta - \beta\gamma)(\gamma^2 + \delta^2)$$

$$s_4 = s \cdot (\gamma\beta - \alpha\delta)(\alpha^2 + \beta^2)$$

$$t_1 = -t \cdot (\alpha^2 + \beta^2 + \gamma\alpha + \beta\delta)(\gamma^2 + \delta^2)$$

$$t_2 = t \cdot (\alpha^3\gamma + \alpha^2\gamma^2 - \alpha^2\delta^2 + \alpha^2\beta\delta + \alpha\beta^2\gamma + 4\alpha\beta\gamma\delta - \beta^2\gamma^2 + \beta^3\delta + \beta^2\delta^2)$$

$$t_3 = -t \cdot (\gamma^2 + \delta^2 + \alpha\gamma + \beta\delta)(\alpha^2 + \beta^2)$$

$$t_4 = t \cdot (\alpha^2\gamma^2 - \alpha^2\delta^2 + \alpha\gamma^3 + 4\alpha\beta\gamma\delta + \alpha\delta^2\gamma + \beta^2\delta^2 + \beta\gamma^2\delta + \beta\delta^3 - \gamma^2\beta^2)$$

$$t_5 = t \cdot (\alpha^3\delta - \alpha^2\beta\gamma + 2\alpha^2\gamma\delta - 2\alpha\beta\gamma^2 + 2\alpha\beta\delta^2 + \alpha\beta^2\delta - \beta^3\gamma - 2\beta^2\gamma\delta)$$

$$t_6 = t \cdot (2\alpha^2\gamma\delta - 2\alpha\beta\gamma^2 + 2\alpha\beta\delta^2 - 2\beta^2\gamma\delta)$$

$$t_7 = t \cdot (-2\alpha^2\gamma\delta + 2\alpha\beta\gamma^2 - \alpha\gamma^2\delta - 2\alpha\beta\delta^2 - \alpha\delta^3 + 2\beta^2\gamma\delta + \beta\gamma^3 + \beta\gamma\delta^2)$$

$$t_8 = t \cdot (-2\alpha^2\gamma\delta + 2\alpha\beta\gamma^2 - 2\alpha\beta\delta^2 + 2\beta^2\gamma\delta)$$

$$t_9 = t \cdot (-2\alpha^2\delta^2 + 4\alpha\beta\gamma\delta - 2\beta^2\gamma^2)$$

$$t_{10} = t \cdot (-2\alpha^2\delta^2 + 4\alpha\beta\gamma\delta - 2\beta^2\gamma^2)$$

$$t_{11} = t \cdot (\alpha\delta - \gamma\beta)(\gamma^2 + \delta^2)$$

$$t_{12} = t \cdot (\gamma\beta - \alpha\delta)(\alpha^2 + \beta^2)$$

$$r_1 = r \cdot (\alpha\delta - \beta\gamma)(\gamma^2 + \delta^2)$$

$$r_2 = r \cdot (\beta\gamma - \alpha\delta)(\alpha^2 + \beta^2)$$

$$r_3 = -r \cdot (\alpha^2\delta^2 + \alpha^2\gamma^2 + \alpha\gamma\delta^2 + \alpha\gamma^3 + \beta^2\delta^2 + \beta^2\gamma^2 + \beta\delta^3 + \beta\delta\gamma^2)$$

$$r_4 = -r \cdot (\alpha^2\beta\delta + \alpha^3\gamma + \alpha^2\delta^2 + \alpha^2\gamma^2 + \alpha\gamma\beta^2 + \beta^2\delta^2 + \beta^2\gamma^2 + \beta^3\delta)$$

$$r_5 = r \cdot (\alpha^2\beta\gamma + \alpha\gamma^2\delta - \alpha^3\delta - \alpha\beta^2\delta + \alpha\delta^3 + \beta^3\gamma - \beta\gamma\delta^2 - \beta\gamma^3)$$

$$r_6 = r \cdot (\alpha^2 + \beta^2 + \beta\delta + \alpha\gamma)(\gamma^2 + \delta^2)$$

$$r_7 = r \cdot (\gamma^2 + \delta^2 + \alpha\gamma + \beta\delta)(\alpha^2 + \beta^2)$$

with

$$\begin{aligned} s &= \frac{(\alpha+\gamma)^2 + (\beta+\delta)^2}{(\alpha+\gamma)^2(\beta+\delta)^2} \\ t &= \frac{-1}{(\alpha^2+\beta^2)(\gamma^2+\delta^2)} \\ r &= \frac{1}{(\alpha^2+\beta^2)(\gamma^2+\delta^2)} \end{aligned}$$

Four two wave computations: Ekman flow (semi-infinite case)

$Re = 120.$	$Re = 180.$
$\epsilon_1 = -9.0$	$\epsilon_1 = -2.0$
$\alpha_1 = .3$	$\alpha_1 = .4$
$c_1 = (.3928, .01957)$	$c_1 = (.2421, .0179)$
$\epsilon_2 = 9.0$	$\epsilon_2 = 13.0$
$\alpha_2 = .54$	$\alpha_2 = .55$
$c_2 = (.07346, .00140)$	$c_2 = (.0223, .01823)$
$k_1 = (-2.27, 7.37)$	$k_1 = (-2.72, 8.29)$
$k_2 = (-6.38, 2.23)$	$k_2 = (-4.31, 2.25)$
$m_1 = (-35.06, -8.26)$	$m_1 = (-6.11, +3.17)$
$m_2 = (-7.81, -3.09)$	$m_2 = (-29.75, -3.37)$

$Re = 130.$	$Re = 220.$
$\epsilon_1 = -2.0$	$\epsilon_1 = 0.0$
$\alpha_1 = .37$	$\alpha_1 = .3$
$c_1 = (.2711, .00611)$	$c_1 = (.2429, .0268)$
$\epsilon_2 = 7.0$	$\epsilon_2 = 13.0$
$\alpha_2 = .55$	$\alpha_2 = .55$
$c_2 = (.09709, .00592)$	$c_2 = (.02296, .0248)$
$k_1 = (-7.08, 5.21)$	$k_1 = (-5.06, 9.06)$
$k_2 = (-6.37, 1.58)$	$k_2 = (-3.51, 2.05)$
$m_1 = (-19.63, -2.86)$	$m_1 = (-8.16, +4.36)$
$m_2 = (-25.03, -1.76)$	$m_2 = (-33.41, +1.39)$

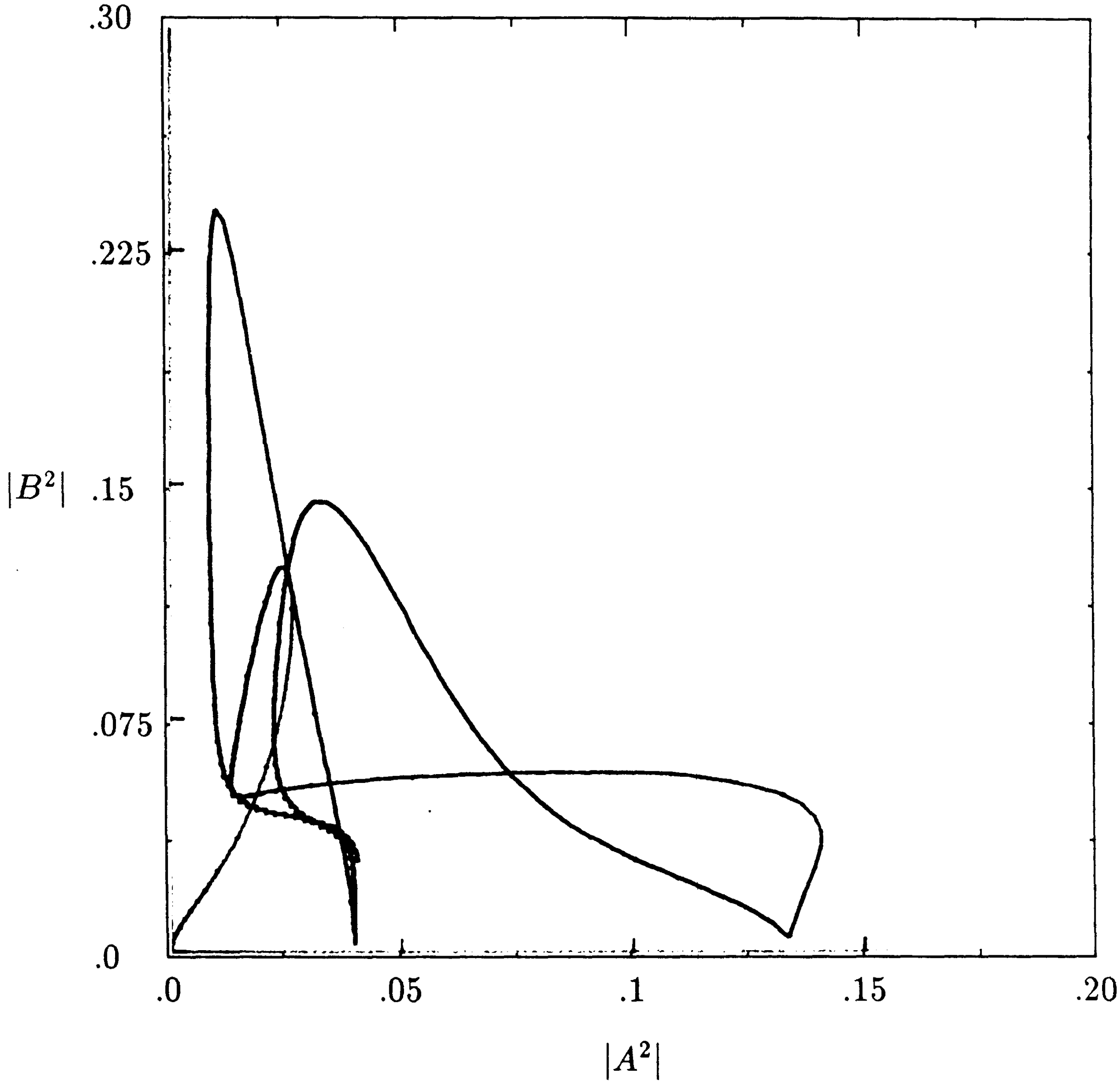

<u>**A Hypothetical two wave interaction displaying intermittency.**</u>

$$\frac{dA}{dt} = .0123A + (-7.58, 1.67)A^2A + (-2.500, -2.508)BB^*A$$

$$\frac{dB}{dt} = .01229B + (-5.27, 1.635)B^2B + (-2.370, 2.720)AA^*B$$

This memo might be read in conjunction with the photographic plates recorded by A.J. Faller (Dynamics of Fluids and Plasmas, Pai Editor, 1966). The coupling coefficients that have been calculated have large negative real parts. There are numerically generated cases where the phase plane is divided into two parts, with trajectories ending up either with $(A_{eq}, 0)$ or $(0, B_{eq})$ depending on initial conditions. In other computations one wave will always suppress the other. That Type II (parallel) waves suppress the first occurrence of the Type I (inviscid) wave is supported by a good deal of evidence (Van Atta, J.F.M). Faller has also observed regions of parameter space exhibiting intermittency of Type I and Type II waves. Ideally this would be modeled in the analogous numerical computation. Although no systematic attempt was made to include every likely two wave interaction this behavior hasn't so far been found numerically. It is however fairly easy to pick coefficients for the model which exhibit this type of behavior. In Figure 6.1 initially linear waves grow along a path in phase space which comes too close to the the unstable equilibrium point (A_{EQ}, B_{EQ}). After a large swing in amplitudes the trajectory approaches the (attracting) limit cycle. The limit cycle displays rapidly oscillating intermittent behavior, where the wave modes alternately predominate.

We mention some of the obvious features of (6.20). If the coupling coefficients are small we expect the equilibration (A_{EQ}, B_{EQ}) to be attained. The magnitude of equilibration amplitudes depends only on the real parts of the landau and coupling constants. If the coupling constants are large there needn't be an equilibrium point, where both A and B are non-zero. A necessary criteria for whether mode A can suppress mode B is that $\alpha_2 c_{i2} < \Re e\{m_2\}|A_{eq}|^2$, where the magnitude of the equilibrium amplitude of A with B = 0 is $|A_{eq}|^2 = \alpha_1 c_{i1}/\Re e\{k_1\}$. We leave as an elementary puzzle for the interested reader the enumeration of all topologically distinct dynamics of the two wave interaction with arbitrary coefficients.

Chapter 7. Resonant Interactions

In this section we formulate two sets of model equations for discrete resonant interactions and give the formulas for their coefficients. The analogy between weakly nonlinear dispersive waves and hydrodynamic stability will be evident. In fact the model equations have appeared in the context of deep water gravity waves (see Equ.s 3.6-3.9 in D.J. Benney (1962)). There is however a distinctive difference between these two situations. The case of surface waves on a body of liquid is one of the classical examples of inviscid irrotational flow. Conservation of energy implies the existence of integrals of the motion and this is reflected in that the model equations have real coefficients. The dissipative nature of waves in the boundary layer with important viscous effects introduces complex coefficients into the equations.

Figure 2-6 (D.K. Lilly, JAS 1966) gives some insight as to how the linear spectrum of basic Ekman flow develops with Reynolds number. This indicates which resonant interactions are allowed (although we still want to know which are the preferred interactions). The model set of equations whose coefficients we wish to derive are for the resonant interactions (1) $k_1 - 2k_2 + k_3 = 0$ and $\omega_1 - 2\omega_2 + \omega_3 = 0$ and (2) $k_1 + k_2 + k_3 + k_4 = \omega_1 + \omega_2 + \omega_3 + \omega_4 = 0$. The first involves resonant coupling between the second harmonic of wave two with the fundamental of waves one and three. It is an asymmetric interaction in that wave two needs to be present for resonance to occur. Waves two and three (or one) will generate wave one (or three), but wave modes one and three will constitute a two wave interaction. The resonant quartet interaction is symmetric in that the presence of any three modes generates the forth. In general the time scale for an $n - wave$ interaction is $o(1/\epsilon^n)$ (where ϵ scales the characteristic wave amplitude) so that low order rather than higher order resonances are likely to be the preferred mechanism when they exist.

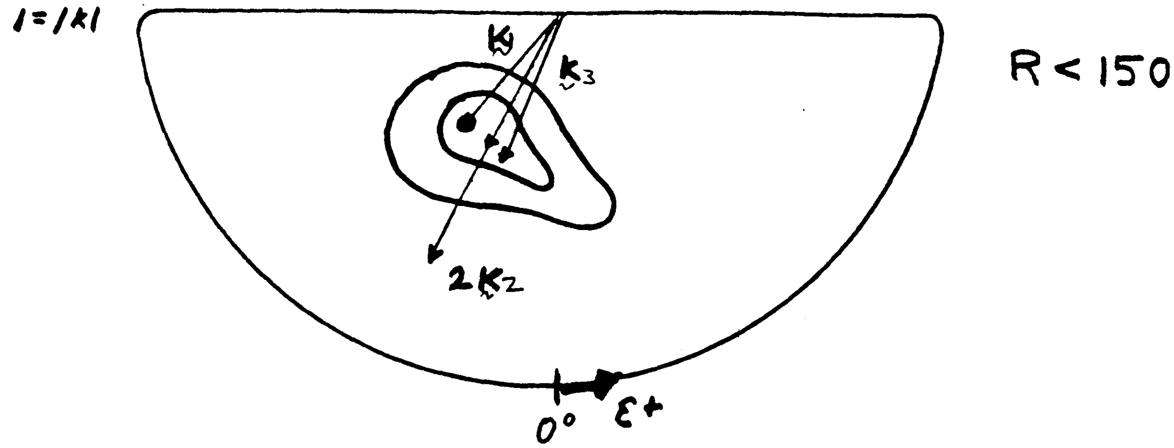

Figure 1: Schematic dispersion diagram for Ekman flow

At Reynolds numbers of roughly 150 the class A mode which is most unstable has characteristics $\alpha_1 \cong .3$, $c_1 \cong .4$ and is oriented 10 degrees clockwise from the geostrophic (0 degrees). The mode which corresponds to the maximal linearly amplified class B mode has wavenumber $\alpha_3 \cong .5$ and phase speed $c_3 \cong 0$ and is directed 10 degrees counterclockwise to the geostrophic. The wave whose second harmonic resonates with these two modes then will have wavenumber $\alpha_2 \cong .4$ and phase speed $c \cong .15$ and is directed approximately 2.5 degrees counterclockwise to the geostrophic. A comparison of the above remarks with figure 2-6(c) shows that the dispersion relation is nearly satisfied by a wave with these properties and indeed this corresponds to a highly unstable wave mode ! In the case where wave A has reached a finite amplitude the nonlinear dispersion relationship has more relevance. However this would entail only a small adjustment of the actual wavenumbers and frequencies of the resonating modes involved.

More generally if a class A mode already exists (at a lower Reynolds number) it should be possible to find a continuous set of resonant interactions of the form (1), which are schematically represented by the three wave vectors. This follows because of the trend to smaller phase speeds and larger wavenumbers for the most highly amplified modes at a fixed angle to the geostrophic as the corresponding wave vector is rotated counterclockwise. (It should be pointed out that 'direct' resonances with weakly damped modes are a possibility. We feel that in a supercritical flow attention should be focused on the linearly unstable waves).

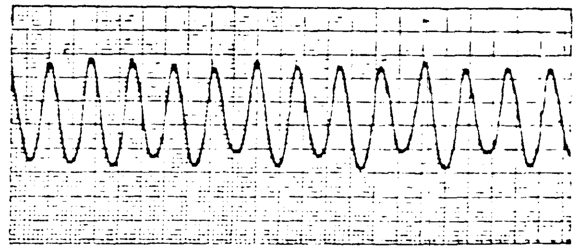

Wave form at Reynolds number = 126

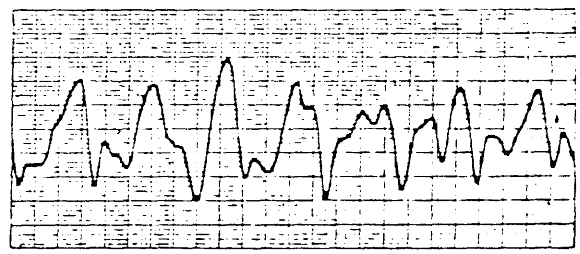

Wave form at Reynolds number = 130

Chart recordings from Tatro & Mollo Christenson. The first occurrence of Class B waves. This was followed by chaotic behavior and the radiation of vertically propagating waves

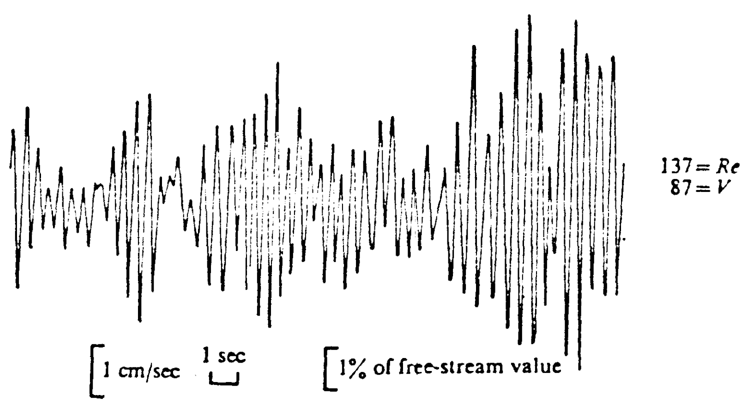

Chart recordings from Caldwell & Van Atta. Observations indicated waves of class A having several different orientations. This led to wave chaos without the presence of class B waves.

This reasoning leads to the conjecture that resonances involving waves of class A alone might occur for the right initial conditions and before class B waves become unstable. This seems to be supported by the observations of Caldwell and Van Atta, and is a more complex situation since a continuous set of wave vector pairs (k_1, k_2) can complete the triad with the most linearly unstable class A wave. The former case in which both a class A wave and a class B wave are involved in a resonant triad could very well be in keeping with the findings of Tatro and Mollo-Christenson. For the triad interaction $k_1 - 2k_2 + k_3 = \omega_1 - 2\omega_2 + \omega_3 = 0$ the model set of asymptotic equations is:

$$\frac{dA}{dt} = l_1 A + A(m_{11}|A|^2 + m_{12}|B|^2 + m_{13}|C|^2) + n_1 B^2 C^*$$

$$\frac{dB}{dt} = l_2 B + B(m_{21}|A|^2 + m_{22}|B|^2 + m_{23}|C|^2) + n_2 ACB^* \tag{1}$$

$$\frac{dC}{dt} = l_3 C + C(m_{31}|A|^2 + m_{32}|B|^2 + m_{33}|C|^2) + n_3 B^2 A^*$$

The determination of the constants l_i, $i = 1, 3$ follows from the respective linear eigenproblems. $m_{i,j}$ are determined by the two wave interaction process; they are either the Landau constants if $i = j$ or the respective coupling constants if $i \neq j$. This leaves n_i, $i = 1, 3$ to be computed. The associated problems at orders B^2C and ACB^* are given on the following pages.

<u>**The Problem at O(B^2C^*):**</u>

$$\frac{1}{R}(D^2-(\alpha^2+\beta^2))^2 w_{002001} - (i\alpha U_E + i\beta V_E - il_1c_1)(D^2-(\alpha^2+\beta^2)w_{002001}$$

$$+(i\beta D^2 V_E + i\alpha D^2 U_E)w_{002001} - \frac{2}{R}\eta_{002001} = n_1(D^2-(\alpha^2+\beta^2))w_{100000}$$

$$+\sigma_1(Dw_{001001})w_{001000} + \sigma_2(Dw_{001000})w_{001001} + \sigma_3\eta_{001001}w_{001000} + \sigma_4\eta_{001000}w_{001001}$$

$$+ox_1(Dw_{002000})w_{000001} + ox_2(Dw_{000001})w_{002000} + ox_3\eta_{002000}w_{000001} + ox_4\eta_{000001}w_{002000}$$

$$+\tau_1(D^3w_{001001})w_{001000} + \tau_2(D^2w_{001001})(Dw_{001000}) + \tau_3(D^3w_{001000})w_{001001} + \tau_4(D^2w_{001000})(Dw_{001001})$$

$$+\tau_5(D^2w_{001001})\eta_{001000} + \tau_6(Dw_{001001})(D\eta_{001000}) + \tau_7(D^2w_{001000})\eta_{001001} + \tau_8(Dw_{001000})(D\eta_{001001})$$

$$+\tau_9(D\eta_{001001})\eta_{001000} + \tau_{10}(D\eta_{001000})(\eta_{001001}) + \tau_{11}w_{001000}(D^2\eta_{001001}) + \tau_{12}w_{001001}(D\eta_{001000})$$

$$+oy_1(D^3w_{002000})w_{000001} + oy_2(D^2w_{002000})(Dw_{000001}) + oy_3(D^3w_{000001})w_{002000} + oy_4(D^2w_{000001})(Dw_{002000})$$

$$+oy_5(D^2w_{002000})\eta_{000001} + oy_6(Dw_{002000})(D\eta_{000001}) + oy_7(D^2w_{000001})\eta_{002000} + oy_8(Dw_{000001})(D\eta_{002000})$$

$$+oy_9(D\eta_{002000})\eta_{000001} + oy_{10}(D\eta_{000001})(\eta_{002000}) + oy_{11}w_{000001}(D^2\eta_{002000}) + oy_{12}w_{002000}(D\eta_{000001})$$

$$\frac{1}{R}(D^2-(\alpha^2+\beta^2))\eta_{002001}-(i\alpha U_E+i\beta V_E-il_1c_1)\eta_{002001}$$

$$(-i\alpha DV_E+i\beta DU_E)w_{002001}+\frac{2}{R}Dw_{002001}=n_1\eta_{100000}$$

$$+\pi_1(D^2w_{001001})w_{001000}+\pi_2(D^2w_{001000})w_{001001}+\pi_3(Dw_{001001})\eta_{001000}+\pi_4(Dw_{001000})\eta_{001001}$$

$$+\pi_5\eta_{001001}\eta_{001000}+\pi_6w_{001000}(\eta_{001001})+\pi_7w_{001001}(D\eta_{001000})$$

$$+oz_1(D^2w_{002000})w_{000001}+oz_2(D^2w_{000001})w_{002000}+oz_3(Dw_{002000})\eta_{000001}+oz_4(Dw_{000001})\eta_{002000}$$

$$+oz_5\eta_{002000}\eta_{000001}+oz_6w_{000001}(\eta_{002000})+oz_7w_{002000}(D\eta_{000001})$$

<u>**The Problem at $O(ACB^*)$:**</u>

$$\frac{1}{R}(D^2-(\gamma^2+\delta^2))^2 w_{100110} - (i\gamma U_E + i\delta V_E - il_2c_2)(D^2-(\gamma^2+\delta^2)w_{100110}$$

$$+(i\delta D^2 V_E + i\gamma D^2 U_E)w_{100110} - \frac{2}{R}\eta_{100110} = n_2(D^2-(\gamma^2+\delta^2))w_{001000}$$

$$+ap_1(Dw_{100010})w_{000100} + ap_2(Dw_{000100})w_{100010} + ap_3\eta_{100010}w_{000010} + ap_4\eta_{000100}w_{100010}$$

$$+ao_1(Dw_{100100})w_{000010} + ao_2(Dw_{000010})w_{100100} + ao_3\eta_{100100}w_{000010} + ao_4\eta_{000010}w_{100100}$$

$$+am_1(Dw_{000110})w_{100000} + am_2(Dw_{100000})w_{000110} + am_3\eta_{000110}w_{100000} + am_4\eta_{100000}w_{000110}$$

$$+bp_1(D^3w_{100010})w_{000100} + bp_2(D^2w_{100010})(Dw_{000100}) + bp_3(D^3w_{000100})w_{100010} + bp_4(D^2w_{000100})(Dw_{100010})$$

$$+bp_5(D^2w_{100010})\eta_{000100} + bp_6(Dw_{100010})(D\eta_{000100}) + bp_7(D^2w_{000100})\eta_{100010} + \tau_8(Dw_{000100})(D\eta_{100010})$$

$$+bp_9(D\eta_{100010})\eta_{000100} + bp_{10}(D\eta_{000100})(\eta_{100010}) + bp_{11}w_{000100}(D^2\eta_{100010}) + bp_{12}w_{100010}(D\eta_{000100})$$

$$+bo_1(D^3w_{100100})w_{000010} + bo_2(D^2w_{100100})(Dw_{000010}) + bo_3(D^3w_{000010})w_{100100} + bo_4(D^2w_{000010})(Dw_{100100})$$

$$+bo_5(D^2w_{100100})\eta_{000010} + bo_6(Dw_{100100})(D\eta_{000010}) + bo_7(D^2w_{000010})\eta_{100100} + bo_8(Dw_{000010})(D\eta_{100100})$$

$$+bo_9(D\eta_{100100})\eta_{000010} + bo_{10}(D\eta_{000010})(\eta_{100100}) + bo_{11}w_{000010}(D^2\eta_{100100}) + bo_{12}w_{100100}(D\eta_{000010})$$

$$+bm_1(D^3w_{000110})w_{100000} + bm_2(D^2w_{000110})(Dw_{100000}) + bm_3(D^3w_{100000})w_{000110} + bm_4(D^2w_{100000})(Dw_{000110})$$

$$+bm_5(D^2w_{000110})\eta_{100000} + bm_6(Dw_{000110})(D\eta_{100000}) + bm_7(D^2w_{100000})\eta_{000110} + bm_8(Dw_{100000})(D\eta_{000110})$$

$$+bm_9(D\eta_{000110})\eta_{100000} + bm_{10}(D\eta_{100000})(\eta_{000110}) + bm_{11}w_{100000}(D^2\eta_{000110}) + bm_{12}w_{000110}(D\eta_{100000})$$

$$
\begin{gathered}
\frac{1}{R}(D^2-(\gamma^2+\delta^2))\eta_{100110}-(i\gamma U_E+i\delta V_E-il_2c_2)\eta_{100110} \\
(-i\gamma DV_E+i\delta DU_E)w_{100110}+\frac{2}{R}Dw_{100110}=n_2\eta_{001000} \\
+cp_1(D^2w_{100010})w_{000100}+cp_2(D^2w_{000100})w_{100010}+cp_3(Dw_{100010})\eta_{000100}+cp_4(Dw_{000100})\eta_{100010} \\
+cp_5\eta_{100010}\eta_{000100}+cp_6w_{000100}(\eta_{100010})+cp_7w_{100010}(D\eta_{000100}) \\
+co_1(D^2w_{100100})w_{000010}+co_2(D^2w_{000010})w_{100100}+co_3(Dw_{100100})\eta_{000010}+co_4(Dw_{000010})\eta_{100100} \\
+co_5\eta_{100100}\eta_{000010}+co_6w_{000010}(\eta_{100100})+co_7w_{100100}(D\eta_{000010}) \\
+cm_1(D^2w_{000110})w_{100000}+cm_2(D^2w_{100000})w_{000110}+cm_3(Dw_{000110})\eta_{100000}+cm_4(Dw_{100000})\eta_{000110} \\
+cm_5\eta_{000110}\eta_{100000}+cm_6w_{100000}(\eta_{000110})+cm_7w_{000110}(D\eta_{100000})
\end{gathered}
$$

The coefficients of the nonlinear terms appearing on the preceding pages are obtained from those of (s, t, r) under the transformations given in the table below.

Table 5.1 Transformations giving the coefficients for nonlinear terms in the Resonant Interaction.

$$(\sigma, \tau, \pi) : (\alpha, \beta, \gamma, \delta) \rightarrow \quad (k_{21}, k_{22}, k_{21} - k_{31}, k_{22} - k_{32})$$

$$(ox, oy, oz) : (\alpha, \beta, \gamma, \delta) \rightarrow \quad (2k_{21}, 2k_{22}, -k_{31}, -k_{32})$$

$$(ap, bp, cp) : (\alpha, \beta, \gamma, \delta) \rightarrow (k_{11} + k_{31}, k_{12} + k_{32}, -k_{21}, -k_{22})$$

$$(ao, bo, co) : (\alpha, \beta, \gamma, \delta) \rightarrow \quad (k_{11} - k_{21}, k_{12} - k_{22}, k_{31}, k_{32})$$

$$(am, bm, cm) : (\alpha, \beta, \gamma, \delta) \rightarrow (k_{11}, k_{12}, k_{31} - k_{21}, k_{32} - k_{22})$$

This is for the resonant interaction $k_1 - 2k_2 + k_3 = \omega_1 - 2\omega_2 + \omega_3 = 0$ Here $k_1 = (k_{11}, k_{12})$ and $k_2 = (k_{21}, k_{22})$ while $\alpha = 2k_{21} - k_{31}$, $\beta = 2k_{22} - k_{32}$, $\gamma = k_{11} - k_{21} + k_{31}$, $\delta = k_{12} - k_{22} + k_{32}$. Also $l_1 = (\alpha^2 + \beta^2)^{1/2}$ and $l_2 = (\gamma^2 + \delta^2)^{1/2}$.

Consider the transformations,

$$A(t) \longrightarrow A_{EQ} + a(t)$$

$$B(t) \longrightarrow B_{EQ} + b(t)$$

$$C(t) \longrightarrow C_{EQ} + c(t)$$

as applied to the model equations (1). Let $\vec{v} = (a, a^*, b, b^*, c, c^*)$ and linearizing about the equilibrium state we obtain the linear system of equations :

$$\frac{d\,\vec{v}}{dt} = [\mathbf{M}] \cdot \vec{v} \tag{2}$$

Then the equilibrium is linearly stable provided the eigenvalues of M have negative imaginary parts. The 6x6 matrix $[\mathbf{M}]$ is given as,

$$[\mathbf{M}] =$$

$$\begin{bmatrix}
(l_1 + 2m_{11}|A_E|^2 + m_{12}|B_E|^2 + m_{13}|C_E|^2) & (m_{11}|A_E|^2) & (m_{12}A_E B_E^* + 2B_E C_E^* n_1) & (m_{12}A_E B_E) & (m_{13}A_E C_E) & (m_{13}A_E C_E + n_1 B_E^2) \\
(m_{11}^* A_E^{*2}) & (l_1 + 2m_{11}^*|A_E|^2 + m_{12}^*|B_E|^2 + m_{13}^*|C_E|^2) & (m_{12}^* A_E^* B_E^*) & (m_{12}^* A_E^* B_E + 2B_E^* C_E n_1^*) & (m_{13}^* A_E^* C_E^* + n_1^* B_E^{*2}) & (m_{13}^* A_E^* C_E) \\
(m_{21}B_E A_E^* + n_2 C_E B_E) & (m_{21}A_E B_E) & (l_2 + m_{21}|A_E|^2 + 2m_{22}|B_E|^2 + m_{23}|C_E|^2) & (m_{22}B_E^2 + A_E C_E n_2) & (m_{23}B_E C_E^* + n_2 A_E B_E^*) & (m_{23}B_E C_E) \\
(m_{21}^* A_E^* B_E^*) & (m_{21}^* B_E^* A_E + n_2^* C_E^* B_E^*) & (m_{22}^* B_E^{*2} + A_E^* C_E^* n_2^*) & (l_2 + m_{21}^*|A_E|^2 + 2m_{22}^*|B_E|^2 + m_{23}^*|C_E|^2) & (m_{23}^* B_E^* C_E^*) & (m_{23}^* B_E^* C_E + n_2^* A_E^* B_E) \\
(m_{31}C_E A_E^*) & (m_{31}C_E A_E + n_3 B_E^2) & (m_{32}C_E B_E^* + 2n_3 B_E A_E^*) & (m_{32}C_E B_E) & (l_3 + m_{31}|A_E|^2 + m_{32}|B_E|^2 + 2m_{33}|C_E|^2) & (m_{33}C_E^2) \\
(m_{31}^* C_E^* A_E^* + n_3^* B_E^{*2}) & (m_{31}^* C_E^* A_E) & (m_{32}^* C_E^* B_E^*) & (m_{32}^* C_E^* B_E + 2B_E^* A_E n_3) & (m_{33}^* C_E^{*2}) & (l_3 + m_{21}^*|A_E|^2 + m_{32}^*|B_E|^2 + 2m_{33}^*|C_E|^2)
\end{bmatrix}$$

The model asymptotic equations for the resonant quartet interaction, (2), are given by :

$$
\begin{aligned}
\frac{dA}{dt} &= l_1 A + A(m_{11}|A|^2 + m_{12}|B|^2 + m_{13}|C|^2 + m_{14}|D|^2) + n_1(BCD)^* \\
\frac{dB}{dt} &= l_2 B + B(m_{21}|A|^2 + m_{22}|B|^2 + m_{23}|C|^2 + m_{24}|D|^2) + n_2(ACD)^* \\
\frac{dC}{dt} &= l_3 C + C(m_{31}|A|^2 + m_{32}|B|^2 + m_{33}|C|^2 + m_{34}|D|^2) + n_3(ABD)^* \\
\frac{dD}{dt} &= l_4 D + D(m_{41}|A|^2 + m_{42}|B|^2 + m_{43}|C|^2 + m_{44}|D|^2) + n_4(BCD)^*
\end{aligned}
\tag{3}
$$

Here the equations for n_i, $i = 1, \ldots, n_4$ can be obtained from the problem at order ACB^* by a suitable adjustment of the subscripts and coefficients that appear there.

Chapter 8. Modulation Theory

It should be emphasized that the results obtained from the preceding Stuart-Watson expansion contain only the first terms of an asymptotic series. In a neighborhood of the critical point the growth rate $\alpha c_i \sim d|R - R_c|$ can be chosen arbitrarily small. It is in this limiting sense that there is agreement with the exact analytical solution for the amplification of a discrete mode of a given wavenumber. Post critically the spectrum will have a range of wavenumbers and phase velocities (connected by a dispersion relationship) which correspond to unstable wave modes. To permit a critical assessment of the weakly non linear wave theories based upon observability, it is desirable to provide a framework in which waves in a narrow wave band can interact. In this section attention is focused on the periodic wave envelope of a group of waves with the most unstable wave at the center of the spectrum. The equations address the question of the stability of the most unstable wave to sideband modes or more generally the development of modulations upon the wave envelope. The description of parallel shear flow instabilities in terms of wave envelopes (also called modulated wave trains) was first given by Stuart and Stewartson (J.F.M. 1971). The work in this chapter is an adaptation of that paper to Ekman flow, with an aim towards a future numerical study of the non-linear Schrödinger equation. The papers of C.S. Bretherton and E.A. Spiegel (Phys. Letters, 1983), and Y. Kuromoto (Prog. Theor. Phys. Suppl., 1978) indicate the kinds of instabilities that can develop from an initial band of wave modes, when nonlinear and dispersive effects are included in the interaction. In the case of a continuous spectrum of participating modes the appropriate model would be a wave packet.

The initial value problem is used as a guide to suggest the appropriate scales. By employing the method of steepest descent (Stuart, *ibid*) it can be shown that in the 'far field' approximation ($|x - c_g t| \ll |a_2 t|$) the eigenfunction ψ is given as

$$\psi \sim \chi(z) \cdot (\exp^{i\alpha_m(x - c_m t)}) \cdot \exp^{-\frac{(x-c_g t)^2}{4a_2 t}} \tag{1}$$

where c_g is the group velocity and a_2 is the group velocity dispersion. Here the expansions proceed about the wavenumber, α_m, and phase speed, c_m , of the fastest growing mode (subscripted with m).

The perturbation equations are again (4.4-5) as before

$$\frac{\partial \xi'}{\partial t} + (V_E + \bar{v} + v')\frac{\partial \xi'}{\partial y} + w'\frac{\partial}{\partial z}(\xi_E + \bar{\xi} + \xi') - \overline{v'\frac{\partial \xi'}{\partial y}} - \overline{w'\frac{\partial \xi'}{\partial z}} =$$

$$\frac{2}{R}\frac{\partial u'}{\partial z} + \frac{1}{R}(\frac{\partial^2 \xi'}{\partial y^2} + \frac{\partial^2 \xi'}{\partial z^2})$$

$$\frac{\partial u'}{\partial t} + (V_E + \bar{v} + v')\frac{\partial u'}{\partial y} + w'\frac{\partial}{\partial z}(U_E + \bar{u} + u') - \overline{v'\frac{\partial u'}{\partial y}} - \overline{w'\frac{\partial u'}{\partial z}} =$$

$$\frac{2}{R}v' + \frac{1}{R}(\frac{\partial^2 u'}{\partial y^2} + \frac{\partial^2 u'}{\partial z^2})$$

But now we consider a modulated wave train so that the expansions assume the form:

$$\left.\begin{aligned} u' &= \textstyle\sum_{n=1}^{\infty}(u_n(Y,T,z)\exp^{in\Theta} + (*)) \\ \xi' &= \textstyle\sum_{n=1}^{\infty}(\xi_n(Y,T,z)\exp^{in\Theta} + (*)) \\ \varphi' &= \textstyle\sum_{n=1}^{\infty}(\varphi_n(Y,T,z)\exp^{in\Theta} + (*)) \end{aligned}\right\} \qquad (2)$$

with $\Theta = \alpha(y - ct)$, and moreover where the slow variables $Y = \epsilon^{1/2}(y - c_g t)$ and $T = \epsilon t$ have been introduced. ϵ is now explicitly taken as αc_i. By the chain rule it is readily determined that:

$$\frac{\partial}{\partial y} \longrightarrow \frac{\partial}{\partial y} + \epsilon^{1/2}\frac{\partial}{\partial Y}$$

$$\frac{\partial}{\partial t} \longrightarrow \frac{\partial}{\partial t} + \epsilon\frac{\partial}{\partial T} - \epsilon^{1/2}c_g\frac{\partial}{\partial Y} \qquad (3)$$

The previously used relations still hold so that in the transformed variables we have:

$$\xi_1 = (\varphi_{1zz} - \alpha^2\varphi_1 + 2i\alpha\epsilon^{1/2}\varphi_{1Y} + \epsilon\varphi_{1YY})$$

$$\xi_2 = (\varphi_{2zz} - \alpha^2\varphi_2 + 2i\alpha\epsilon^{1/2}\varphi_{2Y} + \epsilon\varphi_{2YY})$$

$$w_1 = \frac{\partial \varphi_1}{\partial y} + \epsilon^{1/2}\frac{\partial \varphi_1}{\partial Y}; v_1 = -\frac{\partial \varphi_1}{\partial z}$$

$$w_2 = \frac{\partial \varphi_2}{\partial y} + \epsilon^{1/2}\frac{\partial \varphi_2}{\partial Y}; v_2 = -\frac{\partial \varphi_2}{\partial z}$$

$$(4)$$

Gathering terms in the harmonic expansions the following equations are obtained:

$$
\begin{aligned}
&(-i\alpha c\xi_1 - \epsilon^{1/2}c_g\xi_{1Y} + \epsilon\xi_{1T}) + (i\alpha(V_E+\bar{v})\xi_1 + i\alpha\dot{\varphi}_2\xi_1^* - 2i\alpha\dot{\varphi}_1^*\xi_2 \\
&+\epsilon^{1/2}(V_E+\bar{v})\xi_{1Y} - \epsilon^{1/2}\xi_{2Y}\dot{\varphi}_1^* - \epsilon^{1/2}\dot{\varphi}_2\xi_{1Y}^*) + (-i\alpha\varphi_1\frac{\partial^2}{\partial z^2}(V_E+\bar{v}) \\
&-i\alpha\varphi_1^*\dot{\xi}_2 + 2i\alpha\varphi_2\dot{\xi}_1^* - \epsilon^{1/2}\varphi_{1Y}\frac{\partial^2}{\partial z^2}(V_E+\bar{v}) + \epsilon^{1/2}\dot{\xi}_2\varphi_{1Y}^* + \epsilon^{1/2}\varphi_{2Y}\dot{\xi}_1^*) \\
&\qquad = \frac{2}{R}\dot{u}_1 + \frac{1}{R}(\ddot{\xi}_1 - \alpha^2\xi_1 + \epsilon^{1/2}2i\alpha\xi_{1Y} + \epsilon\xi_{1YY})
\end{aligned}
\tag{5}
$$

$$
\begin{aligned}
&(-i\alpha c u_1 - \epsilon^{1/2}c_g u_{1Y} + \epsilon u_{1T}) + (i\alpha(V_E+\bar{v})u_1 + i\alpha\dot{\varphi}_2 u_1^* - 2i\alpha\dot{\varphi}_1^* u_2 \\
&+\epsilon^{1/2}(V_E+\bar{v})u_{1Y} - \epsilon^{1/2}u_{2Y}\dot{\varphi}_1^* - \epsilon^{1/2}\dot{\varphi}_2 u_{1Y}^*) + (-i\alpha\varphi_1(\dot{U}_E+\dot{\bar{u}}) \\
&-i\alpha\varphi_1^*\dot{u}_2 + 2i\alpha\varphi_2\dot{u}_1^* - \epsilon^{1/2}\varphi_{1Y}(\dot{U}_E+\dot{\bar{u}}) + \epsilon^{1/2}\dot{u}_2\varphi_{1Y}^* + \epsilon^{1/2}\varphi_{2Y}\dot{u}_1^*) \\
&\qquad = -\frac{2}{R}\dot{\varphi}_1 + \frac{1}{R}(\ddot{u}_1 - \alpha^2 u_1 + \epsilon^{1/2}2i\alpha u_{1Y} + \epsilon u_{1YY})
\end{aligned}
\tag{6}
$$

together with,

$$
\begin{aligned}
&(-2i\alpha c\xi_2 - \epsilon^{1/2}c_g\xi_{2Y} + \epsilon\xi_{2T}) + (2i\alpha(V_E+\bar{v})\xi_2 - i\alpha\dot{\varphi}_1\xi_1 + \epsilon^{1/2}(V_E+\bar{v})\xi_{2Y} \\
&-\epsilon^{1/2}\dot{\varphi}_1\xi_{1Y}) + (i\alpha\varphi_1\dot{\xi}_1 - 2i\alpha\varphi_2\frac{\partial^2}{\partial z^2}(V_E+\bar{v}) + \epsilon^{1/2}\varphi_{1Y}\dot{\xi}_1 - \epsilon^{1/2}\varphi_{2Y}\frac{\partial^2}{\partial z^2}(V_E+\bar{v})) \\
&\qquad = \frac{2}{R}\dot{u}_2 + \frac{1}{R}(\ddot{\xi}_2 - \alpha^2\xi_2 + \epsilon^{1/2}2i\alpha\xi_{2Y} + \epsilon\xi_{2YY})
\end{aligned}
\tag{7}
$$

$$
\begin{aligned}
&(-2i\alpha c u_2 - \epsilon^{1/2}c_g u_{2Y} + \epsilon u_{2T}) + (2i\alpha(V_E+\bar{v})u_2 - i\alpha\dot{\varphi}_1 u_1 + \epsilon^{1/2}(V_E+\bar{v})u_{2Y} \\
&-\epsilon^{1/2}\dot{\varphi}_1 u_{1Y}) + (i\alpha\varphi_1\dot{u}_1 + 2i\alpha\varphi_2(\dot{U}_E+\dot{\bar{u}}) + \epsilon^{1/2}\varphi_{1Y}\dot{u}_1 + \epsilon^{1/2}\varphi_{2Y}(\dot{U}_E+\dot{\bar{u}})) \\
&\qquad = -\frac{2}{R}\dot{\varphi}_2 + \frac{1}{R}(\ddot{u}_2 - \alpha^2 u_2 + \epsilon^{1/2}2i\alpha u_{2Y} + \epsilon u_{2YY})
\end{aligned}
\tag{8}
$$

The formal expansion has a hierarchy that increases in powers of $\epsilon^{1/2}$,

$$u_1(Y,T,z) = \epsilon^{1/2}u_{11}(Y,T,z) + \epsilon u_{12}(Y,T,z) + \epsilon^{3/2}u_{13}(Y,T,z) + \ldots$$

$$u_2(Y,T,z) = \epsilon u_{21}(Y,T,z) + o(\epsilon^{3/2})$$

$$\bar{u}(Y,T,z) = \epsilon\bar{u}_{01}(Y,T,z) + o(\epsilon^{3/2})$$

$$\bar{v}(Y,T,z) = \epsilon\bar{v}_{01}(Y,T,z) + o(\epsilon^{3/2})$$

$$\varphi_1(Y,T,z) = \epsilon^{1/2}\varphi_{11}(Y,T,z) + \epsilon\varphi_{12}(Y,T,z) + \epsilon^{3/2}\varphi_{13}(Y,T,z) + \ldots$$

$$\varphi_2(Y,T,z) = \epsilon\varphi_{21}(Y,T,z) + o(\epsilon^{3/2}) \tag{9}$$

and where separability allows the representation to be expressed as:

$$\begin{aligned}
u_{11}(Y,T,z) &= A_{11}(Y,T)u_{11}(z) \quad : \quad \varphi_{11}(Y,T,z) = A_{11}(Y,T)\phi_{11}(z) \\
u_{12}(Y,T,z) &= A_{12}(Y,T)u_{12}(z) \quad : \quad \varphi_{12}(Y,T,z) = A_{12}(Y,T)\phi_{12}(z) \\
u_{21}(Y,T,z) &= A_{21}(Y,T)u_{21}(z) \quad : \quad \varphi_{21}(Y,T,z) = A_{21}(Y,T)\phi_{21}(z) \\
\bar{u}_{01}(Y,T,z) &= A_{01}(Y,T)u_{01}(z) \quad : \quad \bar{v}_{01}(Y,T,z) = A_{01}(Y,T)v_{01}(z)
\end{aligned} \tag{10}$$

These substitutions lead to the set of ordered eigenproblems: At order $\epsilon^{1/2}$ the linear eigenproblem is determined.

$$\mathcal{L}\begin{bmatrix} \phi_{11} \\ u_{11} \end{bmatrix} = 0$$

$$\mathcal{L}\begin{bmatrix} \phi_{11} \\ u_{11} \end{bmatrix} = \begin{bmatrix} i\alpha(V_E - c)(\ddot{\phi}_{11} - \alpha^2\phi_{11}) - i\alpha\ddot{V}_E\phi_{11} - \frac{2}{R}\dot{u}_{11} - \frac{1}{R}(\phi_{11}^{iv} - 2\alpha^2\ddot{\phi}_{11} + \alpha^4\phi_{11}) \\ i\alpha(V_E - c)u_{11} + i\alpha\dot{U}_E\phi_{11} + \frac{2}{R}\dot{\phi}_{11} - \frac{1}{R}(\ddot{u}_{11} - \alpha^2 u_{11}) \end{bmatrix}$$

At order ϵ the group velocity is determined by the Fredholm alternative applied to,

$$\mathcal{L}\begin{bmatrix} \phi_{12} \\ u_{12} \end{bmatrix} =$$

$$\begin{bmatrix} (2\alpha^2(V_E - c) + \ddot{V}_E)\phi_{11} + (\frac{4i\alpha}{R} - (V_E - c_g))(\ddot{\phi}_{11} - \alpha^2\phi_{11}) \\ (\frac{2i\alpha}{R} - (V_E - c_g))u_{11} - \dot{U}_E\phi_{11} \end{bmatrix} \tag{11}$$

Then $A_{11Y} = A_{12}$ and $\begin{bmatrix} \varphi_{12} \\ u_{12} \end{bmatrix} = A_{11Y}\begin{bmatrix} \phi_{12} \\ u_{12} \end{bmatrix} + B\begin{bmatrix} \phi_{11} \\ u_{11} \end{bmatrix}$.

The mean flow distortion is found from the set of equations,

$$i\alpha R\frac{d}{dz}(u_{11}^*\phi_{11} - u_{11}\phi_{11}^*) = 2\bar{v}_{01} + \frac{d}{dz}\bar{u}_{01}$$

$$i\alpha R\frac{d}{dz}(\dot{\phi}_{11}\phi_{11}^* - \dot{\phi}_{11}^*\phi_{11}) = -2\bar{u}_{01} + \frac{d}{dz}\bar{v}_{01}$$

so that $A_{01} = A_{11}A_{11}^*$. The second harmonic component yields the set of simultaneous equations,

$$2i\alpha(V_E - c)(\ddot{\phi}_{21} - 4\alpha^2\phi_{21}) - 2i\alpha\ddot{V}_E\phi_{21} - \frac{2}{R}\dot{u}_{21} - \frac{1}{R}(\phi_{21}^{iv} - 8\alpha^2\ddot{\phi}_{21} + 16\alpha^4\phi_{21})$$

$$= i\alpha\dot{\phi}_{11}(\ddot{\phi}_{11} - \alpha^2\phi_{11}) - i\alpha\phi_{11}\frac{d}{dz}(\ddot{\phi}_{11} - \alpha^2\phi_{11})$$

$$2i\alpha(V_E - c)u_{21} + 2i\alpha\dot{U}_E\phi_{21} + \frac{2}{R}\dot{\phi}_{21} - \frac{1}{R}(\ddot{u}_{21} - 4\alpha^2 u_{21})$$

$$= -i\alpha\phi_{11}\dot{u}_{11} + i\alpha\dot{\phi}_{11}u_{11}$$

and the relationship $A_{21} = A_{11}^2$. Finally at order $\epsilon^{3/2}$ the evolution equation is obtained, again by the application of the Fredholm alternative applied to:

$$\mathcal{L}\begin{bmatrix} \varphi_{13} \\ u_{13} \end{bmatrix} =$$

$$\begin{bmatrix} A_{11YY}(2\alpha^2(V_E - c)\phi_{12} - (V_E - c_g)(\ddot{\phi}_{12} - \alpha^2\phi_{12}) - 2i\alpha(V_E - c_g)\phi_{11} + i\alpha c\phi_{11} \\ +\ddot{V}_E\phi_{12} + \frac{4i\alpha}{R}(\ddot{\phi}_{12} - \alpha^2\phi_{12}) + \frac{2}{R}(\ddot{\phi}_{11} - 3\alpha^2\phi_{11})) \\ +A_{11}^2A_{11}^*(i\alpha\ddot{v}_{01}\phi_{11} - i\alpha v_{01}(\ddot{\phi}_{11} - \alpha^2\phi_{11}) + 2i\alpha\dot{\phi}_{11}^*(\ddot{\phi}_{21} - 4\alpha^2\phi_{21}) + i\alpha\phi_{11}^*\frac{d}{dz}(\ddot{\phi}_{21} - 4\alpha^2\phi_{21}) \\ -2i\alpha\phi_{21}\frac{d}{dz}(\ddot{\phi}_{11}^* - \alpha^2\phi_{11}^*) - i\alpha\dot{\phi}_{21}(\ddot{\phi}_{11}^* - \alpha^2\phi_{11}^*)) \\ -A_{11T}(\ddot{\phi}_{11} - \alpha^2\phi_{11}) \\ A_{11YY}(-(V_E - c_g)u_{12} - \dot{U}_E\phi_{12} + \frac{2i\alpha}{R}u_{12} + \frac{1}{R}u_{11}) \\ +A_{11}^2A_{11}^*(-i\alpha v_{01}u_{11} + 2i\alpha\dot{\phi}_{11}^*\phi_{21} - i\alpha\phi_{11}^*\dot{\phi}_{21} - i\alpha\dot{u}_{01}\phi_{11} + i\alpha\phi_{11}^*\dot{u}_{21} - 2i\alpha\phi_{21}\dot{u}_{11}^*) \\ -A_{11T}u_{11} \end{bmatrix}$$

(12)

The evolution equation for the amplitude A_{11} is thus the nonlinear Schrödinger equation.

$$\frac{\partial A_{11}}{\partial T} - \gamma \frac{\partial^2 A_{11}}{\partial Y^2} = \alpha c_i A_{11} - k A_{11}^* A_{11}^2 \tag{13}$$

The constant $-k$ is the Landau constant as expected. The constant γ is a measure of dispersive effects, and is computed from :

$$\gamma = \frac{\begin{array}{c}\int[(2\alpha^2(V_E - c)\phi_{12} - (V_E - c_g)(\ddot{\phi}_{12} - \alpha^2\phi_{12}) - 2i\alpha(V_E - c_g)\phi_{11} \\ + i\alpha c\phi_{11} + \ddot{V}_E\phi_{12} + \frac{4i\alpha}{R}(\ddot{\phi}_{12} - \alpha^2\phi_{12}) + \frac{2}{R}(\ddot{\phi}_{11} - 3\alpha^2\phi_{11})) \cdot \psi^* \\ + (-(V_E - c_g)u_{12} - \dot{U}_E\phi_{12} + \frac{2i\alpha}{R}u_{12} + \frac{1}{R}u_{11}) \cdot N^*]dz\end{array}}{\int[(\ddot{\phi}_{11} - \alpha^2\phi_{11}) \cdot \psi^* + u_{11} \cdot N^*]dz} \tag{14}$$

where (ψ, N) is the adjoint eigenfunction to the linear problem. The nonlinear Schrödinger equation has the plane wave solution,

$$A = \left(\frac{\alpha c_i}{k_r}\right)^{1/2} \exp(-i\frac{k_i}{k_r}\alpha c_i t) \tag{15}$$

and this is modulationally unstable to sidebands when $k_r\gamma_r + k_i\gamma_i < 0$. This is a direct generalization of the Benjamin-Fier criteria for the stability of a Stokes wave, (A.C. Newell, 1969). For the case of two interacting wave envelopes growing from an undisturbed Ekman flow the asymptotic equations would be a coupled set of nonlinear Schrödinger equations.

$$\frac{\partial A}{\partial T} - \gamma_1 \frac{\partial^2 A}{\partial Y^2} = \alpha c_{i1} A + k_1 A^* A^2 + m_1 B B^* A$$

$$\frac{\partial B}{\partial T} - \gamma_2 \frac{\partial^2 B}{\partial Y^2} = \beta c_{i2} B + k_2 B^* B^2 + m_1 A A^* B \tag{16}$$

Coupled Schrödinger equations also serve as model equations in narrow gap Ekman flow, when vorticity waves generated on opposite boundaries begin to merge. The photographs on the next page, (courtesy of W.V.R. Malkus) are taken of Ekman flow, with a gap separation of 5-6 boundary distances. At this Ekman number, the linear theory predicts a nearly overall minimum critical Reynolds number and wave fronts propagating almost radially inward. In the top photograph, orderly finite amplitude rolls develop post critically. At larger Reynolds numbers (the bottom print) a modulational instability becomes visable. Several scales of motion are simultaneously introduced. Secondary instability is initiated (in theory) at locations where the modulation intensifies the transverse vorticity of the primary wave field.

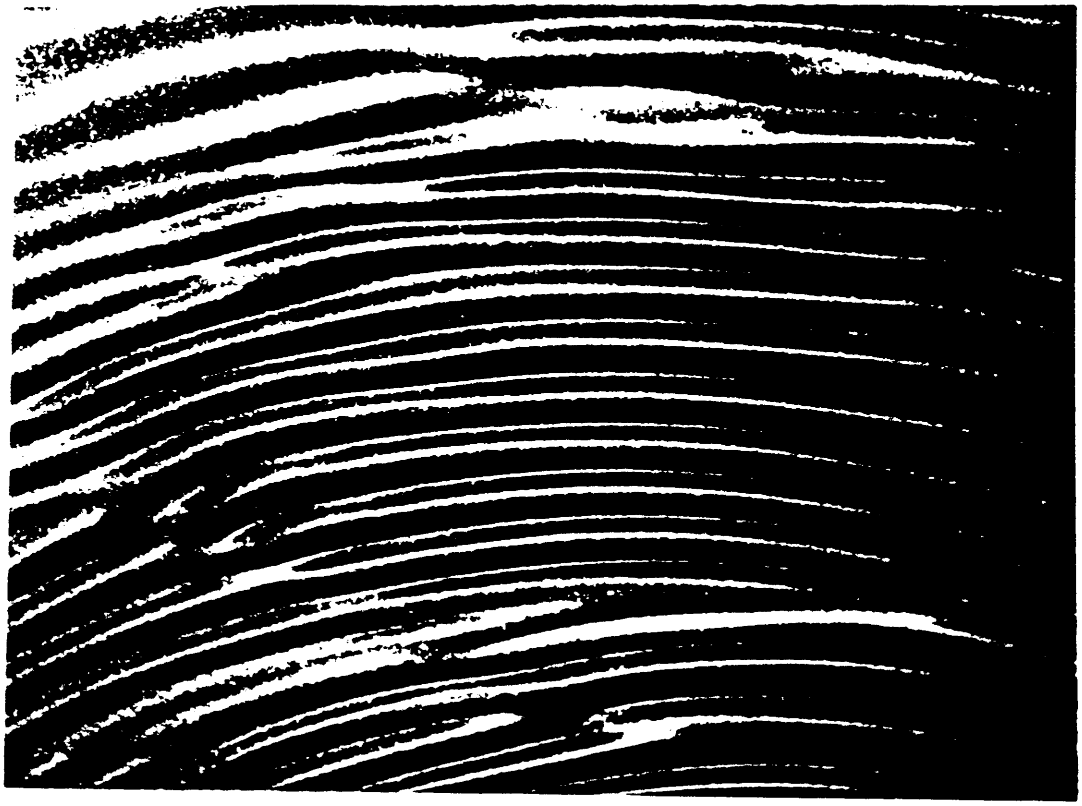

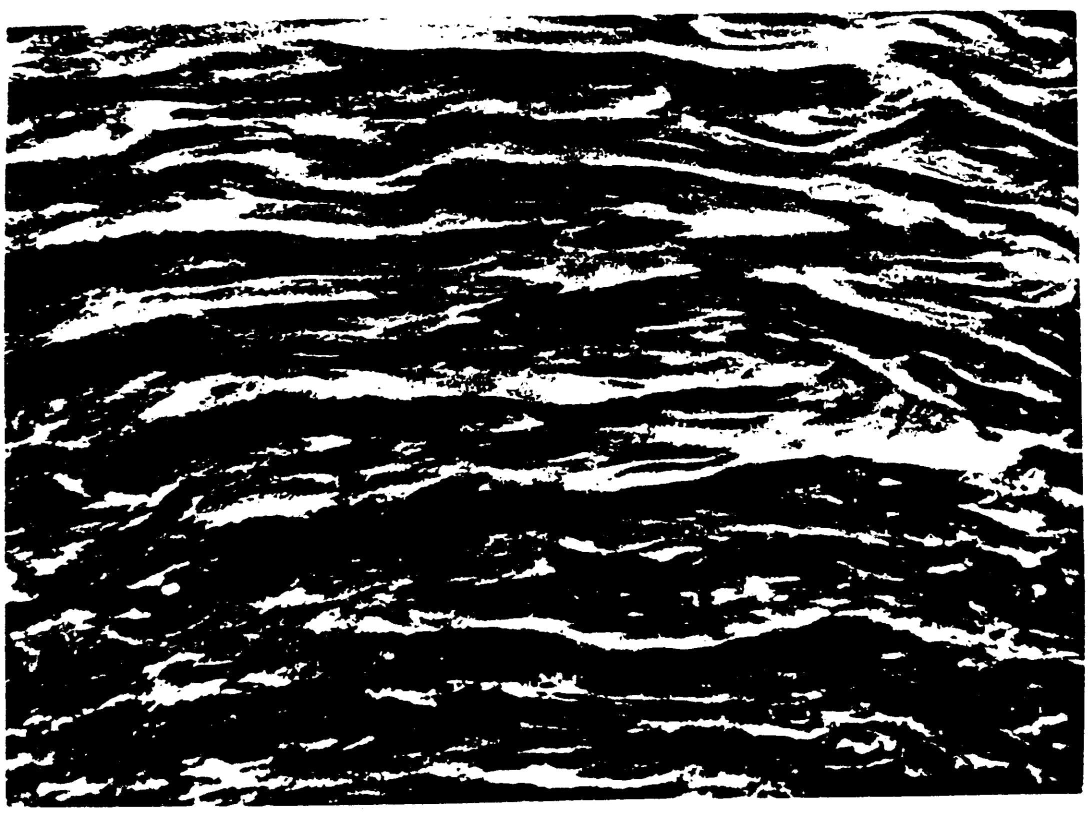

Chapter 9. Secondary Stability of Ekman Flow

We assume a parallel shear flow in a rotating, $\vec{\Omega} = \Omega\hat{k}$, coordinate system. Then the velocity and pressure field satisfies:

$$\frac{d\vec{V}}{dt} = -\nabla p - 2\hat{k}\times\vec{V} + \frac{1}{R}\nabla^2\vec{V} \tag{1}$$

$$\nabla\cdot\vec{V} = 0 \tag{2}$$

We will derive equations for the departure from finite amplitude equilibrium. Here the velocity field has a representation,

$$u(x,y,z,t) = u_B(z) + \sum_{n=-\infty}^{\infty} u_n(z)e^{i\alpha n(x-ct)} + u^*(x-ct,y,z,t)$$

$$v(x,y,z,t) = v_B(z) + \sum_{n=-\infty}^{\infty} v_n(z)e^{i\alpha n(x-ct)} + v^*(x-ct,y,z,t)$$

$$w(x,y,z,t) = \sum_{n=-\infty}^{\infty} w_n(z)e^{i\alpha n(x-ct)} + w^*(x-ct,y,z,t)$$

It is convenient to move into a coordinate system moving with the finite amplitude wave velocity. Then $x' = (x-ct)$ and hence $\partial_t = (\partial_{t'} + c\partial_{x'})$ and $u = (u' - c)$. In this coordinate system (having dropped all primes)

$$\frac{\partial\vec{u}}{\partial t} + \vec{u}\cdot\nabla\vec{u} = -\nabla p - \frac{2}{R}\hat{k}\times\vec{u} + \frac{2}{R}\hat{\jmath}c + \frac{1}{R}\nabla^2\vec{u}$$

$$\nabla\cdot\vec{u} = 0$$

If we let

$$U(x,z) = (u_B(z) + c) + \sum_{n=-\infty}^{\infty} u_n(z)e^{i\alpha nx}$$

$$V(x,z) = v_B(z) + \sum_{n=-\infty}^{\infty} v_n(z)e^{i\alpha nx}$$

$$W(x,z) = \sum_{n=-\infty}^{\infty} w_n(z)e^{i\alpha nx}$$

and

$$u(x,y,z,t) = U(x,z) + u^*(x,y,z,t)$$

$$v(x,y,z,t) = V(x,z) + v^*(x,y,z,t)$$

$$w(x,y,z,t) = W(x,z) + w^*(x,y,z,t)$$

then the full non-linear perturbation equations (which are invariant) are:

$$\frac{\partial \vec{u^*}}{\partial t} + \vec{U} \cdot \nabla \vec{u^*} + \vec{u^*} \cdot \nabla \vec{U} + \vec{u^*} \cdot \nabla \vec{u^*} = -\nabla p^* - \frac{2}{R}\hat{k} \times \vec{u^*} + \frac{1}{R}\nabla^2 \vec{u^*} \tag{3}$$

$$\nabla . \vec{u^*} = 0 \tag{4}$$

We will proceed in a stepwise manner to derive the modal decomposition of (9.3-4). In component form the full non-linear perturbation equations are;

$$\frac{\partial u^*}{\partial t} + U\frac{\partial u^*}{\partial x} + V\frac{\partial u^*}{\partial y} + W\frac{\partial u^*}{\partial z} + u^*U_x + w^*U_z + S_1 = -\frac{\partial p^*}{\partial x} + \frac{2}{R}v^* + \frac{1}{R}\triangle u^*$$

$$\frac{\partial v^*}{\partial t} + U\frac{\partial v^*}{\partial x} + V\frac{\partial v^*}{\partial y} + W\frac{\partial v^*}{\partial z} + u^*V_x + w^*V_z + S_2 = -\frac{\partial p^*}{\partial y} - \frac{2}{R}u^* + \frac{1}{R}\triangle v^*$$

$$\frac{\partial w^*}{\partial t} + U\frac{\partial w^*}{\partial x} + V\frac{\partial w^*}{\partial y} + W\frac{\partial w^*}{\partial z} + u^*W_x + w^*W_z + S_3 = -\frac{\partial p^*}{\partial z} + \frac{1}{R}\triangle w^*$$

$$\frac{\partial u^*}{\partial x} + \frac{\partial v^*}{\partial y} + \frac{\partial w^*}{\partial z} = 0$$

We will now be more specific with regards to the form of the linear 3-D perturbation under investigation. We'll look at the stability of 2-D finite amplitude vorticity waves to that class of 3-D disturbances which have the same periodicity in the downstream direction and arbitrary spanwise periodicity. Therefore

$$\vec{u}^* (x,y,z,t) = \sum_{m=0}^{\infty} \sum_{n=-\infty}^{\infty} [\vec{u}_{n,m} (z) e^{i\alpha nx} e^{i\beta my} e^{im\sigma t} + \vec{u}_{n,-m} (z) e^{i\alpha nx} e^{-i\beta my} e^{-im\tilde{\sigma} t}] \tag{5}$$

with σ being the complex frequency. Note that reality of u^* implies $\vec{u}_{n,m} = \vec{\tilde{u}}_{-n,-m}$ (~ denotes complex conjugation.) For an infinitesimal disturbance, $m = 1$, we have

$$\vec{u}^* (x,y,z,t) = \sum_{n=-\infty}^{\infty} [\vec{u}_{n,1}\, e^{i\alpha nx} e^{i\beta y} e^{i\sigma t} + \vec{u}_{n,-1}\, e^{i\alpha nx} e^{-i\beta y} e^{-i\tilde{\sigma} t}] \tag{6}$$

If for each perturbed quantity in (9.3-4) we substitute an expansion of the form (9.6), neglecting at present nonlinearities, there results a set of equations coupling the modal components of the infinitesimal wave disturbance. These constitute a linear eigenvalue problem in σ, for a 3-D perturbation upon a 2-D finite amplitude wave field:

$$
\begin{aligned}
&[\frac{1}{R}(-k_{n,1}^2 + D^2)^2 - (i\sigma)(-k_{n,1}^2 + D^2)]w_{n,1} - \frac{2}{R}D\eta_{n,1} \\
&+i\alpha nD[(U * u_x)_{n,1} + (V * u_y)_{n,1} + (W * u_z)_{n,1} + (U_x * u)_{n,1} + (U_z * w)_{n,1}] \\
&+i\beta D[(U * v_x)_{n,1} + (V * v_y)_{n,1} + (W * v_z)_{n,1} + (V_x * u)_{n,1} + (V_z * w)_{n,1}] \\
&+ k_{n,1}^2[(U * w_x)_{n,1} + (V * w_y)_{n,1} + (W * w_z)_{n,1} + (W_x * u)_{n,1} + (W_z * w)_{n,1}] = 0
\end{aligned}
\qquad (7)
$$

$$
\begin{aligned}
&[\frac{1}{R}(-k_{n,1}^2 + D^2) - (i\sigma)]\eta_{n,1} + \frac{2}{R}Dw_{n,1} \\
&-i\alpha n[(U * v_x)_{n,1} + (V * v_y)_{n,1} + (W * v_z)_{n,1} + (V_x * u)_{n,1} + (V_z * w)_{n,1}] \\
&+ i\beta[(U * u_x)_{n,1} + (V * u_y)_{n,1} + (W * u_z)_{n,1} + (U_x * u)_{n,1} + (U_z * w)_{n,1}] = 0
\end{aligned}
\qquad (8)
$$

as the vertical component of vorticity is given by $\eta \triangleq (\frac{\partial v}{\partial x} - \frac{\partial u}{\partial y})$ the relations

$$u_{n,1} = (i\alpha nDw_{n,1} + i\beta\eta_{n,1})/k_{n,1}^2$$

$$v_{n,1} = (i\beta Dw_{n,1} - i\alpha n\eta_{n,1})/k_{n,1}^2$$

are obtained, with $k_{n,1}^2 = (n\alpha)^2 + \beta^2$. The convolution product $(F * g)_{n,m} = \sum_{p+q=n} F_p \cdot g_{q,m}$.

The most significant result of the secondary stability calculation of Patera and Orzag is the prediction of transition at Reynolds numbers of the order of 1000, in Poiseuille and Couette flow. This is in agreement with the observations of bursts and the appearance of spots that occur at about this number. The predictions are based on a quasi steady equilibrium approximation which balances 2-D viscous decay rates with convective 3-D growth rates to obtain an instability cutoff.

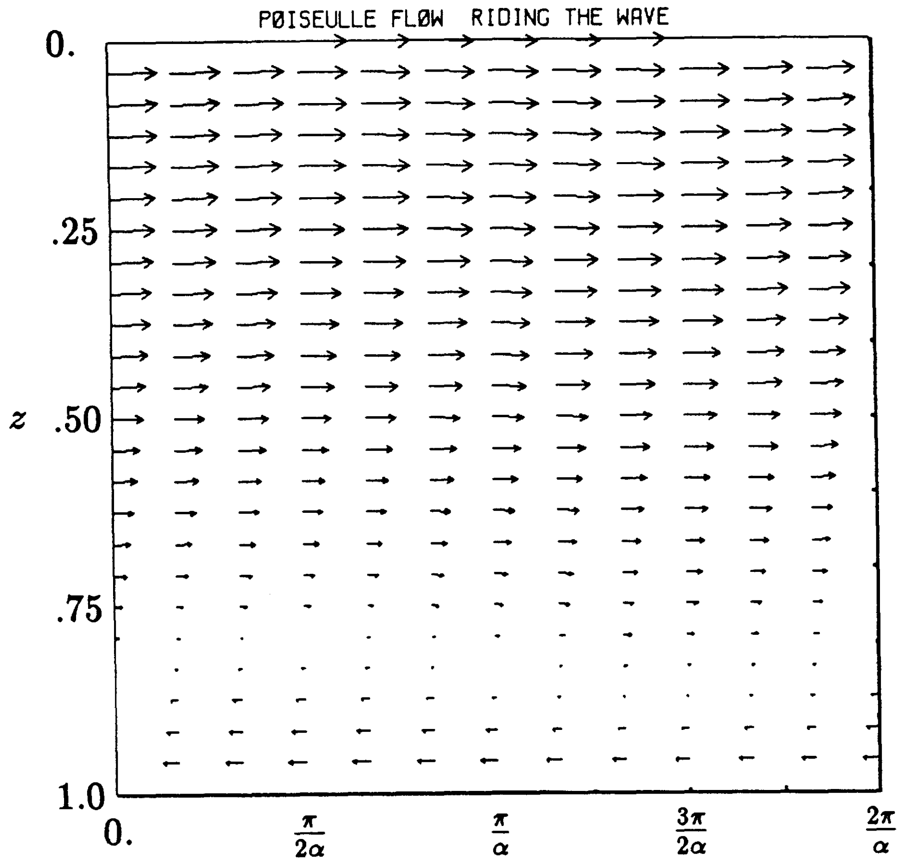
PØISEULLE FLØW RIDING THE WAVE
0.
.25
z .50
.75
1.0
0.
$\frac{\pi}{2\alpha}$
$\frac{\pi}{\alpha}$
$\frac{3\pi}{2\alpha}$
$\frac{2\pi}{\alpha}$

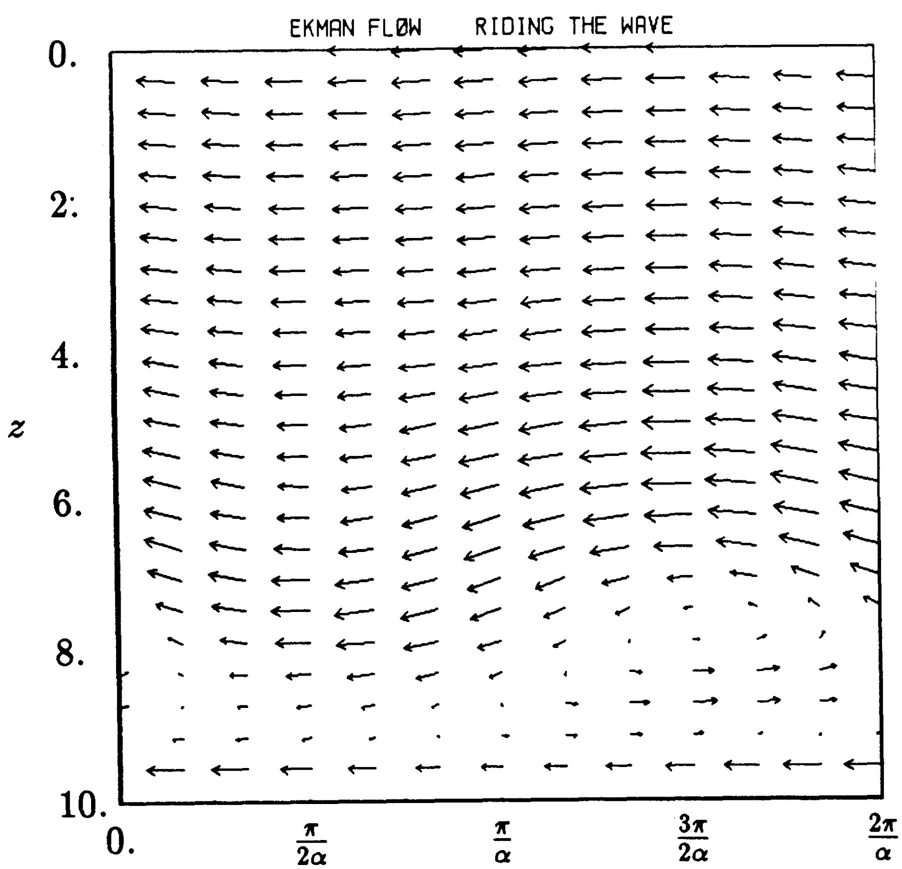
EKMAN FLØW RIDING THE WAVE
0.
2.
4.
z
6.
8.
10.
0.
$\frac{\pi}{2\alpha}$
$\frac{\pi}{\alpha}$
$\frac{3\pi}{2\alpha}$
$\frac{2\pi}{\alpha}$

Figure 9.1 shows the finite amplitude velocity fields for (a) Poiseuille and (b) Ekman flow, in a reference frame moving at the 2-D wave speed. It can be seen that a finite amplitude 2-D wave produces a local vorticity maximum. Early theories attempted to relate secondary instability with local velocity inflections and generalized Rayliegh criteria. A WKB type argument applied around the inflection point would indicate inviscid instability to small length scale disturbances, provided the local Reynolds number was large enough. This argument fails to account for the fundamental physical characteristic of the instability, namely its '3-dimensional' signature. Additionally only a small threshold 2-D amplitude is required to initiate the secondary instability, which can occur prior to the establishment of a local inflection. While a subcritical secondary instability might conceivably produce its own local inflections, the 3-D instability considered here grows from infinitesimal amplitude as a rapidly growing linear perturbation on a 2-D wave field.

For the case of primary transverse vorticity waves, as in Poiseuille flow or the Ekman boundary layer the '3-D' eigenvalue is accurately given by the lowest consistent three mode fourier truncation. For Poiseuille flow this involves the downstream roll ($\leadsto e^{i\beta y}$, the $n = 0$ mode) and two symmetric oblique modes ($\leadsto e^{\pm i\alpha x + i\beta y}$, the $n = \pm 1$ modes). At Reynolds numbers of 1000 each of these modes would individually decay fairly rapidly. Squires theorem precludes the possibility of a linearly unstable downstream roll (which, in the absence of the primary 2-D wave, would have a sinusoidal eigenstructure, i.e. a the solution of a forth order constant coefficient O.D.E.). The primary transverse 2-D wave serves to link the oblique and streamwise fourier components of the secondary perturbation. The streamwise mode is altered near the boundary (inside the viscous sublayer) through coupling with the oblique component (Figure 9.2). A large forced streamwise velocity, u_0^{3d}, response is induced. Strong '3-D' growth results because the downstream mode is very effective in generating power via the correlation $u_0^{3d}(w_0^{3d})^*(dU_M/dz)$. The linear streamwise

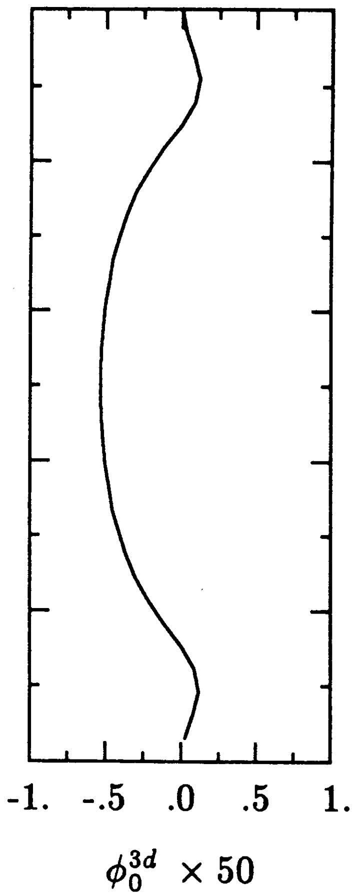
-1.
-.5
.0
.5
1.
$\phi_0^{3d} \times 50$

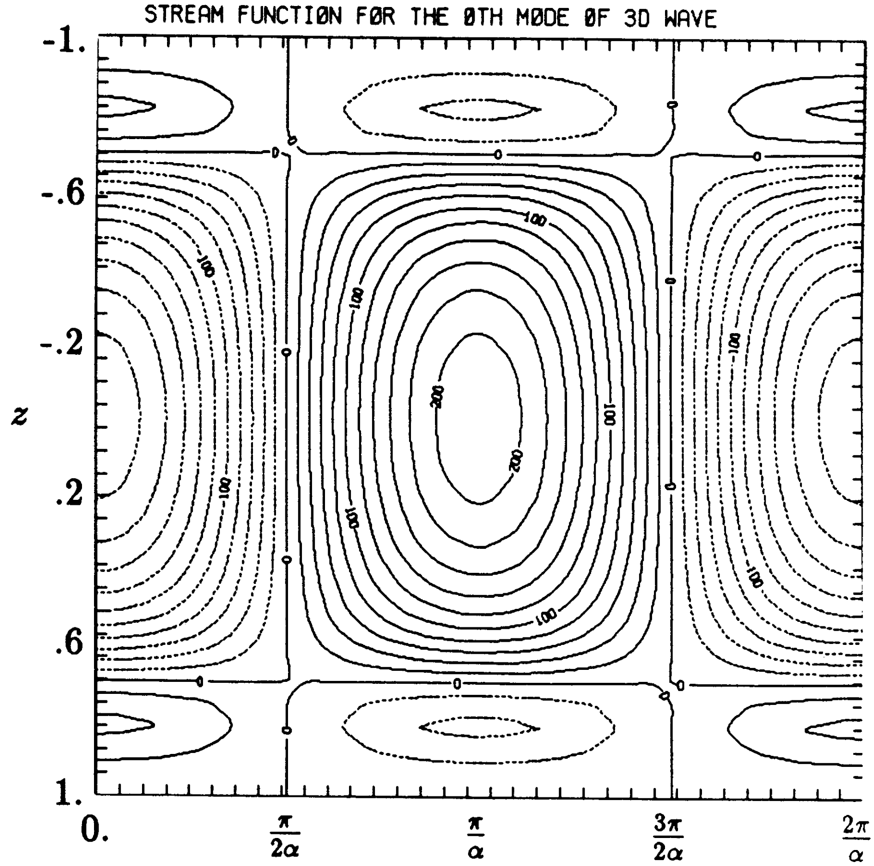
STREAM FUNCTIØN FØR THE ØTH MØDE ØF 3D WAVE
-1.
-.6
-.2
.2
.6
1.
z
0.
$\frac{\pi}{2\alpha}$
$\frac{\pi}{\alpha}$
$\frac{3\pi}{2\alpha}$
$\frac{2\pi}{\alpha}$
0
100
200

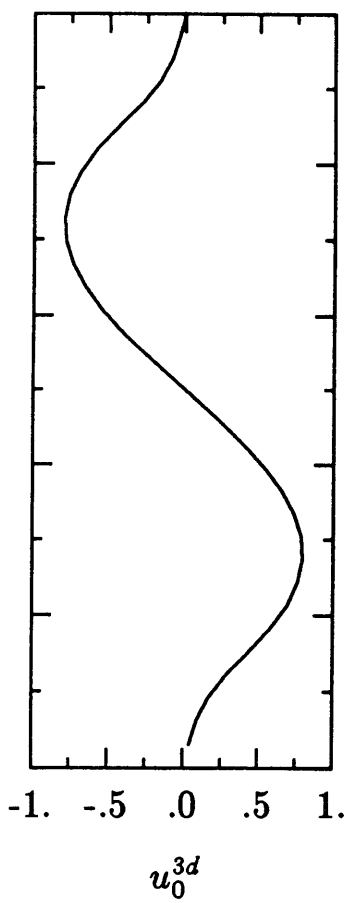
-1.
-.5
.0
.5
1.
u_0^{3d}

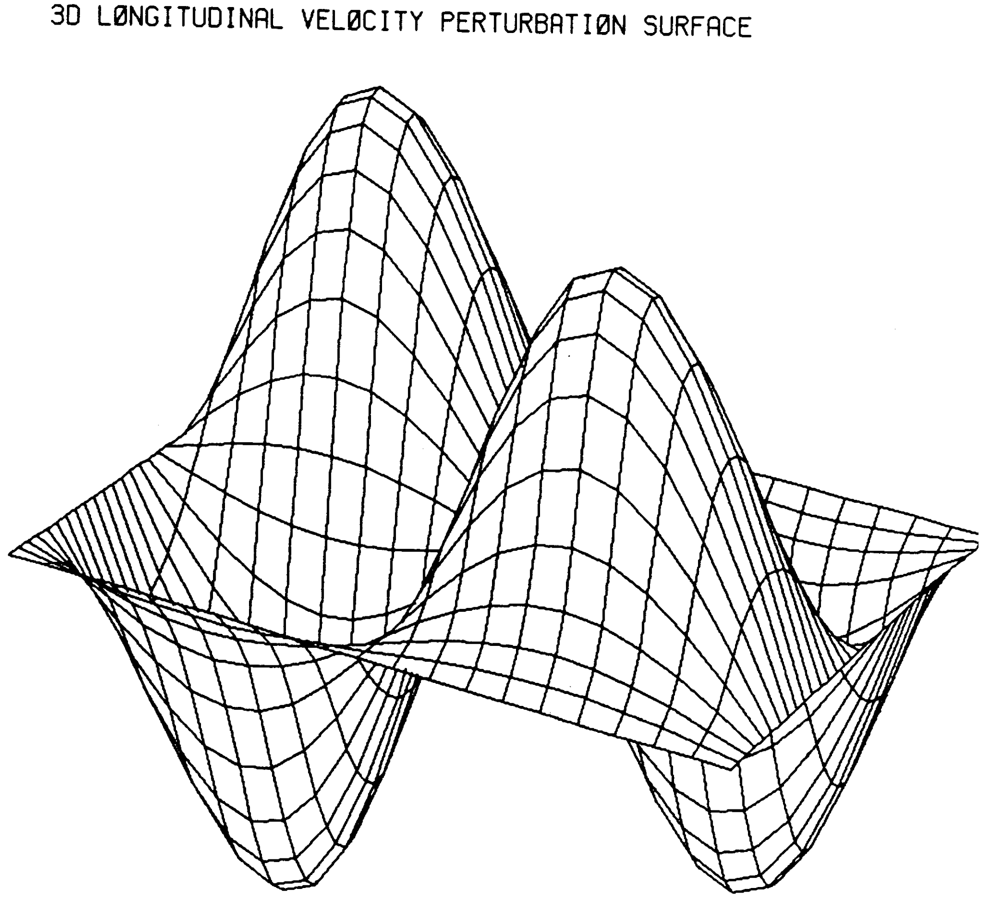
3D LØNGITUDINAL VELØCITY PERTURBATIØN SURFACE

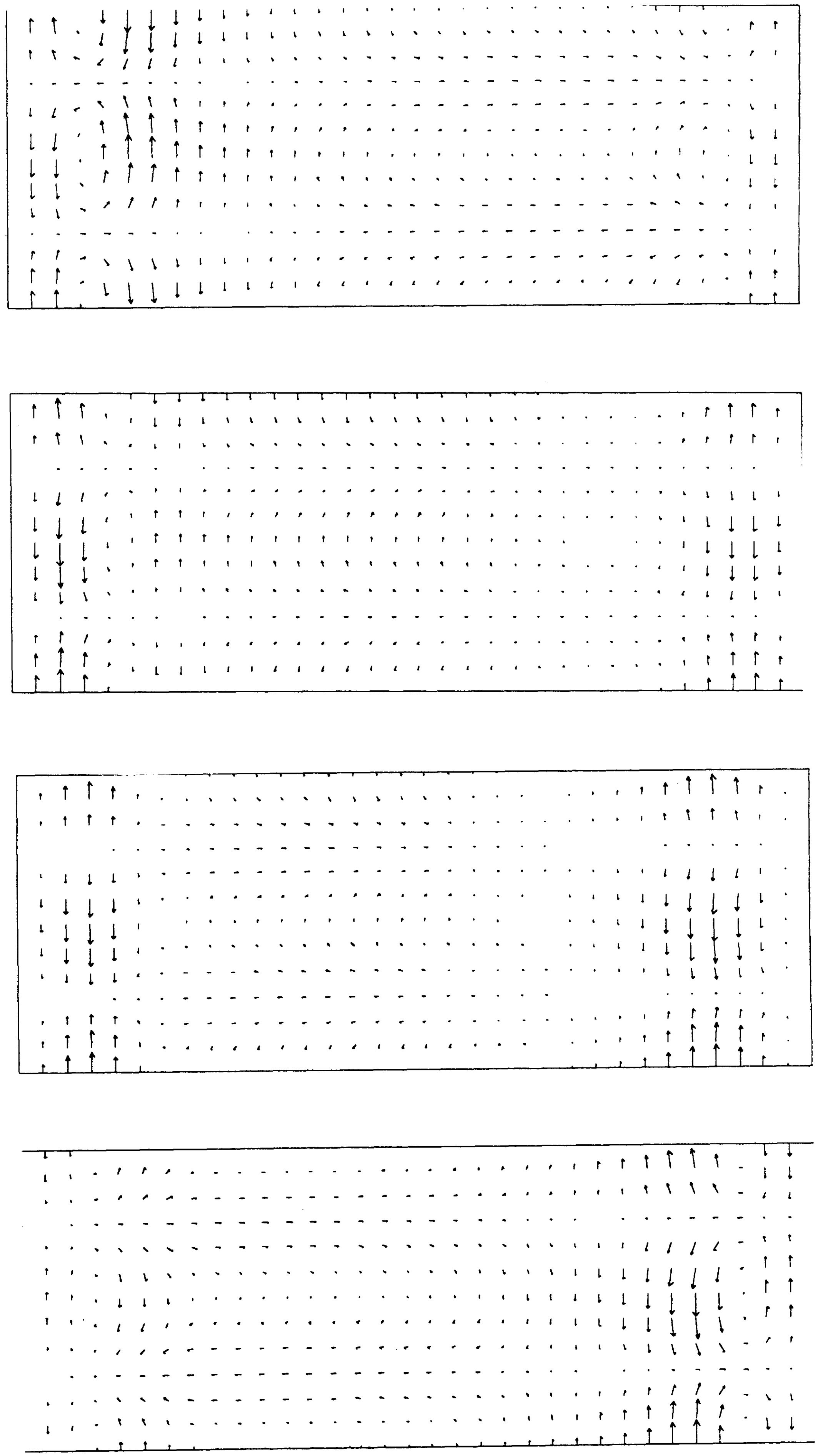

component is locked into a '3-D' eigenstructure together with the oblique and higher wave modes. The total perturbation would not have the appearance of simply a downstream roll. For the three mode truncation in Poiseuille flow, the vorticity of the oblique component (which is somewhat larger in magnitude than the vorticity associated with the streamwise mode) will alternately enhance and detract from the streamwise vorticity of the downstream mode. This is illustrated in Figure 9.3, which shows four cuts of the total '3-D' perturbation velocity field (v^{3d}, w^{3d}), at downstream locations separated a distance $\pi/(4\alpha)$ apart.

Many of the parametric dependencies of the '3-D' instability model are in keeping with an inviscid mechanism. For uni-directional mean flows the '3-D' instability travels at the 2-D phase speed. For Poiseuille and Couette flow there is no large wave number cutoff. After reaching a maximum the growth rate curve asymptotes off, slowly decreasing with increasing wave numbers. Most revealing, however, is that '3-D' growth rates increase with Reynolds number, and the instability is maintained in the inviscid limit. This latter holds for secondary instability in Ekman flow, and is generic to the kind of secondary instability considered here.

The spectra of Ekman flow differs from Poiseuille flow in that the phase speed is not zero in the frame of reference moving with the primary wave velocity. The 3-D disturbance can be advected by the geostrophic flow above the boundary layer, in the large gap case. For the narrow gap case the 3-D disturbance is similarly advected by the mean velocity field orthogonal to the inflectional profile. As can be seen from the wave number dependence of the 3-D growth rates (Figures 9.4(a)-(d)) there is a well defined maximum and wavenumber cutoff. An additional complication, that appears in many of the cases examined, is the competition of two 3-D modes. There is still a predicted critical Reynolds number for the onset of secondary instability. Because of the large parameter space involved with this problem we limit attention to a few gap cases, and the zero Rossby number limit. The amplitude of the 2-

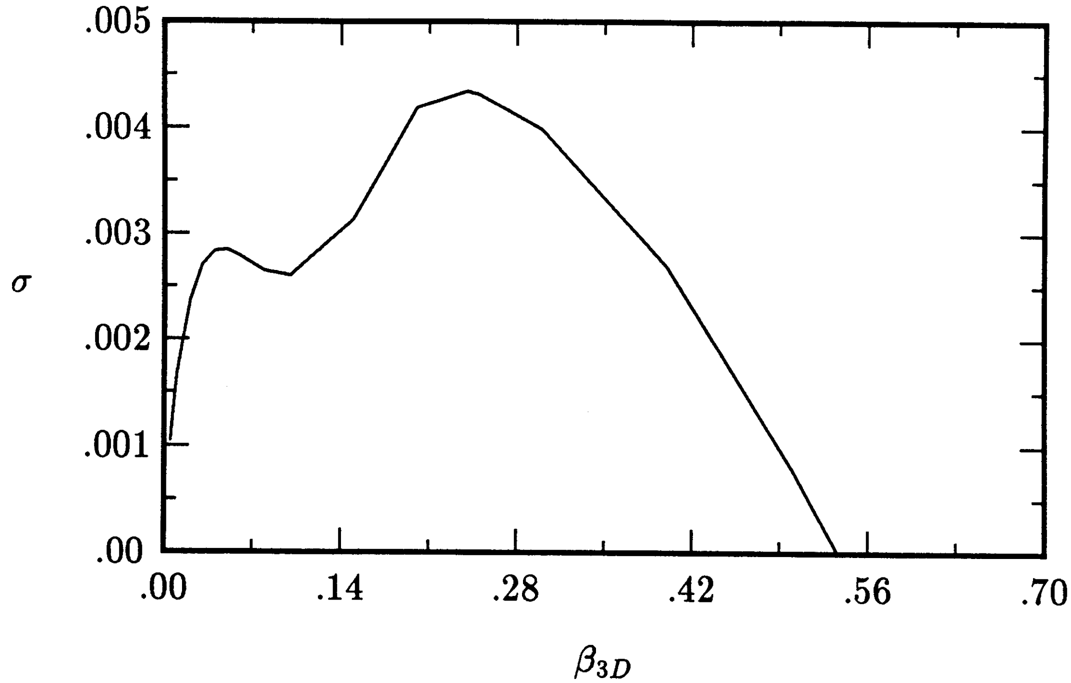

Figure 1: Growthrate vs Wavenumber: (Gap = 20.,Re=80.,Amp=.03)

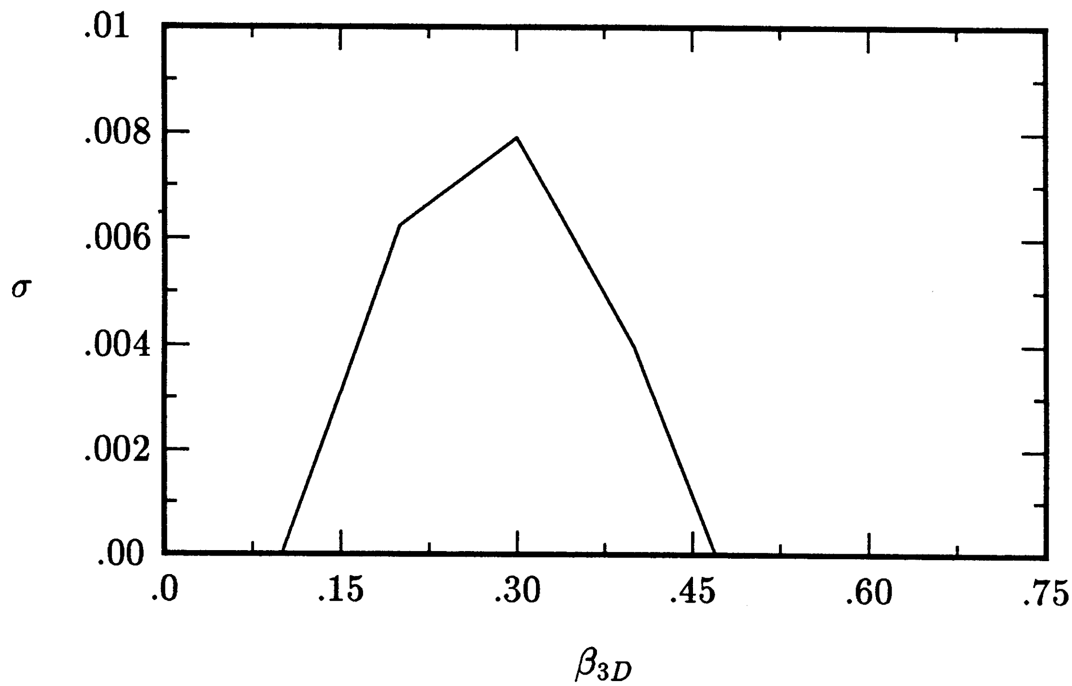

Figure 2: Growthrate vs Wavenumber: (Gap = 6.,Re=102.,Amp=.06)

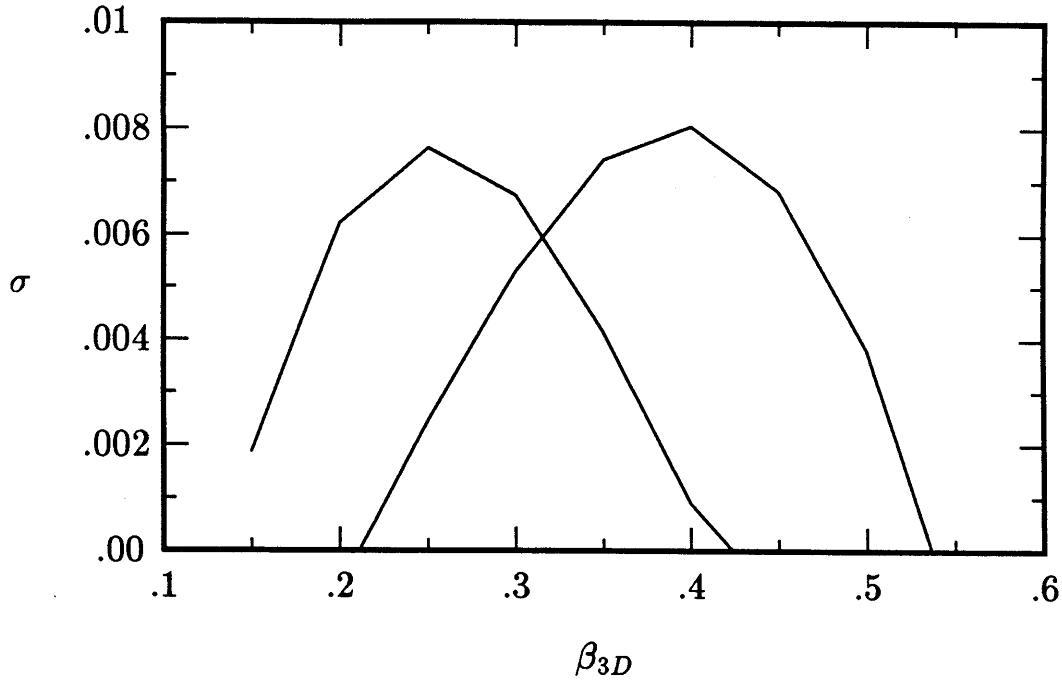

Figure 3: Growthrate vs Wavenumber: (Gap = 4.,Re=200.,Amp=.08)

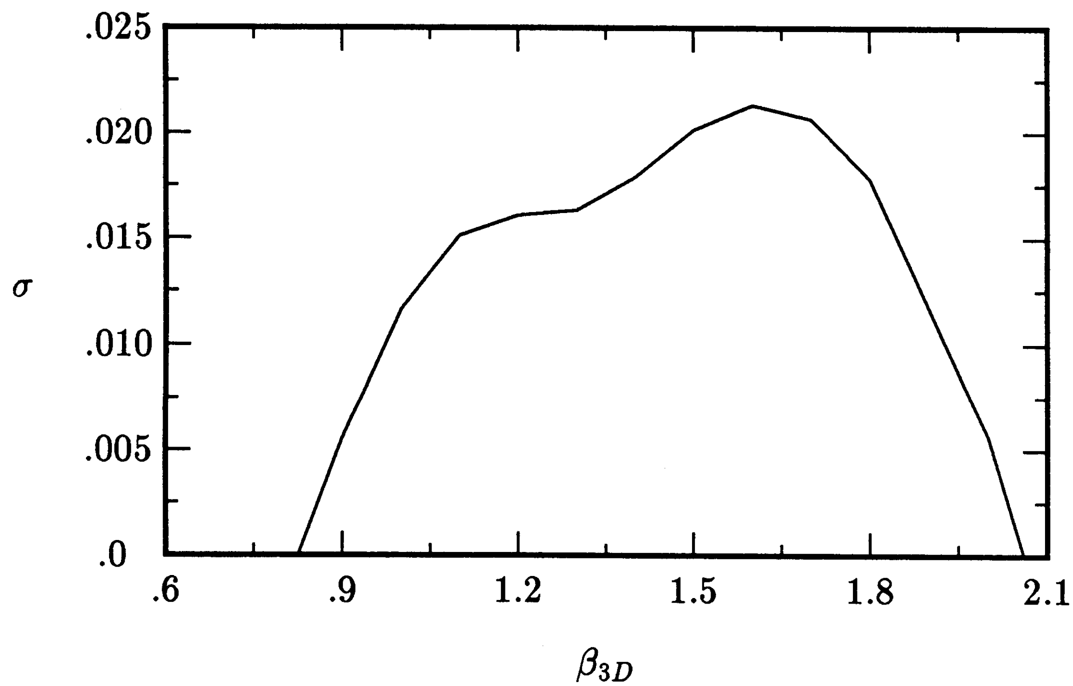

Figure 4: Growthrate vs Wavenumber: (Gap = 2.5.,Re=1000.,Amp=.15)

D wave is a given, predicted from the finite amplitude expansions. *Unlike the numerical experiments done with Poiseuille flow, we are not testing if there exists some threshold 2-D amplitude, but whether the realized flow at a given Reynolds number becomes unstable.*

Each of the cases considered is of interest in its own right, although the semi-infinite and small gap cases represent the two extremes of transverse and streamwise primary vorticity. The large gap case (G = 20.) is naturally close in behavior to the semi-infinite Ekman boundary layer. The primary roll is a taken to be a type II (class A) mode with $R_{cr}^{2D} = 53.$ and oriented $-20.^o$ counterclockwise from the geostrophic. There is a large asymmetry between the n=1 and n=-1 modes. This is the best computational example of a '3-D' disturbance reducing to a low order wave interaction, which can't be accounted for in terms of the WNLTs. If the 2-D wave amplitude is artificially decreased to zero the '3-D' eigenvalue traces back to a slightly damped type I (class B) mode. The $n = 1$ component is a type I mode in the sense that its orientation to the geostrophic is 13^0, and it is similar in eigenstructure to the linear Type I mode. Its wave number is not that normally associated with type I instability but has been selected by optimal growth rate considerations. When the type II mode achieves an amplitude of .02 at Reynolds number 80 it becomes unstable to this secondary instability. The phase speed of the '3-D' disturbance is nearly that given by the type I eigenvalue. Increasing the number of modes to 5 produces very little change in the '3-D' eigenvalue. The type I wave serves as the oblique, n=1 , mode allowing the n=-1 component, to generate power from the mean shear. The n=-1 mode is not found in the classical picture of Ekman flow. In terms of its energy producing ability, it corresponds to the downstream rolls of uni-directional flows. This is a bonafide 3-D instability. A two wave interaction (Chapter 5) consisting of a Type I and Type II wave never generates the n = -1 mode. Even a three wave resonance could at best generate the n=-1 mode by coupling the Type I wave and with the second harmonic of the Type II mode. This is not the process involved in this '3-D' instability. Here the n=-1 mode is generated through a more complex locking of the Type I, and n=0 components without the inclusion of the second harmonic of the primary Type II wave. It is the 3-D perturbation and not just a single wave mode that is growing, and more that half the power to sustain the instability comes from the n=-1 mode.

The case of G=6. is also of special interest. This corresponds with nearly a minimum critical Reynolds number, 34, for the onset of primary waves. Secondary instability is predicted at Reynolds numbers as low as 60, at 2-D amplitudes of about .04 . This is also a case where experimental observations indicate a modulational type instability, with energy spreading out into a wave band of modes, and secondary instability originating at locations near the wave peaks where the modulation reinforces the primary vorticity.

G = 4 is marked by two secondary instabilities almost equally unstable at Reynolds numbers of about 100. and primary wave amplitudes .06 . At this gap separation the secondary instability receives energy from both the mean shear and wave (chapter 10).

G = 2.5 is a case where the primary wave rolls can be considered to be nearly longitudinal with respect to the mean shear. The inflectional velocity component which generates the instability is small compared to the radial velocity profile which is nearly Poiseuille. Secondary instability can occur at Reynolds numbers over 900, if the primary wave amplitude is .145 or larger. The growth rate has a sharp amplitude cutoff. As discussed in the next chapter the energy pathway for the instability of longitudinal rolls is different. Any physically realized instability depends on a large primary wave amplitude. Figure 2.5 (a,b) shows the total longitudinal velocity, where the linear wave is added to the mean velocity so that ratio of the maximum amplitude of the perturbation velocity to the maximum mean velocity is (a) 15%

and (b) 30%. The location where the maximum wave velocity contributes to the total velocity determines its relative importance. If for example the maximum was located near a boundary where the mean velocity is small the effected change would be dramatic. Because the perturbation is a wave, it will alternately steepen and flatten the total velocity in the spanwise direction. The resulting 'warped' velocity fields have local inflections. These periodic local vorticity maxima are most likely instrumental in initiating possible secondary instability to primary streamwise directed waves.

The numerical work by A. Patera and S. Orzag on Poiseuille flow and the experimental observations of S. Widnall and others in boundary layers indicate that the occurrence of secondary instability overlaps with transition to a turbulent flow involving small scales of motion, and immediately precedes the appearance of spots. The results here suggest that the '3-D' instability initiates or triggers the appearance of further burstlike instabilities, (which are determined by the local physics), rather than itself developing into a global 'turbulent' spot.

In the subcritical case it has been speculated that turbulent spots are a manifestation of a fully nonlinear interaction. As conjectured (Malkus' hypothesis), the physical realization does not make use of a quasi steady 2-D viscous wave. Rather the spot initiates a self perpetuating process. This 'island' instability is isolated in phase space, inaccessible through perturbation techniques that start with only a mean shear flow. Its origins are local and it propagates through the fluid much as a pressure pulse would.

Since the current work reports only on the linear aspects of 3-D instability, the analysis applies only to the initial growth. However certain aspects of the linear secondary solution will influence even the fully nonlinear disturbance. It is believed that the secondary instability in Ekman flow is supercritical. Therefore at slightly post critical Reynolds numbers it will retain much of its linear character. Under these conditions the secondary instability may, heuristically, be viewed in terms of modal wave couplings. *The energetics of the instability indicate the rapid channeling of energy into the downstream velocity component,* u_0^{3d} *, of the streamwise mode.* Where as in the absence of a primary wave linearly unstable longitudinal rolls are prohibited, the presence of a small amplitude transverse wave permits a more complex '3-D' disturbance, with a streamwise fourier component, to effectively grab energy from the mean shear. This results in the appearance of intense longitudinal streaks just prior to boundary layer transition. Any one who has looked over a body of water on a windy day has seen longitudinal streaks in the rough patches of water swept by gusting wind. A similar coupling mechanism is responsible for transferring energy from the wind shear into the 'helical' streamwise velocity perturbation. For layered flows with two mean velocity components the situation is complicated in that more than one orientation may be capable of generating the large correlations normally associated with the downstream direction. The instability mechanism is however the same.

Finally it appears that primary streamwise rolls are relatively stable, but become unstable at high Reynolds numbers, where large wave amplitudes produce local inflections in the velocity field. For narrow gap Ekman flow with $G \cong 2.5$, this instability has the appearance of a 'string of beads', a finely hashed small scale disturbance running parallel along individual vortex filaments. The hashings have a preferred orientation with respect to the primary wave. The onset of the instability occurs sporadically within narrow spanwise intervals. The 'strings' start independent of one another. As the disturbance is advected into higher Reynolds number regions the instability spreads out contaminating neighboring filaments and becoming more intense. Eventually patches where the primary wave field is nearly obscured result. This has a substantially milder character than bursting phenomenon associated with the subcritical Poiseuille instability.

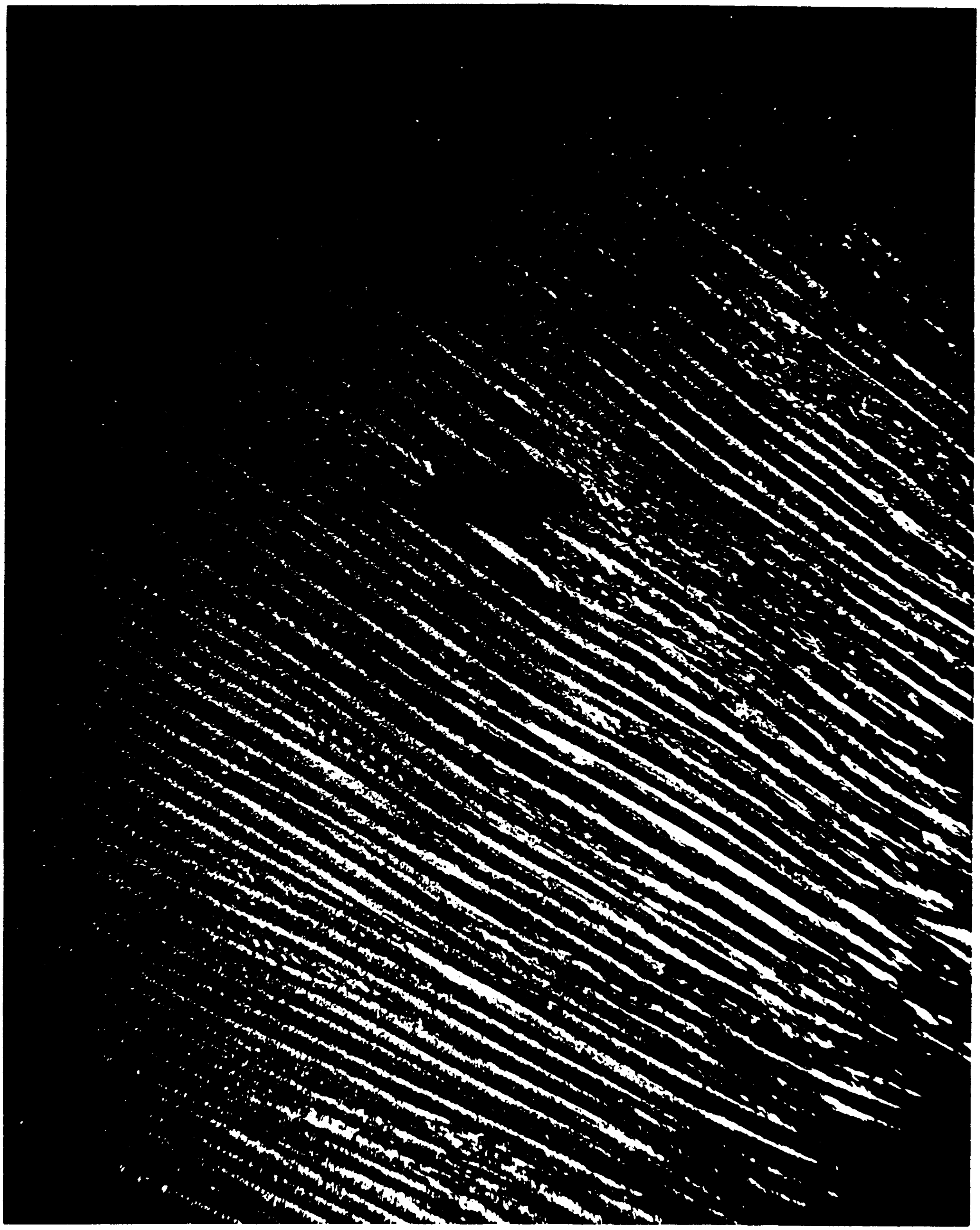

Chapter 10. The Energetics of the Linear 3-D Instability.

There are two complimentary features of 3-D instability that wave energetics helps to clarify. The first is the strong instability of finite amplitude 2-D transverse waves to 3-D instability. A small transverse wave results in convectively large 3-D growth rates. Longitudinal or streamwise vorticies must achieve a relatively large amplitude to initiate 3-D instability. The energy transfer to the secondary instability in each case relies on quite different pathways.

Ekman flow with variable gap width provides a class of flows where the orientation of the vortex waves to the mean shear varies. For large gap widths the two mean velocity profiles are comparable in magnitude. The inflectional profile, which generates the primary rolls, is substantial enough to supply the secondary disturbance with power. At small gap widths the inflectional component of the mean is only a fraction of the radially directed and nearly Poiseuille velocity component. The rolls that are initiated can then be considered to lie longitudinally with respect to the mean shear.

Energy transfer in Poiseuille flow has been examined by A. Patera, (J.F.M., 1982) where it is shown that the secondary instability receives an order of magnitude more power from the mean flow directly, than from the 2-D wave. This same result holds for Ekman flow and is a general characteristic of transverse vorticies. However when the gap width is sufficiently small, so that the primary waves are longitudinally directed, any secondary instability which occurs is delivered power directly from the wave, and necessarily relies on a very large 2-D amplitude.

The motive behind this section is to determine specifically how the 3-D instability can derive energy from an equilibrated or quasi-equilibrated 2-D finite amplitude state. We introduce a modal decomposition of the Reynolds stress tensor in terms of the harmonic (fourier) velocity components. The principle result is that *the energy transfer responsible for the instability is supplied to the 3-D perturbation directly from the mean shear, through the correlation* $u_0^{3d}(w_0^{3d})^*(dU_M/dz)$.

We work first with Poiseuille flow then return to Ekman flow, where the same results hold except for the case of streamwise vorticity waves. These longitudinally directed waves are stable against 3-D instability until the maximum primary perturbation velocity reaches about 15% of the maximum mean velocity. They then can become unstable via an alternate pathway involving a correlation between the 2-D *wave* and the 3-D perturbation. For $G \tilde{>} 2.0$ the realized equilibrated waves achieve sufficient amplitude to become unstable to the secondary instability, before the onset of subcritical instability. As mentioned at the end of the Chapter 9, observations indicate that the secondary instability initially takes on the form of a string of beads, along streamwise vortex filaments. The instability prefers a given orientation with respect to the primary wave. Although the large amplitude required to initiate the secondary instability probably places the computation of the equilibration in a range beyond that which can be accurately predicted from the finite amplitude expansions used, the stability calculations for this case can be performed by artificially varying the 2-D amplitude and Reynolds number. Then numerical model predicts primary rolls (of reasonable amplitudes) should remain stable to '3-D' disturbances untill a Reynolds number of about 900 (compare this with the 2-D onset at a Reynolds number of 204). The Reynolds number regime over 1000 is particularly interesting because of the appearance of a subcritical instability from the Poiseuille velocity profile. A competition between these two mechanisms would result. Whether this beadlike instability works to delay the occurrence of bursts or helps in their initiation it is not known.

We will make use of several simplifications in an attempt to leave the equations unfettered with superfluous terms, while still retaining all the essential physical effects. Thus (i) the basic flow $(U_M(z), 0, 0)$ is taken to be unidirectional, (ii) the 2-D wave $\left\{(u^{2D}(z), 0, w^{2D}(z))e^{i\alpha(x-ct)} + (*)\right\}$ is assumed to be sinusoidal, neglecting its higher harmonics, and (iii) the 3-D perturbation is truncated to three modes, its lowest order representation, consisting of two complimentary oblique components and a longitudinal mode.

Let the time dependent velocity field be decomposed as $v = v^{eq} + u$ where v^{eq} is the equilibrated finite amplitude flow and u the 3-D perturbation. Let $\mathcal{V}(x, y, z)$ be the region given by $\left\{ x \in [0, \frac{2\pi}{\alpha}],\ y \in [0, \frac{2\pi}{\beta}],\ z \in [-1, 1] \right\}$ so that the velocity vectors vanish on the boundary. The fundamental equation for the perturbation kinetic energy, $\mathcal{K} = \frac{1}{2}\int u \cdot u d\mathcal{V}$ is

$$\frac{d\mathcal{K}}{dt} = -\int_{\mathcal{V}} \left(u \cdot D \cdot u + \nu \nabla u : \nabla u\right) d\mathcal{V} \tag{1}$$

where

$$[D]_{i,j} = \frac{1}{2}\left(\frac{\partial v_j^{eq}}{\partial x_i} + \frac{\partial v_i^{eq}}{\partial x_j}\right)$$

is the deformation matrix of the equilibrium flow, and

$$[\nabla u]_{i,j} = \frac{\partial u_j}{\partial x_i}$$

The approximate form of the 3-D perturbation in component form is

$$u = \left(\sum_{n=-1,0,1} \left(u_n^{3D}, v_n^{3D}, w_n^{3D}\right) e^{i\alpha n(x-ct)} e^{i\beta y} e^{\sigma t} + (*) \right) \tag{2}$$

The second integrand of Equation (1) is negative definite. Therefore the first integrand of Equation (1) must be positive and large enough over a sufficient region of $\mathcal{V}$ in order for the perturbation to grow. Upon substitution the deformation matrix becomes

$$D = D_1 + D_2 = \frac{1}{2}\begin{bmatrix} 0 & 0 & U_M'(z) \\ 0 & 0 & 0 \\ U_M'(z) & 0 & 0 \end{bmatrix} +$$

$$\left\{ \begin{bmatrix} i\alpha u^{2D} & 0 & \frac{1}{2}\left(\frac{du}{dz}^{2D} + i\alpha w^{2D}\right) \\ 0 & 0 & 0 \\ \frac{1}{2}\left(\frac{du}{dz}^{2D} + i\alpha w^{2D}\right) & 0 & \frac{dw}{dz}^{2D} \end{bmatrix} e^{i\alpha(x-ct)} + (*) \right\} \tag{3}$$

The part of the integration involving D_1 represents an energy contribution occurring through the action of Reynolds stresses, involving the shear in the mean flow, $U'_M(z)$, and the individual modes of the 3D perturbation. After making use of the symmetry relations $(u_{-1}^{3D}, v_{-1}^{3D}, w_{-1}^{3D}) = (u_1^{3D}, -v_1^{3D}, w_1^{3D})^*$ and $(u_0^{3D}, v_0^{3D}, w_0^{3D}) = (u_0^{3D}, -v_0^{3D}, w_0^{3D})^*$ the second part of the first integral reduces to

$$\int_{\mathcal{V}} (u \cdot D_2 \cdot u) \, d\mathcal{V} = \frac{4\pi^2}{\alpha\beta} e^{2\sigma t} \int_{-1}^{1} \Big\{ 4i\alpha u^{2D} u_0^{3D} (u_1^{3D})^*$$
$$2(\frac{du}{dz}^{2D} + i\alpha w^{2D}) \left(u_0^{3D} (w_1^{3D})^* + (u_1^{3D})^* w_0^{3D} \right) +$$
$$4 \frac{dw}{dz}^{2D} w_0^{3D} (w_1^{3D})^* \Big\} + \{*\} \, dz \qquad (4)$$

There is no instability without the 2-D wave. A stability calculation based on the the mean shear alone amounts to solving uncoupled Orr-Sommerfeld equations for each of the 3-D wave components separately. This results only in decaying modes. In light of the above Reynolds stress decomposition, there are three alternatives to consider. (i) The 2-D wave could conceivably supply energy to the 3-D perturbation directly, through the second of the two integrals (Eq. 4). (ii) The finite amplitude 2-D wave could distort the mean, allowing a modified mean shear to become unstable to 3-D disturbances. (iii) The 2-D wave could, through nonlinear wave couplings, permit the 3-D eigenstructure to assume a form capable of extracting energy from the mean shear. The second phenomenon, mean flow distortion is important to 2-D equilibration but plays an inconsequential role for the type of 3-D growth considered here. The eigenvalue computations with or without the correction to the mean show little difference. Merely altering the mean shear, but setting the 2-D wave amplitude to zero, again results in uncoupled eigenproblems with only decaying modes.

The computation of the power integrals shows that terms from the second integral, which are proportional to the 2-D wave amplitude, are much smaller than the contribution from the mean shear that result from the first integral. Of the terms in the second integral the largest is the correlation $\left\{ u^{2D} u_0^{3D} (u_1^{3D})^* \right\}$. This contributes positively to

3-D growth, but is considerably smaller than (about one sixth of) the energy transfer from the mean shear, at near critical wave amplitudes. Therefore, in the presence of a finite amplitude 2-D wave, nonlinear wave couplings permit a modified 3-D eigenstructure to draw energy directly from the mean shear. This is the mechanism responsible for large 3-D growth rates. The downstream component (the 0^{th} fourier mode) delivers six times the power as the oblique component to the 3-D perturbation. With increasing Reynolds number, the streamwise velocity component u_0^{3D} becomes proportionately larger and the correlation product $u_0^{3D}(w_0^{3D})^*(dU_M/dz)$ more significant.

This model is consistent with a further simplified interpretation along the lines of the three mode fourier truncation. Where as in the absence of a primary wave linearly unstable downstream rolls are prohibited, the presence of a small amplitude transverse wave permits of a more complex '3-D' disturbance, with a downstream fourier component. The downstream component is very effective at producing energy through the correlation product $u_0^{3d}(w_0^{3d})^*(dU_M/dz)$ and this results in the large '3-D' amplification rates that calculations predict. While for an infinitesimal 2-D wave the 3-D eigenvalue problem decouples into modal components, a small but critical primary amplitude is the essential ingredient necessary for secondary instability. The sensitivity of the 3-D eigenstructure to variations in amplitude make it believable that beyond some large 2-D amplitude the eigenstructure is modified so as to effect a decrease in the growth rate or energy cutoff. This is a parametric feature of the model found by Orzag and Patera for Poiseuille flow.

Figure 10.1 shows respectively the 2-D power integral (a), the power produced by the downstream mode (b), and the oblique component (c) of the 3-D perturbation, and the largest of the dynamic energy terms (d), for Poiseuille flow.

Poiseuille flow secondary instability case

$Re^{3d} = 1000.$
$\alpha = 1.25$
$\beta = 2.$
$c_{2d} = (.3054, -.01765)$
$w(.0) = 1.$
$amp^{2d} = .002$
$(NN, Q, M) = (1, 1, 0)$

(Table 10.1) INTEGRALS OF THE MODAL ENERGY TERMS

$E^{3d}_{-1,13} = -1.314e-03$	$E^{3d}_{0,13} = -1.498e-02$	$E^{3d}_{+1,13} = -1.314e-03$
$E1 = -1.8689e-03$	$E3 = 5.323e-04$	$E5 = -3.661e-6$

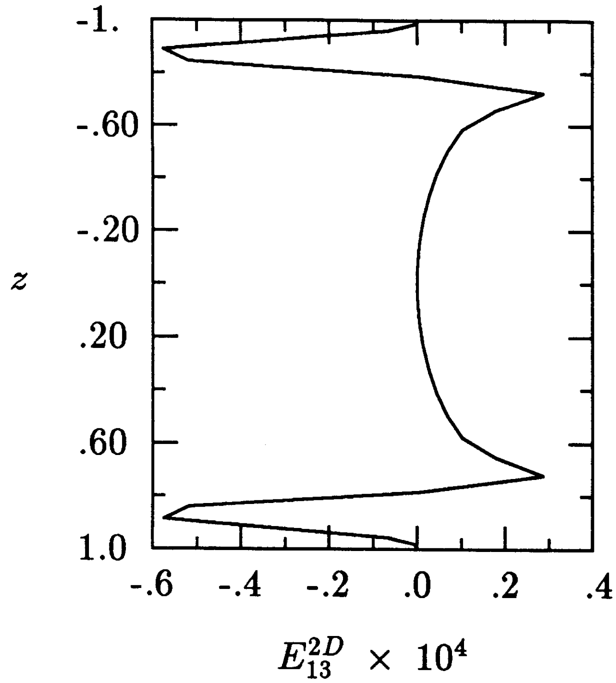

Figure 1: Poiseuille 2D Power Integral

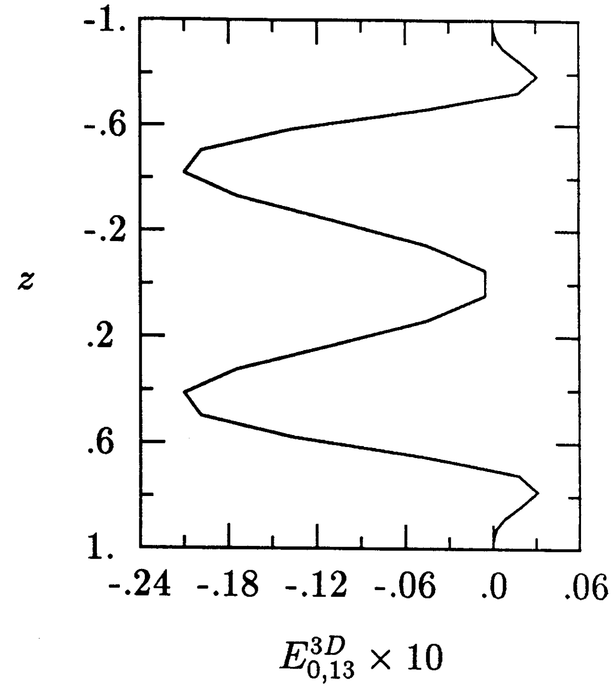

Figure 3: Power from o'th mode

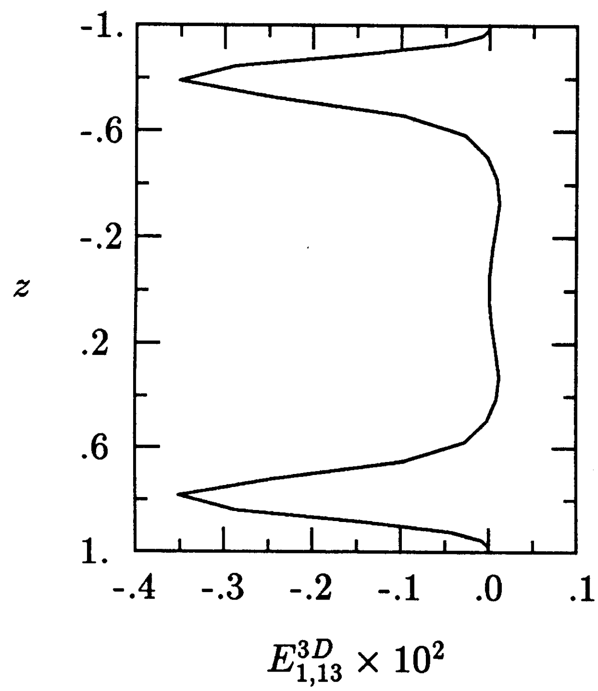

Figure 2: Power from n=1 mode

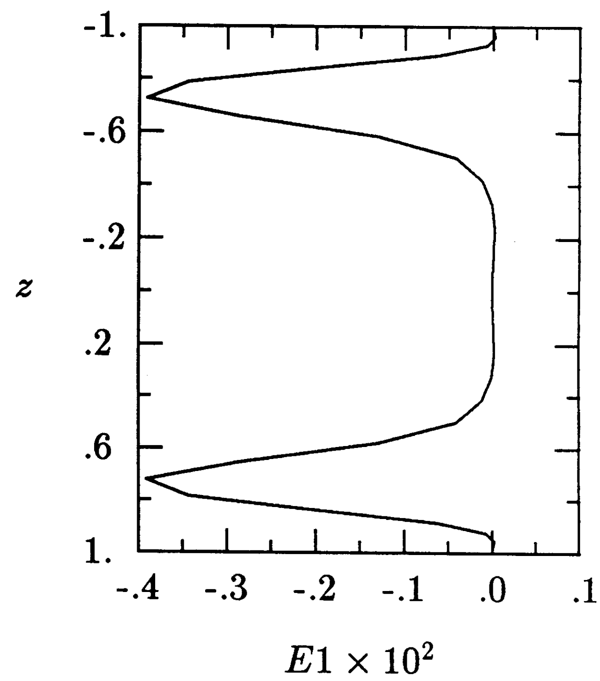

Figure 4: Dynamic term

For mean profiles $(U_M(z), V_M(z), 0)$ and a 2-D primary wave $\left\{(u^{2D}, v^{2D}, w^{2D})e^{i\alpha(x-ct)} + (*)\right\}$ the decomposition $D = D_1 + D_2$ proceeds just as before. A number of new correlation products appear and the symmetry $y \to -y$ is broken. Then Equation (4) is modified to:

$$\int_{\mathcal{V}} (u \cdot D_2 \cdot u)\, d\mathcal{V} = \frac{4\pi^2}{\alpha\beta} e^{2\sigma t} \int_{-1}^{1} \Big\{ 2i\alpha u^{2D} \left(u_0^{3D} (u_1^{3D})^* + u_{-1}^{3D} (u_0^{3D})^* \right) +$$
$$i\alpha v^{2D} \left(u_0^{3D} (v_1^{3D})^* + u_{-1}^{3D} (v_0^{3D})^* + (u_1^{3D})^* v_0^{3D} + (u_0^{3D})^* v_{-1}^{3D} \right)$$
$$(\frac{du}{dz}^{2D} + i\alpha w^{2D}) \left(u_0^{3D} (w_1^{3D})^* + u_{-1}^{3D} (w_0^{3D})^* + (u_1^{3D})^* w_0^{3D} + (u_0^{3D})^* w_{-1}^{3D} \right) +$$
$$\frac{dv}{dz}^{2D} \left(v_0^{3D} (w_1^{3D})^* + v_{-1}^{3D} (w_0^{3D})^* + (v_1^{3D})^* w_0^{3D} + (v_0^{3D})^* w_{-1}^{3D} \right)$$
$$2\frac{dw}{dz}^{2D} \left(w_0^{3D} (w_1^{3D})^* + w_{-1}^{3D} (w_0^{3D})^* \right) \Big\} + \{*\}\ dz \tag{5}$$

These are referenced as the five dynamic terms, $E1, \ldots, E5$. i.e.

$$E1 = 2i\alpha u^{2D} (u_0^{3D} (u_1^{3D})^* + u_{-1}^{3D} (u_0^{3D})^*)$$

Now six terms couple the two mean profiles directly with the three wave mode components. (The terms arising from the contribution of D_1 in the energy equation.) These are the terms usually associated with the Reynolds stress of individual waves. The eigenstructure of a linear '3-D' perturbation is affected by the presence of a 2-d finite amplitude primary wave, which couples (and locks) the component fourier modes. In the terminology in use

$$E_{1,13}^{3D} = (u_1^{3d} (w_1^{3d})^* + (u_1^{3d})^* w_1^{3d}) \frac{dU_M}{dz}$$
$$E_{0,23}^{3D} = (v_0^{3d} (w_0^{3d})^* + (v_0^{3d})^* w_0^{3d}) \frac{dV_M}{dz}$$

... etc. Figure 10.2 shows the important correlations for G = 20, where primary transverse vorticity enables the '3-D' instability to draw energy directly from the mean shear. In Figure 10.3, G = 2.5, the correlations proportional to the 2-d amplitude of the streamwise directed primary vorticity wave produce the energy necessary to maintain the secondary instability. In the convention adopted below, negative terms supply power to the disturbance.

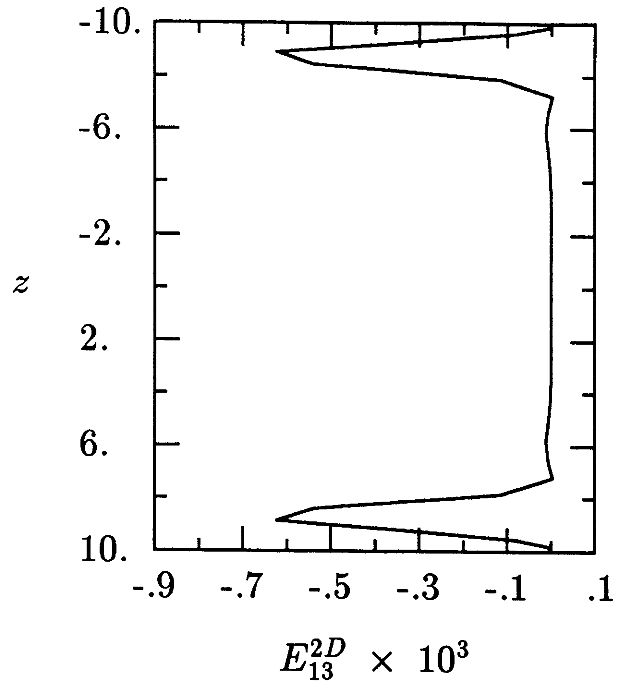

Figure 1: Ekman 2D Power Integral

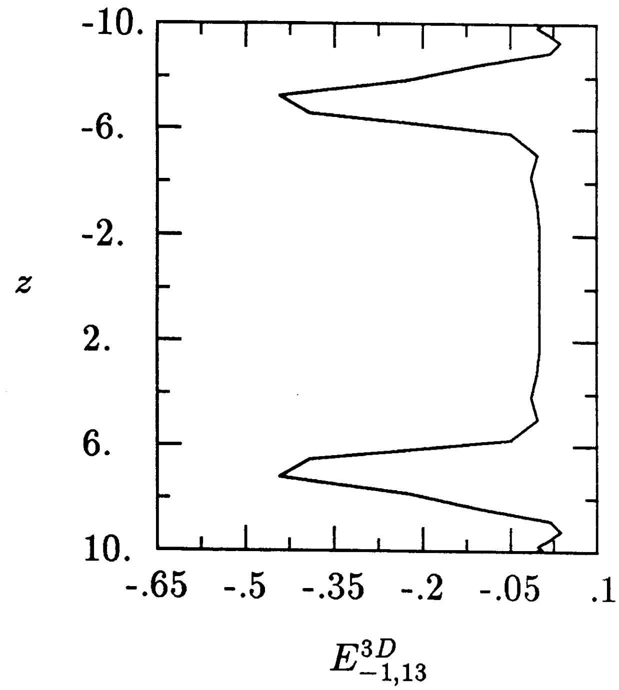

Figure 3: Power from n=-1 mode

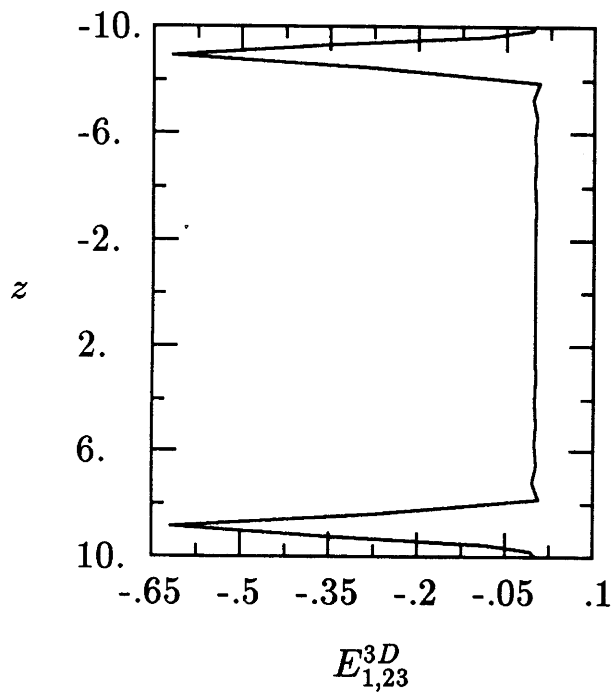

Figure 2: Power from Type I mode

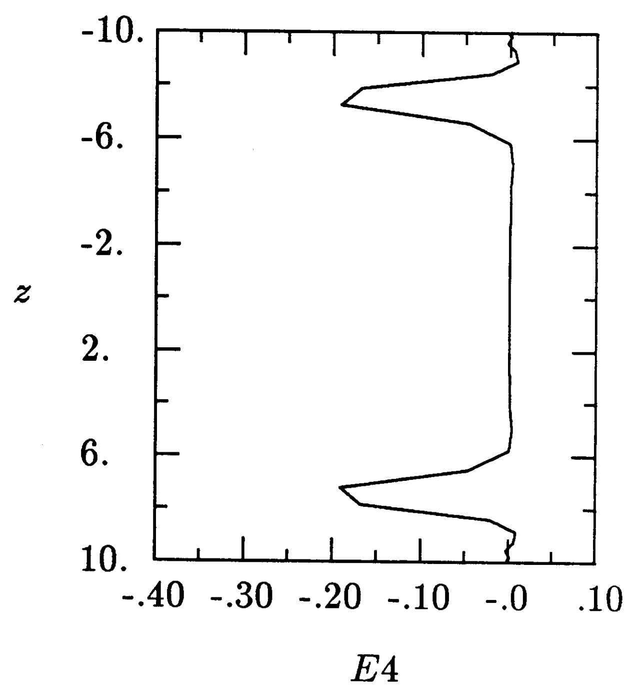

Figure 4: dynamic term

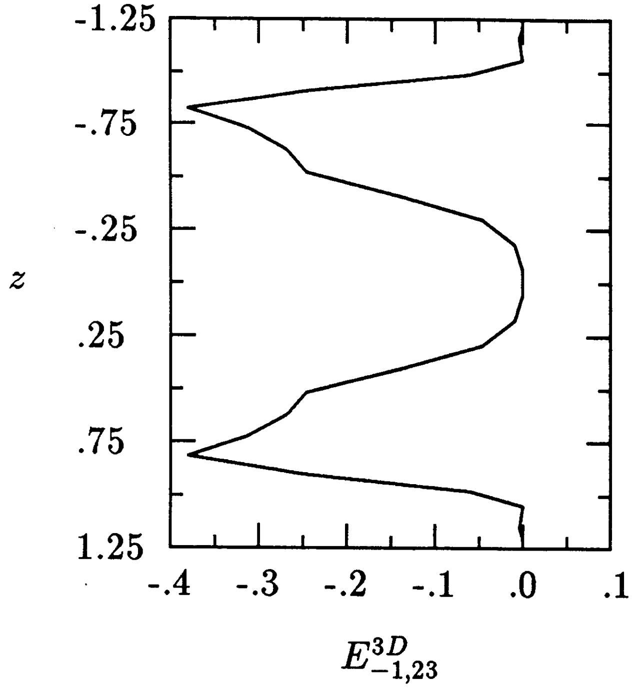

Figure 1: Power from n=-1 mode

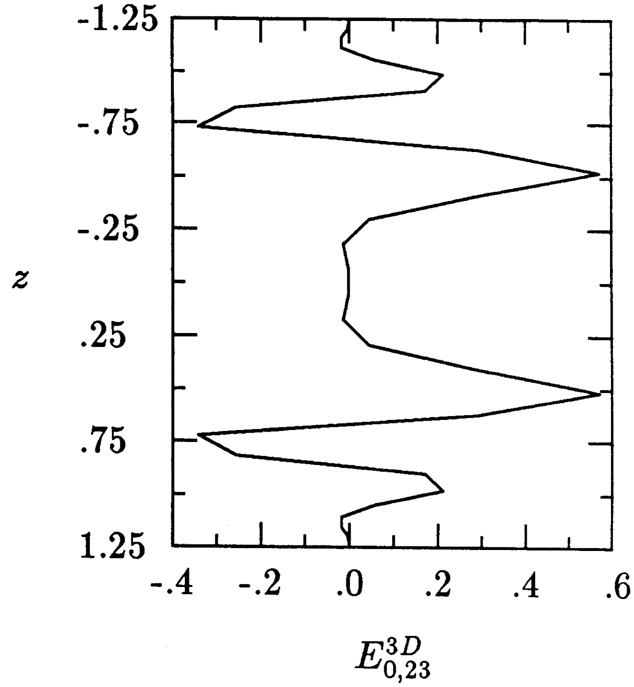

Figure 3: Power from n=0 mode

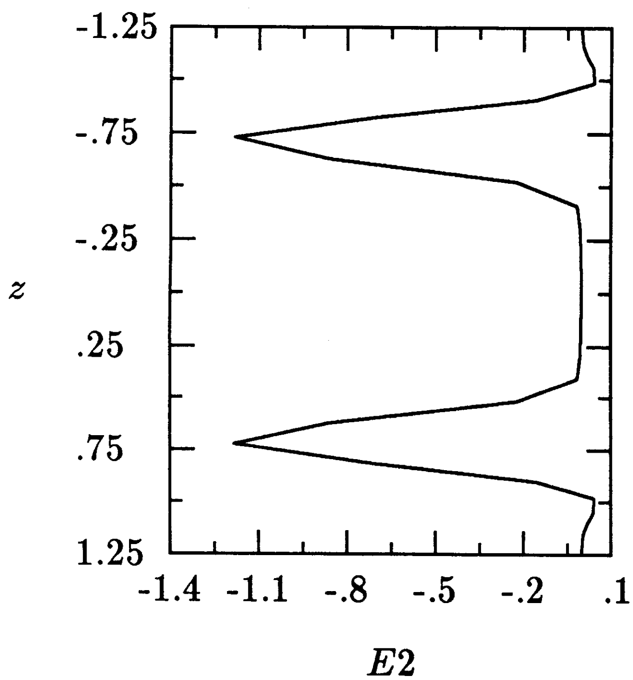

Figure 2: dynamic term

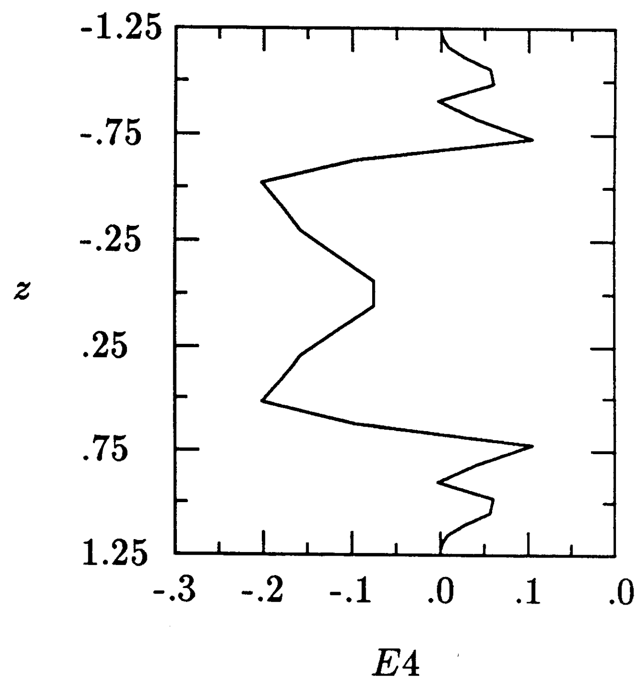

Figure 4: dynamic term

Narrow gap Ekman flow secondary instability models

$$Gap = 20.$$
$$Re^{2d} = 100.$$
$$\epsilon = -20.0^o$$
$$\alpha = .3$$
$$c_{2d} = (.5415, .01765)$$
$$w(.8) = 1.$$
$$\beta = .2$$
$$amp^{2d} = .02$$
$$\sigma = (-.1454, 7.58e-4)$$
$$(NN, Q, M) = (1, 1, 0)$$

$$Gap = 4.$$
$$Re^{2d} = 90.$$
$$\epsilon = 7.5^o$$
$$\alpha = .75$$
$$c_{2d} = (.2210, .0192)$$
$$w(.0) = 1.$$
$$\beta = .4$$
$$amp^{2d} = .08$$
$$\sigma = (-.0473, .0503)$$
$$(NN, Q, M) = (1, 1, 0)$$

$$Gap = 6.$$
$$Re^{2d} = 84.$$
$$\epsilon = -5.0^o$$
$$\alpha = .4$$
$$c_{2d} = (.3909, .0325)$$
$$w(.0) = 1.$$
$$\beta = .3$$
$$amp^{2d} = .06$$
$$\sigma = (-.1423, 2.79e-3)$$
$$(NN, Q, M) = (1, 1, 0)$$

$$Gap = 2.5$$
$$Re^{2d} = 1000.$$
$$\epsilon = 36.0^o$$
$$\alpha = 1.2$$
$$c_{2d} = (.0563, .0087)$$
$$\eta(.5) = 1.$$
$$\beta = 1.6$$
$$amp^{2d} = .15$$
$$\sigma = (-.8912, .02196)$$
$$(NN, Q, M) = (1, 1, 0)$$

Table 10.2 INTEGRALS OF THE MODAL ENERGY TERMS

NARROW GAP EKMAN FLOW				
	GAP = 20.	GAP = 6.0	GAP = 4.0	GAP = 2.5
$E^{3D}_{-1,13}$	-.15796	-.760	-6.71e-3	-5.46e-2
$E_{-1,23}$	-3.46e-3	-.7559	-5.20e-2	-.2662
$E^{3D}_{0,13}$	-1.25e-3	-2.77e-3	-2.44e-3	3.47e-2
$E^{3D}_{0,23}$	5.85e-4	.557	2.05e-3	.1640
$E^{3D}_{1,13}$	-5.76e-3	-.760	8.51e-3	1.05e-2
$E^{3D}_{1,23}$	-.1116	-.9218	-.2639	-.2435

Table 10.3 INTEGRALS OF THE DYNAMIC ENERGY TERMS

NARROW GAP EKMAN FLOW				
	GAP = 20.	GAP = 6.0	GAP = 4.0	GAP = 2.5
E_1	-4.06e-2	.1954	-2.93e-2	4.1e-4
E_2	-1.64e-2	-.4038	-.2893	-.4795
E_3	4.94e-4	-.9928	-7.936e-3	-1.436e-2
E_4	-5.21e-2	-.6207	-1.71e-2	-.1106
E_5	3.20e-3	-1.84e-2	-5.07e-4	-6.71e-3

Concluding Remarks.

Various non-linear wave interactions and secondary instabilities have been examined in the context of Ekman flow. Ekman flow has the virtue of being supercritical, which allows the formulation of stability theories in terms of weakly non-linear wave dynamics. The evolution of Ekman flow also displays several of the many routes to transition, and their dependence upon the flow parameters, such as the Reynolds and Rossby numbers, and on initial conditions, such as the existing wave amplitudes. The orientation of the primary vorticity wave to the mean shear has a dramatic effect on secondary instability.

Each of the routes to transition involves physically distinct mechanisms. We mention three different regimes which, experimental observations indicate, are reliably interpreted in terms of the models considered.

The weakly nonlinear wave theories, i.e. amplitude expansions, correctly predict phenomenon of the sort observed near criticality and the onset of primary waves. The coupling equations are in agreement with the experimental observations of Faller and Kallor and Van Atta in predicting the suppression of type I waves by the type II modes. The coupling coefficients that have been computed have large negative real parts indicating their inhibitory affect. A hypothetical two wave computation shows that this model is also capable of exhibiting intermittent behavior where the wave modes alternately predominate in close proximatity of each other. Such behavior has been observed by Faller. Some numerical simulations show limit cycles with large swings several times the equilibrium amplitude. Caution should be exercised when the amplitude equations are applied far from criticality, as the perturbation scheme used to derive them rapidly becomes 'disordered'. Malkus (private communication) has suggested an alternative approach which should exhibit better convergence properties.

As the amplitude of the primary wave grows, there are several ways in which the spectrum of the flow field might change. The development of a modulation instability could result in wave chaos, should the initial wave be unstable to sideband modes. Dispersive effects have been incorporated into the weakly nonlinear framework, by introducing multiple scales. This leads to coupled nonlinear Shrödinger equations. A secondary instability might receive additional encouragement near the wave envelope peaks.

One important kind of oscillation, which has been neglected in this study, is the subharmonic instability. In the case of narrow gap Ekman flow photographic evidence suggests parameter regions where wave 'defects' play an initiating role in transition. Here neighboring vortex tubes begin to merge giving the perturbation a wavelength twice the original. The most unstable oscillations involve spanwise dependence and would have a three dimensional character.

For the fast growth and introduction of small scales that accompany the bursting phenomenon, a different process has to be considered. The secondary instability considered here, in the context of narrow gap Ekman flow, results from a three dimensional linear instability to a finite amplitude primary wave field. The primary wave links fourier components of the secondary disturbance. If the primary vorticity is transverse to the shear, the primary wave permits the secondary disturbance to effectively tap available energy in the shear that it otherwise couldn't utilize. The energy is channeled into large streamwise velocity perturbations. These warp the underlying mean flow, alternatively steepening and flattening the flow field. If the primary vorticity wave is originally longitudinally directed then secondary instability relies on a large primary wave to supply energy to the secondary disturbance.

Appendix 1: On the Summation Algorithm for Non-Linear Terms.

1. It is convenient to keep things in terms of the components w and η, remembering that for wave mode $e^{i(\alpha x+\beta y)}$ we have the transformation:

$$\begin{pmatrix} \hat{u} \\ \hat{v} \end{pmatrix} = \frac{i}{l^2} \begin{pmatrix} \alpha & \beta \\ \beta & -\alpha \end{pmatrix} \begin{pmatrix} \frac{d\hat{w}}{dz} \\ \hat{\eta} \end{pmatrix}$$

2. Introduce the nonlinear quadratic forms, $\phi_{m,n}(f,g) = \phi_{A^m,A^{*n}}(f,g)$ for $m \neq n$, by the rules:

$$\phi_{m,n}(f,g) = \sum_{i=0}^{m} \left(\sum_{j=0}^{n} \hat{f}_{\,m-i,n-j}\hat{g}_{i,j} \right)$$

and whenever $(i = j)$ or $(m - i) = (n - j)$ that product is neglected from the summation.

3. Let Φ denote a 'tensor' of rank two defined as the dyadic sum

$$\Phi(f,g) = \sum_{m} \sum_{n}^{(m \neq n)} \left\{ A^m A^{*n} \phi_{m,n}(z) e^{(m-n)\theta} \right\} \hat{\imath}_m \hat{\imath}_n$$

(Where $\theta = (\alpha x + \beta y)$.)

4. We invent, for convenience, two dyadic wave number (m,n)-*tuples*. They have components

$$\begin{aligned} (\varepsilon)_{m,n} &= (m-n)(\alpha) \\ (\nu)_{m,n} &= (m-n)(\beta) \end{aligned}$$

$m \neq n$ and we give them the following two properties

- (m,n)-*tuples* are closed under multiplication which is performed componentwise, leaving a dyadic of the same order.
- (m,n)-*tuples* multiply tensors of rank two via contraction over both indices which gives a scalar.

Then we can write the nonlinear products for the Navier-Stokes Equation

$$\begin{pmatrix} S_1 \\ S_2 \\ S_3 \end{pmatrix} = \begin{pmatrix} i\varepsilon \cdot \Phi(u,u) + i\nu \cdot \Phi(v,u) + \Phi_z(w,u) \\ i\varepsilon \cdot \Phi(u,v) + i\nu \cdot \Phi(v,v) + \Phi_z(w,v) \\ i\varepsilon \cdot \Phi(w,u) + i\nu \cdot \Phi(v,w) + \Phi_z(w,w) \end{pmatrix}$$

also note the symmetry $\Phi(u,v) = \Phi(v,u)$.

5. It can readily be determined that

$$\left(\frac{\partial^2}{\partial x^2} + \frac{\partial^2}{\partial y^2}\right)S_3 = -(\varepsilon^2 + \nu^2)\left[i\varepsilon\Phi(w,u) + i\nu\Phi(v,w) + \Phi_z(w,w)\right]$$

$$-\left(\frac{\partial^2 S_1}{\partial z \partial x} + \frac{\partial^2 S_2}{\partial z \partial y}\right) =$$

$$\left[\varepsilon^2\Phi_z(u,u) + \nu^2\Phi_z(v,v) + 2\varepsilon\nu\Phi_z(u,v) - i\varepsilon\Phi_{zz}(w,u) - i\nu\Phi_{zz}(w,v)\right]$$

$$\left(\frac{\partial S_2}{\partial x} - \frac{\partial S_1}{\partial y}\right) =$$

$$\left[\varepsilon\nu\Phi(u,u) - \varepsilon\nu\Phi(v,v) + (\nu^2 - \varepsilon^2)\Phi(v,u) - i\nu\Phi_z(w,u) + i\varepsilon\Phi_z(w,v)\right]$$

6. Now the final measure of nonlinear terms at a given order of $\epsilon^2 = AA^*$ is a summation of the above terms after being multiplied by the Reynolds number, $R = R_0 + \epsilon^2 R_1 + \epsilon^4 R_2 + \epsilon^6 R_3 + \epsilon^8 R_4 + \ldots$

Appendix 2: The Numerics of the Linear Eigenvalue Problem.

The differential eigenvalue problem to be solved consists of two sets of coupled equations for the fourier components of the vertical velocity, $w_{n,m}$, and the vertical vorticity, $\eta_{n,m}$.

$$[\frac{1}{R}(-k^2_{n,m}+D^2)^2-(i\sigma m)(-k^2_{n,m}+D^2)]w_{n,m}-\frac{2}{R}D\eta_{n,m}$$

$$+i\alpha nD[(U*u_x)_{n,m}+(V*u_y)_{n,m}+(W*u_z)_{n,m}+(U_x*u)_{n,m}+(U_z*w)_{n,m}]$$

$$+i\beta mD[(U*v_x)_{n,m}+(V*v_y)_{n,m}+(W*v_z)_{n,m}+(V_x*u)_{n,m}+(V_z*w)_{n,m}]$$

$$+k^2_{n,m}[(U*w_x)_{n,m}+(V*w_y)_{n,m}+(W*w_z)_{n,m}+(W_x*u)_{n,m}+(W_z*w)_{n,m}]=0 \qquad (1)$$

$$[\frac{1}{R}(-k^2_{n,m}+D^2)-(i\sigma m)]\eta_{n,m}+\frac{2}{R}Dw_{n,m}$$

$$-i\alpha n[(U*v_x)_{n,m}+(V*v_y)_{n,m}+(W*v_z)_{n,m}+(V_x*u)_{n,m}+(V_z*w)_{n,m}]$$

$$+i\beta m[(U*u_x)_{n,m}+(V*u_y)_{n,m}+(W*u_z)_{n,m}+(U_x*u)_{n,m}+(U_z*w)_{n,m}]=0 \qquad (2)$$

Both the limitation of memory space and the need for high accuracy in manipulating the eigensolution are imperatives for using the Chebychev formulation (Orzag, JFM 1971). The linear eigenstructure representation is given by

$$w(x,y,z,t)=\sum_{n=-N}^{N}\sum_{p=0}^{P}w_{m,n,p}e^{i\alpha nx}e^{i\beta my}e^{im\sigma t}T_p(z)+(*) \qquad (3)$$

$$\eta(x,y,z,t)=\sum_{n=-N}^{N}\sum_{p=0}^{P}\eta_{m,n,p}e^{i\alpha nx}e^{i\beta my}e^{im\sigma t}T_p(z)+(*) \qquad (4)$$

(with m = 1 for linear theory.) The differential eigenproblem is reduced to the matrix equation $([A]+\sigma[B])X=0$, where the structure of the $[A]$ and $[B]$ matrices are schematically illustrated as follows,

$$
\begin{array}{c}
n=-N \\ \text{Eq's} \\ w_{1,n,p} \\ n=N \\ \\ n=-N \\ \text{Eq's} \\ \eta_{1,n,p} \\ n=N
\end{array}
\left(\begin{array}{c|c}
\begin{array}{ccc} p=0\ldots P & & \\ \boxed{P\times P} & \cdots & \boxed{P\times P} \\ \vdots & \text{Vars } w_{1,n,p} & \\ \boxed{P\times P} & \cdots & \boxed{P\times P} \end{array} & \text{Vars } \eta_{1,n,p} \\ \hline
\text{Vars } w_{1,n,p} & \text{Vars } \eta_{1,n,p}
\end{array}\right) + \sigma \left(\begin{array}{ccccc} \boxed{P\times P} & & & & \\ & \cdot & & 0 & \\ & & \cdot & & \\ & 0 & & \cdot & \\ & & & & \boxed{P\times P} \end{array}\right)
$$

The dimensions of the complex matrices A and B are 2(2N+1)(P+1) although by making use of cross stream symmetry this can be halved. In the case of Poiseuille (unidirectional) flow a further reduction which makes A and B real is possible (symmetry under $y \to -y$). It is useful to fill in some details with regards to the matrix eigenvalue problem. Each row of the matrix equation could be thought of as an equation for $w_{1,n,p}$ or $\eta_{1,n,p}$. Line [(N+n)(P+1)+(p+1)] corresponds to the equation for $w_{1,n,p}$ and line [(2N+1)(P+1)+(N+n)(P+1)+(p+1)] corresponds to the equation for $\eta_{1,n,p}$. Obviously $w_{1,n,p}$ is the [(N+n)(P+1)+(p+1)]th component of the eigenvector while $\eta_{1,n,p}$ is the [(2N+1)(P+1)+(N+n)(P+1)+(p+1)]th component of the eigenvector. The convolution products in Equations (1-2) are a coupling between the variables and fill a diagonal band of A of width 2*Q+1 blocks, where Q is the number of harmonics included in the primary wave approximation. The eigenvalue problem is then solved by inverting B and applying a Q-R algorithm to determines all the eigenvalues of AB^{-1}. The eigenfunction is then determined by inverse iteration.

Bibliography.

(1) H.P. Greenspan,(1966), 'The theory of rotating fluids', Camb. Univ. Press.
(2) C.C. Lin, (1954), 'The theory of hydrodynamic stability', ibid.
(3) G.B. Whitham, Linear and Nonlinear Waves, Wiley -Interscience (1972).
(4) D.K. Lilly, (1966), 'On the instability of Ekman boundary flow', J.A.S., Vol. 23.
(5) A.J. Faller, (1963), 'An experimental study of the instability of the laminar Ekman boundary layer', J.F.M..
(6) A.J. Faller and R.E. Kaylor, 'A numerical study of the instatbility of the laminar Ekman boundary layer', J.A.S.
(7) A.J. Faller and R.E. Kaylor (1966), 'Investigations of Stability and Transition in Rotating Boundary Layers', Dynamics of Fluids and Plasmas, (Edited by Pai).
(8) W.V.R. Malkus and G. Veronis, 'Finite Amplitude Cellular Convection', J.F.M. (1958), Vol. 4.
(9) W.V.R. Malkus, 'Turbulent Velocity Profiles From Stability Criteria', J.F.M. (1979), Vol. 90.
(10) J.T. Stuart, (1960), 'On the Nonlinear Mechanics of Wave Disturbances in Stable and Unstable Parallel Flows', J.F.M.
(11) J. Watson, (1960), 'On the Nonlinear Mechanics of Wave Disturbances in Stable and Unstable Parallel Flows', J.F.M..
(12) E.L. Mollo-Christenson and P.R. Tatro, (1967), 'Experiments on Ekman layer instabilities', J.F.M.
(13) D.R. Caldwell and C.W. Van Atta, (1970), 'Characteristics of Ekman layer instabilities', J.F.M.
(14) K. Stewartson and J.T. Stuart, (1972), 'Nonlinear stability of plane Poiseuille flow', J.F.M.
(15) C.C. Lin, (1954), 'Some physical aspects of the stability of parallel flows', Proc. N.A.S..
(17) R.A. Brown, (1970), 'A secondary flow model for the planetary boundary layer', J.A.S..
(18) D.J. Benney and H. Gustavson, (1980), 'A new mechanism hydrodynamic instability', Studies in Applies Math.
(19) T.R. Akylas and D.J. Benney, (1980), 'Direct resonance in nonlinear wave systems', Studies in Applied Math.
(20) D.J. Benney, (1962), 'Nonlinear gravity wave interactions', Journal of Mathematical Physics.
(21) D.J. Benney and A.C. Newell, (1966), 'The propagation of Nonlinear wave envelopes', Journal of Math Physics.
(22) A.C. Newell and J. Whitehead, (1969), 'Finite bandwidth finite amplitude convection', J.F.M., Vol 38.
(23) T.B. Benjamin and J.E. Fier, 'The disintegration of wavetrains on deep water',

J.F.M. (1967).
(24) N. Itoh, 'Nonlinear stability of parallel flow with subcritical Reynolds numbers', Part I and II, J.F.M. (1977).
(25) A. Davey, 'On Itoh's finite amplitude stability theory for pipe flow', J.F.M. (1978), Vol 86.
(26) D.D. Joseph and D.H. Sattinger, 'Bifurcating time periodic solutions and their stability', Archives for Rational Mechanics and Analysis, (1972), Vol 45.
(27) J.P. Zahn, J. Toomre, E.A. Spiegel, and D.O Gough, 'Nonlinear cellular motions in Poiseuille channel flow', (1974), J.F.M..
(28) W.C. Reynolds and M.C. Potter, 'Finite amplitude instability of parallel shear flows', J.F.M. (1967), Vol 27.
(29) G Iooss, H. Nielson, and H. True, 'Bifurcation of stationary Ekman flow into stable periodic flow', Archive for Rational Mechanics and Analysis, (1978), Vol 68.
(30) K.K. Tung, 'Barotropic Instability of Zonal Flows', J.A.S. (1980), Vol 38.
(31) Arthur Rosenthal and Richard Lindzen, 'On the the instability of Helmholtz velocity profiles', Journal of Geophysical Research
(32) Th. Herbert, 'On perturbation methods in nonlinéar stability theory', J.F.M. (1983).
(33) Th. Herbert, 'Nonlinear stability of parallel flows by High order amplitude expansions', (1980) A.I.A.A.
(34) Th. Herbert and M.V. Morkovin, 'Dialogue bridging some gaps in stability and transition research', I.U.T.A.M. Symposium, (1979), (Edited R. Eppler).
(35) J.T. Stuart and D. Meksyn, (1954), Proc. Royal Soc. A, Vol. 208.
(36) J.T. Stuart, N. Gregory, W.S. Walker, Phil. Trans. A, Vol 248, (1955).
(37) J.T. Stuart, (1962), ' Three-Dimensional nonlinear effects in the stability of parallel flows', Adv. Aero Sci., Vol. 3.
(38) Ince, 'Ordinary Differential Equations', Dover.